Concordia's First Supersonic Sounding Rocket

Team 79 Project Technical Report to the 2018 Spaceport America Cup

Olivier D'Angelo
Co-Technical Lead, Concordia University, Montreal, QC, H3K 1M8

Oleg Khalimonov
Co-Technical Lead, Concordia University, Montreal, QC, H3K 1M8

Anania Yeghikian
Avionics Lead, Concordia University, Montreal, QC, H3K 1M8

Matthieu Hoang-Cao
Recovery Lead, Concordia University, Montreal, QC, H3K 1M8

Juan Sebastian Prieto
Legal Team, Concordia University, Montreal, QC, H3K 1M8

Camille Bernier-Tremblay
Recovery Team, Concordia University, Montreal, QC, H3K 1M8

Kevin Bolusi
Payload Lead, Concordia University, Montreal, QC, H3K 1M8

Diego Canizales
Payload Team, Concordia University, Montreal, QC, H3K 1M8

Slater Covenden
Payload Team, Concordia University, Montreal, QC, H3K 1M8

The following document consists of the summary of the functionality and operations of *Supersonice*, a sounding rocket competing in the 2018 Spaceport America Cup. Team 79 will be competing in the Advanced Category, for a 30,000 ft apogee target with a COTS motor system. For the first time at the SAC, the rocket fuselage will be entirely manufactured by automated fibre placement using thermoplastic composites in two components. This allows for rapid assembly of the vehicle and omits the use of doors which can be a source of weakness in the body of rocket. The rocket's payload will observe the sloshing effects of launch while validating two different types of SRAD baffles, simulating a liquid rocket propellant draining simulated system. Each subsystem will validate the requirements set forth by the team, in addition to those outlined by the competition rules and requirements documentation.

I. Nomenclature

A = amplitude of oscillation
A_D = drag area
A_{DA} = drag area of aft
A_{DF} = drag area of forward
a = cylinder diameter
a_g = gravitational acceleration
C_D = coefficient of drag
C_p = pressure coefficient

Cx = force coefficient in the x direction
Cy = force coefficient in the y direction
c = chord
c_p = constant pressure specific heat
c_v = constant volume specific heat
dt = time step
F_D = Drag
Fx = X component of the resultant pressure force acting on the vehicle
Fy = Y component of the resultant pressure force acting on the vehicle
f, g = generic functions
K = trailing-edge (TE) nondimensional angular deflection rate
m = mass
n = number of moles
P = pressure
R = ideal gas constant
R_c = combustion gas constant
r_w = weight ratio
□ = fluid density
T = temperature
V = volume
v_f = fluid velocity

II. Introduction

Space Concordia is a student society which aims to promote aerospace and astronautical engineering within Concordia University and Montreal by taking on projects and participating in competitions in these fields. Space Concordia's Rocketry Division is one of the four divisions which are supported by the society, alongside Spacecraft, Robotics and Special Projects. The rocketry team benefits from a society level management on several aspects, and is part of a "bigger picture". It is the rocketry team's mission to develop concordia's rocket technology to the point where we can house our Spacecraft team's CubeSat and eventually launch suborbital flights. This year, the team focused on achieving supersonic flight for the first time at Concordia. To further push the capabilities of the team, all structural components were student researched and developed (SRAD), from the carbon fibre boat tail to the sears-haack tip of the rocket. Additionally, research was conducted on a thermoplastic composite material used in sounding rocket airframes: glass fibre reinforced polyethylene terephthalate (PET). The research project conducted by one of our members served to validate the new composite fuselage through analysis and destructive testing.

This rocket is meant to be a milestone for Space Concordia as our first entry in IREC's advanced category, first supersonic vehicle first rocket to house CubeSat format (our previous rockets used PocketCube). We also believe that we built the first rocket fuselage, built completely using Automated Fiber Placement (AFP) technology.

AFP technology is a new way of laying up composite materials, by using a powerful robotic arm to wrap individual tapes of fiber (toes) around a mandrel while applying high pressure and heat. This allows us to produce composite wraps that have extremely low void content (a very common defect in composites) and denser composite parts, dramatically increasing its strength to weight ratio. Previous iterations of our rockets have used this technology, but only to make simple cylindrical shapes. This year, we have done enough research to attempt to have the cylinder taper, and have the arm layup over a changing geometry, allowing us to make the nose cone on the machine. Due to the machine's ability to make "perfect" layups, this prompted us to integrate the nose cone with the forward section, thus greatly improving the load pathways on the rocket, and reducing its complexity, allowing the whole structure stronger and easier to analyze.

Fig. 1 AFP Machine

The purpose of this rocket is to validate this new method of manufacturing, validating our supersonic analysis and performing a fluid slosh experiment during acceleration of the rocket to test the effects of our SRAD baffles on draining fuel simulant tanks. Our dual deployment rocket will allow us to validate out deployment bag design, while using for the first time GPS along with telemetry to ensure recovery of the rocket post flight.

The project is funded partially by the Engineering and Computer Science Association and by various sponsors. The team structure is divided into 5 subdivisions: structure, recovery, avionics, payload and flight performance, each responsible for their own subsystem and member productivity.

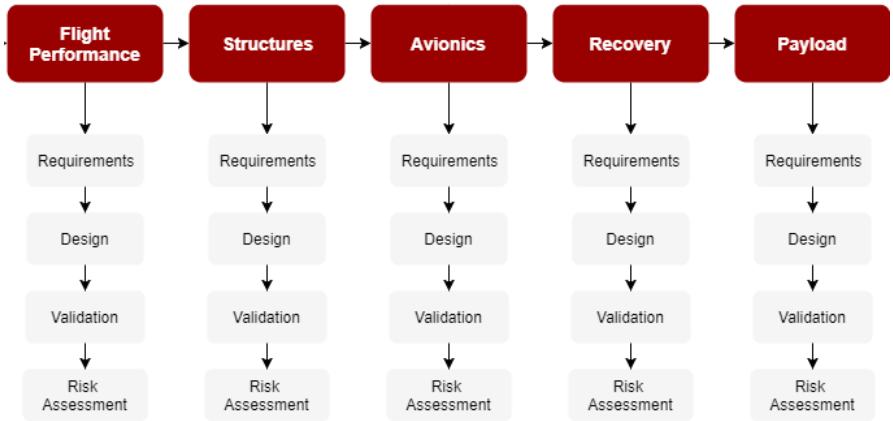

Fig. 2 Team Structure

III. System Architecture Overview

The purpose of this rocket is to validate this new method of manufacturing, validating our supersonic analysis and to perform a fluid slosh experiment during acceleration of the rocket. A new structure was developed that has undergone heavy analysis and validation. The forward section of the rocket houses the avionics system which records the barometric pressure, temperature, 3-axis acceleration, pitch roll and yaw, battery voltage and GPS coordinates. Data is collected with both a commercial system and a SRAD system. Avionics is used to deploy the drogue chute at apogee, using an SRAD recovery system that separates the rocket by releasing pressurized gas. After the rocket has descended to a satisfactory height, the main cute is released by the recovery system to slow the rocket before landing. Throughout the flight, our payload will be testing the effects of our SRAD baffles on actively draining tanks. The payload will be using an analogue to RP1 (kerosene) and will compare the effectiveness of ball baffle design vs. ring baffle design, as well as study the inertial forces acting on a spray nozzle.

This will also be our first single deployment rocket, therefore would be validating our deployment bag design, and also our first rocket using GPS along with telemetry to ensure recovery of the rocket post flight.

Fig. 3 Rocket Assembly Rendering

A. Flight Performance

Requirements (Design, Test & Evaluation Guideline)

8.1. Launch Azimuth and Elevation
8.2. Launch Stability
8.3. Ascent Stability
8.4. Over-Stability

The flight simulation and analysis software selected was RASAero, which is known to be more precise for supersonic ballistic flights. Table 1 lists the input flight conditions used to simulate the rocket's flight.

Table 1 Simulation Inputs

Simulation Conditions	Value
Launch Alt., AGL (ft.)	4595
Launch Elevation (deg.)	84±1°
Rail Length (ft.)	17
Avg. Wind (mph)	10
Worst Wind (mph)	20
High Temperature (F)	100
Avg. Temperature (F)	86

Table 2 represents the output data at notable flight phases which was used for the flight phase analysis. From the above simulation inputs, an altitude of **3149 ft** was attained in the least favorable conditions. Note that although this is higher than the desired altitude target, certain masses cannot be accurately accounted for until the full assembly of the launch vehicle, therefore giving a safety factor.

Table 2 Flight Phase Acquired Data

Phase	Time	Flight Conditions	Velocity (m/s)
Ground Handling	0	Static Loading: 362 N	N/A
Ignition	0	Thrust: 8034 N (17.5 G)	N/A
Rail Clearance	0.25	Stability Caliber: 2.7	43.2
Motor Burnout	3.4	Drag: 930 N Bending: 2011 N-m	567.5 (Mach 1.64)
Drogue Deployment	40.6	Altitude: 30,149 ft.	73.2

		Deployment Load: 838 N	
Main Deployment	287.6	Altitude: 755 ft. Deployment Loads: 1604 N	25.23
Ground Impact	305	N/A	9.2

B. Structures

Requirements

The following requirements further define the scope of the launch vehicle:

6.1 Adequate venting: 1/8" to 3/16" through any isolated compartment or bay

6.2 Overall Structural Integrity (See Table 3 for more details on the structural analysis)

- 6.2.1 Material Selection: No PVC, low temp polymers or plastics were used in the fuselage structure
- 6.2.3 Implementing Coupler Tubes: minimum coupler length used is 1.5 times the caliber
- 6.2.4 Launch lug mechanical attachment: Implemented hardpoints able to lift vehicle by lugs
- 6.2.5 Aft most launch lug: Support vehicles fully loaded weight while vertical prior to launch

6.3 RF Transparency: Implement radio frequency transparent windows at the top of motor mount and near greatest concentration of payload mass

Design Overview

The structure is composed of two components coupled together using coupler, as seen in Fig. 4.This design was chosen for several reasons. Consolidating the forward and the nose cone reduces weight while adding structural rigid and simplifying assembly procedures. The two sections are assembled together using a ring of equally spaced shear pins.

Fig. 4 Rocket Assembly

Fig. 5 Forward Section Assembly

The forward section consists of a rail system composed of 4 L-extrusions, used to support the bulkheads, housing the ballast, Payload, Avionics, and Recovery sections respectively from tip to aft. The rail system is first assembled

out of the rocket for ease of access, then slid into the fuselage secured by an array of machine screws to the fuselage, and at the nose using a threaded aluminum tip.

Fig. 6 Aft Section Assembly

The aft section of the rocket houses the motor casing, aerodynamic boat tail fairing, recovery hoist ring coupler and fins. All components in the section were student developed. The boat tail mold was designed to minimize wave drag and weight, then manufactured by CNC lathe in Concordia's Engineering, Design and Manufacturing Laboratory (EDML), then layed up using a prepreg carbon fibre. The aluminum thrust ring was optimized by iterating over several finite element analysis (FEA) using ANSYS explicit dynamics, to simulate the shock wave generated by the impulse of launch. To manufacture the entire fuselage on the AFP machine, an aluminum mandrel was designed with the following specifications:

- The end of the mandrel must extend 10 in passed the end of the effective layup section to avoid robotic head collision with the mandrel support.
- The straight sections could not be longer than 30 in, to accommodate the maximum working length of EDML's largest lathe.
- The curved sections could not be longer than 17 in, to accommodate the maximum working length of EDML's CNC lathe.
- The mandrel must be within a cylindricity tolerance of 0.002 in.
- A perpendicular through hole of 1 in diameter at 5 in length from the edge must be machined for the bolt used for the extraction of the composite final product
- Surface finish must be less than 1.6 μm

Fig. 7 Mandrel Assembly

Further details on the mandrel can be found in Appendix E. The mandrel is then mounted to a rotating chuck and to apply the PET glass fibre composite using a hot gas torch to heat the thermoplastic to its melting temperature, bonding it to subsequent layers. Fig. 8 demonstrates the process during the forward fuselage layup. Given the change in material, the layer orientation was optimized to satisfy the structural loading requirements. This resulted in a quasi-isotropic layup sequence Further details research report can be found in Appendix F.

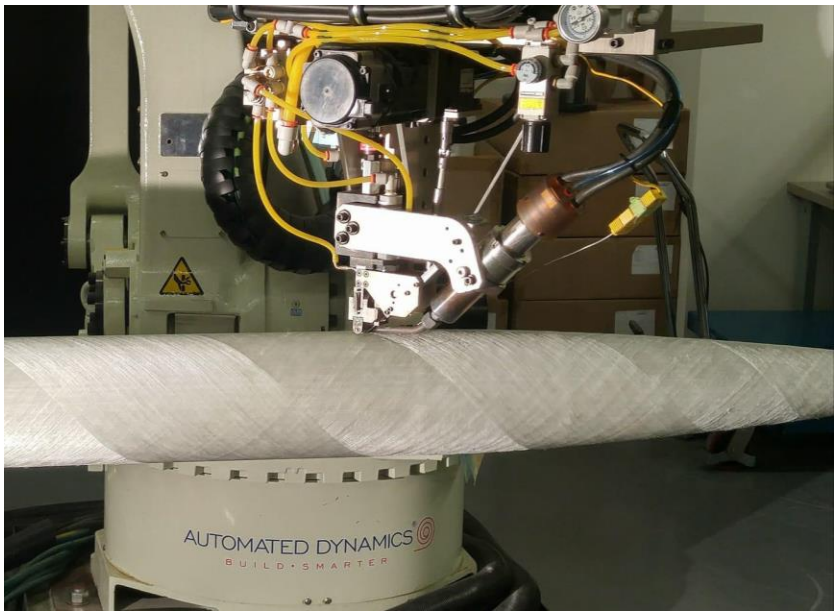

Fig. 8 Forward Section Layup on Aluminum Mandrel

Validation

To validate the structural integrity of the launch vehicle, each critical structural component was analyzed to determine the Factor of Safety. Other critical flight phases will be further details in the CONOPS section.

Table 3 Structural Analysis

P/N	Component	Event	Load (N)	FoS	Method of Analysis
SR18-AF-00-001	Aft Fuselage	Ignition	8034	9	FEA Explicit Dynamic
SR18-AF-02-003	Thrust Ring	Ignition	8034	4.4	Rated Strength
SR18-AF-00-006A	Center Rings	Ignition	8034	17.2	Lap Shear Strength
SR18-PA-01-012	Payload Bulkhead	Ignition	8034	8.2	FEA Explicit Dynamic
SR18-FR-00-05	Fuselage Screw	Ignition	8034	4.5	Screw Shear
SR18-FR-00-001	Rail	Ignition	8034	14	Rated Strength

C. Avionics

Requirements

The avionics systems onboard Supersonice shall meet both the SA Cup - IREC requirements as well as the internal requirements and specifications.

(Design, Test, & Evaluation Guide)

3.1 Dual-Event Parachute and Parafoil Recovery
3.1.1 Initial Deployment Event
3.1.2 Main Deployment Event
3.3 Redundant Electronics
3.3.1 Redundant COTS Recovery Electronics
3.3.2 Dissimilar Redundant Recovery Electronics

3.4 Safety Critical Wiring
3.4.1 Cable Management
3.4.2 Secure Connections
3.5 Recovery System Energetic Devices
4.1 Energetic Device Safing and Arming
4.1.1 Arming Device Access
4.1.2 Arming Device Location
(Rules and Regulations)
2.4 Range Tracking
2.5 Official Altitude Logging

Design Overview

The Altus Metrum Telemetrum is used in the rocket as the primary deployment device, and a PerfectFlite StratoLogger SL100 Altimeter is used as the redundant system. (3.3, 3.3.1) Each device is set to fire the drogue system at apogee event and the main deployment system at 755 feet AGL. (3.1, 3.1.1, 3.1.2) Both the Telemetrum and the Stratologger devices are COTS flight computers and will record flight data including Apogee. (2.5) Both the Telemetrum and the Stratologger devices are NOT modified and will be used as per manufacturer's recommendations and guidelines. (3.3.2)

The Telemetrum has its own 3.7V Li-Po battery to power its sensors and a standard 9V battery to fire the recovery systems. The stratologger will have its own standard 9V battery to power itself and the recovery firing systems. Each device has its own switch that can be physically activated/deactivated from outside the rocket easily and efficiently. (3.5, 4.1, 4.1.1, 4.1.2)

The wiring of each device going to each of the two recovery systems has its own shunt system. This will allow the recovery systems to not be armed until the physical pin is removed from the rocket. (3.5, 4.1, 4.1.1, 4.1.2) All the wiring is done with accordance to the guidelines of the competition. (3.4.1, 3.4.2)

The Telemetrum features a transmitting telemetry RF signal at 434 MHz that will be used to locate and track the movement of the rocket. (2.4) A Remove Before Flight (RBF) module with snap action switches and 3D printed guides serve as a safing mechanism for the recovery system and power switches for each avionic system. Below is a system overview of the onboard avionics systems.

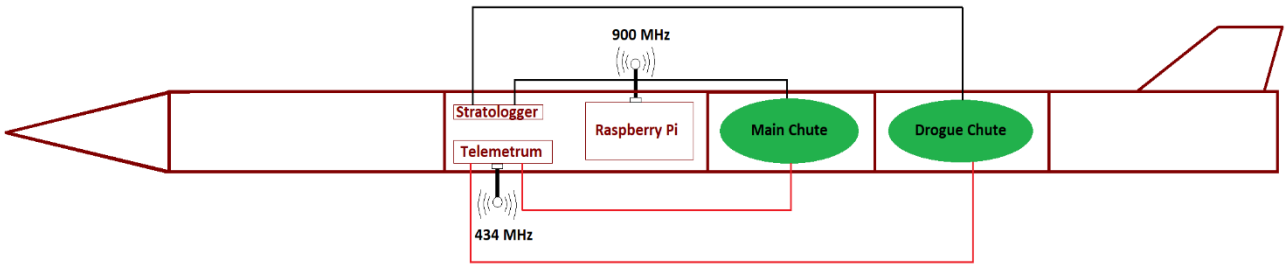

Fig. 9 Overview of the Avionics Systems

***Note that this is not a representation of the structure and look of the rocket, simply a rough figure showing the deployment firing systems boards are not connected.*

As depicted in the Fig. 9, there will also be a Raspberry Pi 3 Model B onboard with RF capabilities. We have chosen to do so to have a custom-made system transmitting telemetry using a few sensors. This system will also use the data to do some processing onboard that will predict the apogee in real time. The sensors and devices connected to the Raspberry Pi 3:

1. Adafruit Ultimate GPS breakout V3.
2. MPL3115A2 I2C Barometric Pressure/Altitude/Temperature Sensor
3. Pololu AltIMU-10 V5 Gyroscope and Accelerometer LSM6DS33, Magnetometer LIS3MDL
4. RFD 900+ RF Transceiver with 2 Dipole Antennas

The callsign used with these frequencies is: KM6TKP registered with FRN number: 0027529932 to Anania Yeghikian. This is an American callsign associated with a Technician class amateur radio licence. Each of these devices have been picked to withstand the forces of flight as well as the temperature changes that the vehicle will encounter. The main goal of this system is to create a modular device that can hold various sensors that are not dependent on one another. This method is meant to be a foundation which allows future students to swap sensors and implement them to use in the way that they choose.

All the sensors will be connected to the Pi by means of a PCB shield with headers. The connection will be solid without a need for any wiring. The RFD transceiver is an exception as it will be connected to the Pi via USB. A portable power bank will power the Pi via micro-USB connection and the Pi in turn will supply all the power to the sensors. Data will be recorded onto a micro-SD card and some (speed, location, etc) of it will be transmitted to a ground station computer. All USB and SD card connections will be securely fastened to prevent them from disconnecting. Below is a 3D image of the avionics bay.

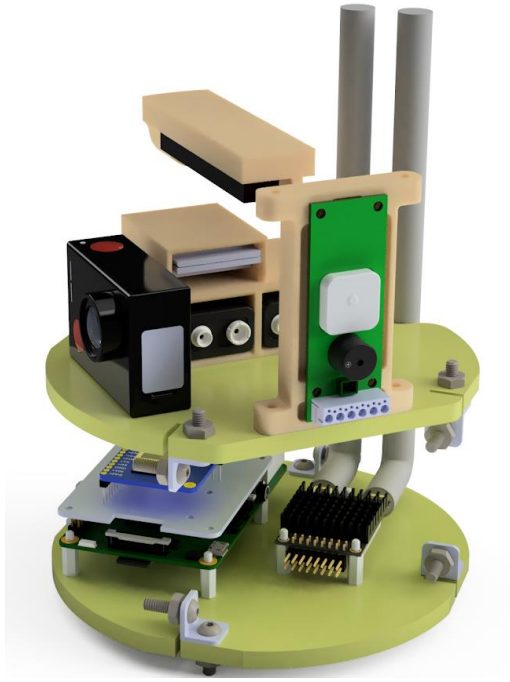

Fig. 10 3D Image of the avionics bay and its components

The avionics systems will undergo various testing including deployment, telemetry and range. The Telemetrum and Stratologger will be tested in high power rockets, going to altitudes from 1000 feet to 3000 feet and more while experiencing between 4g and 20g with possibly speeds over Mach 1. Vacuum tests will also be done prior to flights to ensure proper functionality of the firing systems of the boards. The devices will be carried onboard a drone and flown away from the ground station to test the maximum range of the connection to better prepare and set expectation for the competition. The Pi will undergo heavy programming loads to ensure it can handle a lower load during flight as well as staying within the power consumption rate expected.

D. Recovery

Requirements

(SAC Rules & Requirements)

3.1 Dual-Event Parachute and Parafoil Recovery
3.1.1 Initial Deployment Event
3.1.2 Main Deployment Event
3.1.3 Ejection Gas Protection
3.1.4 Parachute Swivel Links
3.1.5 Parachute Coloration and Marking

3.6.1 Ground Test Demonstration
4.1 Energetic Device Safing and Arming
6.2.1 Material Selection
6.2.2 Load Bearing Eye Bolts and U-Bolts

(Internal Requirements)

1. Bulkheads, eye bolts, and shock cords must be able to withstand the impulse generated by the deployment of the parachutes with a minimum factor of safety of 1.5.
2. The rocket must not separate before drogue deployment.
3. Main parachute must be retained in the forward section until it reaches an altitude of 755 ft.
4. The deployment system must be redundant. Meaning that a completely independent backup system must be able to deploy the parachutes in the case the main system fails. Completely independent is defined as a system that runs on its own flight computer, own battery and works regardless of the state of the other system.

Design Overview

The recovery device is a two-parachute system, which will be deployed at apogee and at 755 ft. AGL. At apogee, the drogue parachute (4, Recovery IPC) will be released by decoupling the rocket via chamber pressurization using a CO_2 canister (1, Recovery IPC). The main parachute (6, Recovery IPC) is released using a tender descender system where the deployment is triggered via a pyro system containing black powder (NI).

All deployment events are actuated by the avionic systems when target altitudes are reached. An E-Match will ignite a black powder charge to puncture a CO_2 canister. The gases released will generate pressure on the bulkheads causing a breach allowing the drogue parachute to evacuate. The piston bulkhead (5, Recovery IPC) serves to lessen the pressurized volume to optimize the ejection force. At 755ft, an E-Match will ignite black powder in a separate enclosure which will trigger the tender descender, allowing the main parachute to evacuate.

This design features 2 parachute deployments, but with only one decoupling. This allows all avionics to be installed in one location and improved safety. All components are designed with a minimum factor of safety of 1.5. Furthermore, double canisters and tender descenders are employed for redundancy. Spacers are also used to prevent the shock cords from damaging the fuselage due to deployment forces.

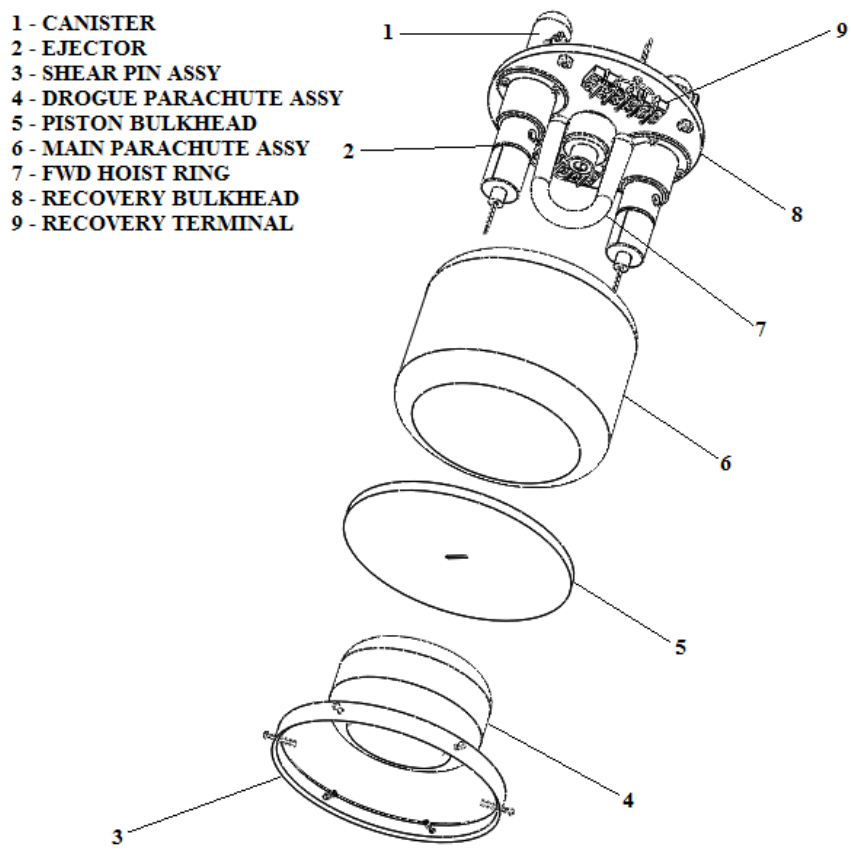

Fig. 11 Recovery System IPC

Parachute Selection

The requirements state that under the drogue parachute, the rocket's speed should be between 21.3-46 m/s, and under the main parachute, the speed should be below 9 m/s. The speed was found by rearranging Newton's laws and the drag equation:

$$\frac{1}{2}\rho {v_f}^2 C_D A_D - m a_g = 0 \tag{1}$$

$$v_f = \sqrt{\frac{2 m a_g}{\rho C_D A_D}} \tag{2}$$

The selected drogue chute is the 30" elliptical from Fruity Chutes. The speed under the drogue parachute at 30,000 ft. with a 27 kg load is 41.1 m/s. The selected main parachute is the 72" Iris Ultra, also from Fruity Chutes. The speed under this main parachute AGL with a 27.2 kg load is 8.6m /s. Both parachutes were chosen due their availability in the Space Concordia inventory, and their designed properties.

Drag Forces (Number of Shear Pins)

The drag difference between the forward and the aft puts stress on the shear pins in the coupler. Thus, their number must be sufficient to resist these forces, but be broken at apogee. The difference in force was found using the drag force equation.

$$\Delta F_D = \frac{1}{2}\rho {v_f}^2 (C_D A_{DF} - C_D A_{DA}) \tag{3}$$

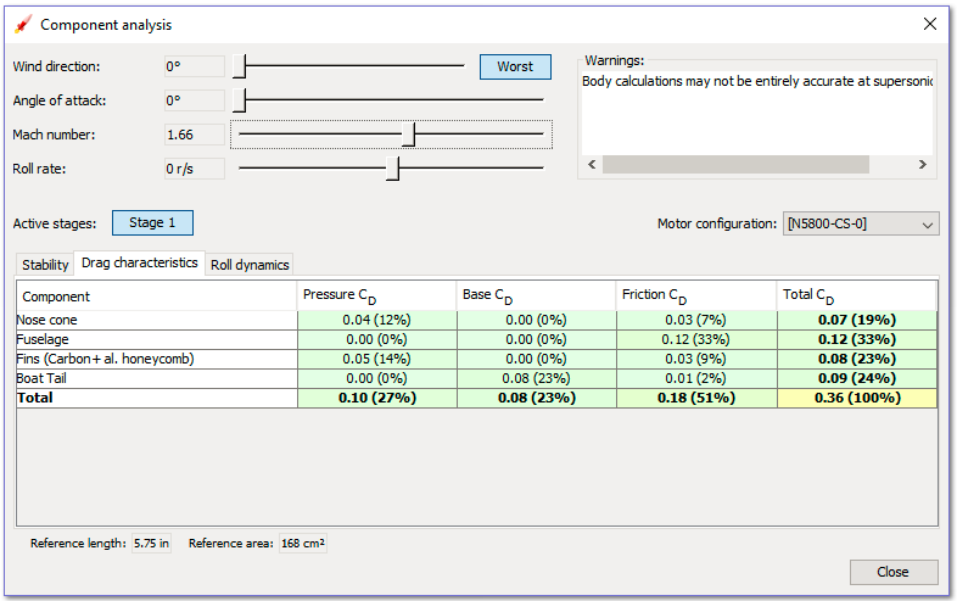

Component	Pressure C_D	Base C_D	Friction C_D	Total C_D
Nose cone	0.04 (12%)	0.00 (0%)	0.03 (7%)	**0.07 (19%)**
Fuselage	0.00 (0%)	0.00 (0%)	0.12 (33%)	**0.12 (33%)**
Fins (Carbon+al. honeycomb)	0.05 (14%)	0.00 (0%)	0.03 (9%)	**0.08 (23%)**
Boat Tail	0.00 (0%)	0.08 (23%)	0.01 (2%)	**0.09 (24%)**
Total	**0.10 (27%)**	**0.08 (23%)**	**0.18 (51%)**	**0.36 (100%)**

Fig. 12 Drag Data

The data above was used to find the area drag coefficient of the forward section (0.066 m^2) and of the aft (0.068 m^2). The air density was taken at the estimated motor burnout altitude, 3962 ft. Applying the above equation to both sections of the rocket, the net force was found to be 376N. The forward and aft sections will be held together by six shear pins, needing a total force of 570N to break. Therefore, the shear pins chosen are adequate (FoS 1.52), as the rocket will not separate due to the drag forces on the rocket. In practice, we believe that this FoS will be higher due to the fluid compression at the nose and subsonic flow at the aft.

Deployment Forces

The parachute deployment loads were found via the drag equation using the flight conditions during deployments. The force is distributed amongst the forward and the aft as a function of their weight ratio.

$$F_D = \frac{1}{2}\rho v_f C_D A_D r_w \tag{4}$$

The drogue parachute deployment was found to generate a force of 838N (310N on the AFT & 528N on the FWD), and the main parachute deployment, 1604N (594N on the AFT & 1010N on the FWD). These values were used to determine the factor of safety (FoS) for all affected parts using the heaviest load felt:

Table 4 Structural Analysis

P/N	Component	Event	Load (N)	FoS	Method of Analysis
SR18-FW-RE-01-001	Recovery Bulkhead	Main Deploy.	1010	2.5	FEA
SR18-FW-RE-01-002	Hoist Swivel	Main Deploy.	1010	4.4	Rated Strength
SR18-FW-RE-01-004	Hoist Nut	Main Deploy.	1010	74.3	Rated Strength
SR18-FW-RE-01-006	4 x Bulkhead Screw	Main Deploy.	252.5	15.3	Rated Strength
SR18-FW-RE-01-007	4 x Bulkhead Nut	Main Deploy.	252.5	91.4	Rated Strength

SR18-FW-RE-03-003	2 x Tender Descender	Drogue Deploy..	264	33.7	Rated Strength
SR18-FW-RE-03-005/ SR18-FW-RE-03-006	Shock Cords	Main Deploy.	1010	15.9	Rated Strength
SR18-FW-RE-03-007	Quicklink	Main Deploy.	1010	7.8	Rated Strength

Black Powder Mass

A force of 196.2 N in needed to pierce the CO_2 canister. The following formula was used to calculate the pressure created by the detonation of FFFFG black powder (12.1579 m/K).

$$P = \frac{mR_c T a_g}{V} \tag{5}$$

The pressure generated by the detonation is 21.796 Mpa, or a force of 4395.2N yielding a factor of safety of 22. Less black powder could be used, however this calculation does not account for pressure losses or inefficiencies during detonation. Smaller amounts of powder are also harder to manipulate.

Ejection Pressure

As mentioned previously, the required force to break the Shear Pins is 570N. Using the ideal gas law and isentropic expansion formula, the pressure created can be calculated according to the following equation.

$$P_2 = \frac{nRT}{V_1}\left(\frac{V_1}{V_2}\right)^{\frac{c_p}{c_v}} \tag{6}$$

The final pressure was found to be 5,810 KPa in the recovery chamber, yielding a total force of 973 N and a safety factor of 1.7.

Shock Cord Length

The shock cord length is recommended to be three times the rocket length. Consequently, the shock cords will be 50 ft long, as per SR18-FW-RE-03, Parachute Assembly.

System Integration

The recovery system is part of the forward compartment and is attached to the Rails P/N SR18-FW-FR-00-001 via L-Brackets. The drogue parachute will be attached to both forward and aft compartments via a hoist swivel. Furthermore, 2 holes are drilled in the bulkhead for avionics wire routing.

E. Payload

The rocket is designed to accommodate a functioning payload conforming to the CubeSat standard. The experiment aims at building and further developing a slosh experiment by studying and understanding the influence of 2 types of baffles on slosh dynamics systems under varying gravity and loads. Such experimentations will provide us understanding about the behavior of fluids in space and varying effects of prominent parameters such as pressure, temperature, velocity, etcetera on fluids. The experiment is accomplished by using 3 polycarbonate transparent tanks accompanied by 2 high speed cameras mounted to record the video footage. The recorded data can further be utilized for post-flight analysis and to further understand the sloshing effect of liquid propellent in sounding rocket flight.

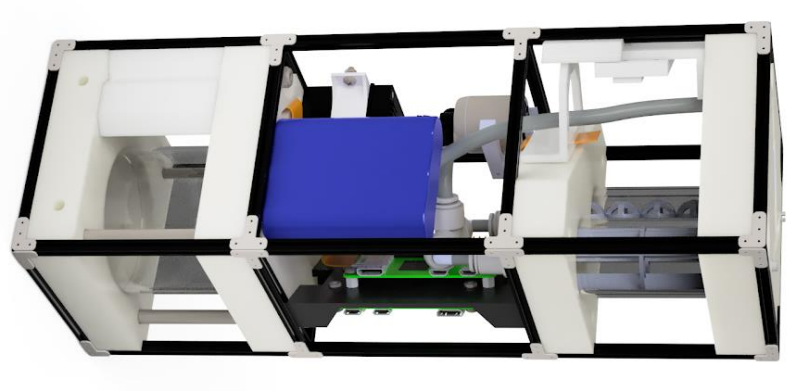

Fig. 13 Payload Assembly Internal Requirements

Requirements

Considering the IREC requirements, along with our internal Space Concordia Rocketry Division Specifications and Requirements, the below mentioned guidelines were formulated for the design of payload:

1. The payload should perform a scientific experiment.
2. It should have a minimum weight of 8.8lbs and a maximum of 10 lb.
3. It must function independent of the rocket with no interference with the vehicle's stability and performance.
4. Must not contain any form of Toxic Materials.
5. Should have a CubeSat format
6. The payload should have a maximum weight of 9.5 lb.
7. It must be Structurally sound and should withstand 17.5 G launch force
8. Should be Watertight to avoid any leakage to the other components of the rocket.
9. It should be able to take all the required electronic components such as cameras, computer board for the performance of both the experiments.

Design Overview

The Payload constitutes two separate experiments. The objective of the first experiment is the study, analyze and record the influence of two different types of baffles (Vertical baffles and Baffle balls) on sloshing phenomenon under different atmospheric conditions, varying loads and gravity forces. The two upper smaller tanks located in the top unit contain the two different types of baffles, filled with demineralized water that been mixed with two different fluorescent pigments. Both the smaller tanks are identical in shape, structure, dimensions and contain the same fluid (demineralized water) filled up to same level in the tanks. This experiment will be captured through a Pi Zero camera pointed at both tanks. The bottom bigger tank is the collector tank as the liquid drains from the upper tanks to the bottom tank during the flight. in this tank we can also see the flight effects of the two fluids mixing during flight through the color ratio between the two liquids. which will show the effects of the baffles in terms of flow rates.

The second experiment is meant to study and examine the atomized fluid motion during the supersonic flight. This allows us to study the gaseous dynamics under the effect of varying forces, pressure and velocity. This is accomplished using a spray nozzle to spray the fluid coming from the upper smaller tanks into the bottom tank with a much higher force. The spraying rate of the atomized fluid will be observed by a secondary Pi Zero camera in the bottom unit. Both experiments will be conducted before the rocket hits apogee.

The liquid (demineralized water) used for the experimentation will be mixed with fluorescent particles that glow under ultra-violet LED light to obtain better contrast footage and to facilitate the observation of liquid sloshing. Both experiments will be conducted starting from the initial launch and will record data 10 seconds after launch and before the rocket has reached apogee.

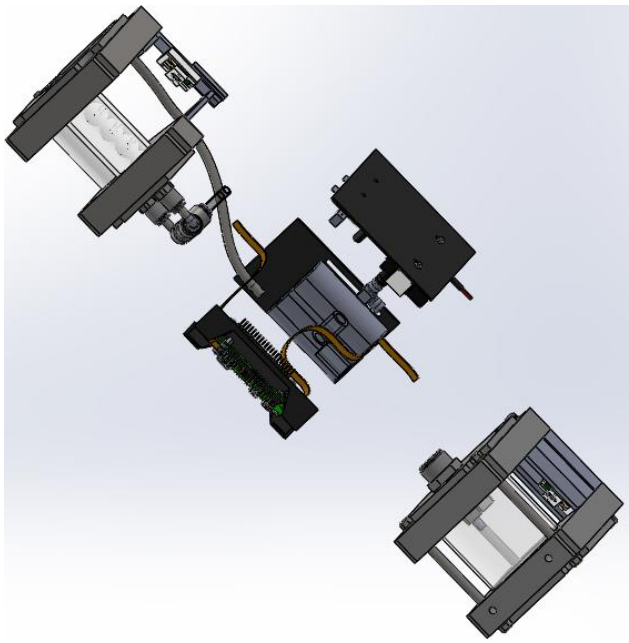

Fig. 14 Payload exploded view

Validation

1. **Performing a scientific experiment**

As specified, the motive of this payload is to test the performance of two different types of baffles in reducing the sloshing phenomenon by placing them in two identical polycarbonate smaller tanks having same dimensions. The level of the working fluid which is alcohol is maintained same in both the tanks during the starting of the experiment. The second experiments involve the study of atomized fluid motion through a spray nozzle. It will help us to study the gaseous dynamics and record the obtained data for further implications in the future.

2. **The weight requirement of 8.8 – 10 lb.**

To meet the weight requirements and to avoid any violations due to the overweight of the payload, all the materials are carefully chosen according to the design requirements. The 3 tanks (2 top and 1 bottom) are made from polycarbonate material which is lightweight and delivers the same strength and purpose which is required as per the experiment. Further, the piping is made of plastic in addition to the 4 bulkheads made of steel to meet the weight requirements. Being within the weight requirements also provides better flexibility.

3. **No interference with vehicle's stability and performance**

It is of optimum priority that payload works independent of the rocket without any sort of interference. This payload is designed in such a way that that it does not interfere with the functionality and efficiency of other systems of the rocket. Moreover, required safety measures are taken so that each sub-part of the payload does not affect the working of other sub- parts. The selection of the liquid is based on the condition that it is non- conductive and non-toxic to avoid any chances of sparks and damage which can cause any damage to the payload and further to the rocket. Moreover, the payload has its own avionics for its functioning and performance. This enables payload work independent of the rocket and if the avionics of payload encounter any sort of malfunctioning or undesirable problem (which won't happen but considering the worst cases), it will not affect the stability, functioning and performance of the other parts of the rocket and the rocket itself.

4. **CubeSat format of payload and use of non-toxic materials**

The payload should have the dimensions of 10 x 10 x 30cm. This is the standard dimensions for the CubeSat (3U) and this is according to the rules of the competition for payload. Keeping the dimensions of the payload strictly as per

the directions of the competition is our main priority and this is taken care by using metric extrusions, which helped us to make a frame of specified dimensions. In addition to that, selection of size of all the components to be used in the payload including the piping arrangement was with respect to the CubeSat format of the payload. Hence, pre-planning and calculative manufacturing of all the payload parts helped us to remain within the desired dimensions of final payload.

It is well taken care of that there is no use of toxic element of any form within the payload no matter what purpose it may serve. This is as per the rules of the competition. The liquid which is used to conduct the 2 experiments is also carefully chosen after detailed study of its properties both physical and chemical. It is important to avoid the use of toxic things in the payload as it possess great danger to the internal parts of the payload and then further to the rocket in worst cases.

5. It should be structurally sound and watertight

This is one of the most prominent factor that affects the performance and working of the payload. The more structurally sound a system is, the more is its output and lesser are the chances of any failure or malfunctioning. The payload is designed to withstand 17.5G's to conserve the structural integrity of the payload. Hence, specified tests are conducted using the shaker table for vibration testing to ensure that payload do not add unwanted vibrations to the rocket. This is taken care of by using self-locking nylon nuts for securing bulkheads together. Also, strong materials with high impact strength and the ones which can withstand maximum loads such as steels, aluminum, polycarbonate and plastics are being used for numerous specified purpose to impart strength to the payload. This will help the payload withstand worst conditions and still function and perform its task as desired. Moreover, sensitive and important components such as Avionics and cameras are fitted and adjusted with care to avoid getting detached and thus damaging the payload.

Also, to ensure that there is no leakage from the payload or within the payload subsystems due to the flow of the fluid under varying pressure and temperature conditions, redundant sealing of the parts wherever necessary is done. For instance, compressed gaskets are being used to avoid leakage of fluid. In addition to that, O-rings are also used to take every preventive measure to avoid any problem that the payload may encounter during the flight.

IV. Mission Concept of Operations Overview

The launch vehicle flight phase analysis is organized into six separate phases, which outlines the worst conditions encountered at each stage. A governing safety factor is determined to validate the vehicle's integrity at each stage.

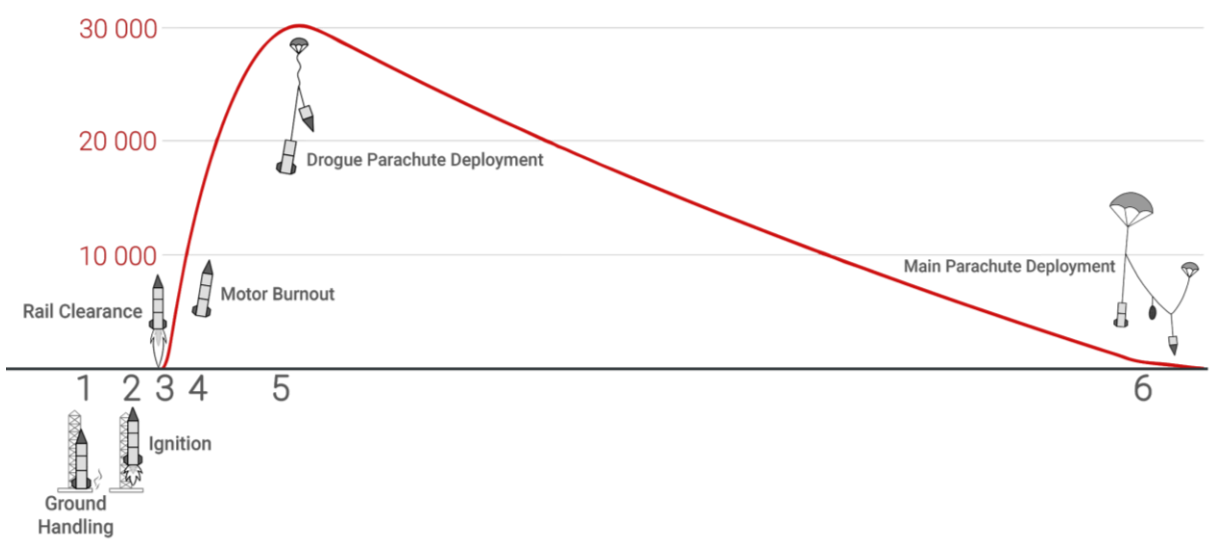

Fig. 15 Flight Phase Graph

A. **Phase 0: Ground Handling**

As the rocket sits statically on the launch rod, the lugs support the vehicle's full weight. The lugs must therefore be analyzed for worst case scenario, which considers a vertical launch rod. Thus, the reactions at the bottom lug and top lug were calculated, and a safety factor of 9.3 was found. Although this factor of safety is very high, its consideration comprises an important portion of the flight's nominal operation.

B. **Phase 1: Motor Ignition**

The ignition of the motor creates a large initial shock on the system. This has a maximum force of 8034N. The force is handled by the motor block and thus, the motor block must be analyzed with respect to this initial force. Thus an FEA model was built in ANSYS consisting of the assembly of the aft section was conducted, where the maximum thrust was applied to the motor block and boat tail. The resulting safety factor for the correct operation of the vehicle was 7.8. This section is considered safe, as it last year's rocket was made of the same composites, thus has flight heritage.

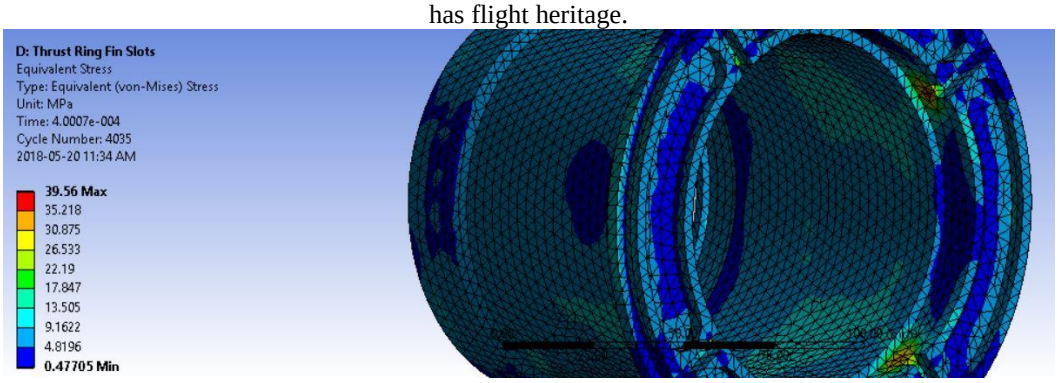

Figure 17. ANSYS Explicit Dynamic Simulation

C. **Phase 2: Launch Rod Clearance**

When the rocket leaves the rod, it encounters two issues: the tendency of the rocket to be unstable at low velocities and high wind speeds and the risk the lugs may detach from the rocket. Both these conditions are considered at the maximum wind condition (8.33 m/s).

A minimum dynamic stability caliber was calculated to give a safety factor of 2.7. A one kilogram ballast can be removed or added to accommodate varying wind conditions. The dynamic forces on the launch lugs caused by the high wind speeds were within operational limits of the vehicle, after calculations were conducted.

D. **Phase 3: Maximum Dynamic Pressure**

The third phase begin right before motor burnout, at maximum velocity. At this point in flight, the rocket has reached transonic speeds (Mach 1.7). Due to these high speeds, the rocket's dynamic pressure is at a maximum of 930 N. At this point, fin flutter is most likely to occur. Using the NACA TN-4197 equation, a flutter velocity of 693 m/s was found, which, given the ANSYS analysis performed previously demonstrates the equation to be conservative, thus validating the fins at a safety factor of 4.8. Additionally, the honeycomb fins are part of the many components with flight heritage.

E. **Phase 4: Drogue Deployment**

On drogue deployment, a shock will travel through several components, including the parachute swivel, shock cord, quick link, eye bolt, shear pins, and bulkhead. These components' rated strengths were compared with the ejection shock force of 167N. A governing safety factor was given by the array of 6 shear pins, meant to withstand only the shock of the drogue chute, to avoid deployment of the main chute at apogee. To simulate worst case conditions, the force of shock for the drogue was calculated for the rocket after 4 seconds of freefall. This allows ample time for the deployment system to notice a change in pressure due to altitude.

F. **Phase 5: Main Deployment**

As the rocket, falls below 755 ft, the deployment of the main parachute will be triggered, thus shearing the nylon screws, and ejecting the main chute. The shock of the main deployment, considered the second largest load to act on the launch vehicle, was calculated to 1604 N. Once again, structural components were analyzed, and the

forward recovery bulkhead assembly was analyzed in ANSYS resulting in a safety factor of 2.5.

IV. Conclusions and Lessons Learned

This has been one of the most ambitious projects conducted by Space Concordia's rocketry team, with many "firsts". We are very proud of our team and accomplishments this year. In order to achieve all these milestones, we were required to find workarounds to multiple problems. Due to our annual budget ($11,000), we were required to manufacture every single mechanical component in house. This meant we had to learn to use new manufacturing techniques that we have never used before such as CNC machining and complex AFP layup in parallel with improving our previous techniques of hand layups and manual machining. We also worked to acquire a total in-kind sponsorship value of over $45,000.

We quickly learned that to achieve our goals, we needed to adhere to a very tight and rigid development cycle. There must be a priority to projects, and sacrifices might need to be made to achieve more important goals. Examples of projects that were cut this year: fall away launch lugs, transition sections, ejecting payload and downwards facing cameras. These projects, nonetheless exciting, take time away from the team that needs to focus on our fundamentals. We learned that having a strong foundation is more important than a feature-filled rocket.

We have attempted to do more than any previous iteration before us. With regards to the design, manufacturing, analysis, and performance of this rocket, the scope of this project has dwarfed anything that has come before. The ambition, dedication and hard work shown by the entire team has made this a reality. We are very proud of our team and accomplishments this year. We look forward to launching our rocket at Spaceport America and cannot wait to apply what we learn to our future designs and further push the limit of what we are capable.

APPENDIX A: SYSTEM WEIGHTS, MEASURES, AND PERFORMANCE DATA

Spaceport America Cup

Intercollegiate Rocket Engineering Competition

Entry Form & Progress Update

Color Key	SRAD = Student Researched and Designed	v18.1

Must be completed accurately at all time. These fields mostly pertain to team identifying information and the highest-level technical information.

Should always be completed "to the team's best knowledge" , but is expected to vary with increasing accuracy / fidelity throughout the project.

May not be known until later in the project but should be completed ASAP, and must be completed accurately in the final progress report.

Date Submitted:	2018-03-23
Team ID:	79

* You will receive your Team ID after you submit your 1st project entry form.

Country:	Canada
State or Province:	Quebec

State or Province is for US and Canada

Team Information

Rocket/Project Name:	Supersonice
Student Organization Name	Space Concordia - Rocketry Division
College or University Name:	Concordia University
Preferred Informal Name:	Optional
Organization Type:	Club/Group
Project Start Date	2017-09-01
Category:	30k – COTS – All Propulsion Types

Projects are not limited on how many years they take

Member	Name	Email	Phone
Student Lead	Olivier D'Angelo	olivier.dangelo@spaceconcordia.ca	5142416115

Alt. Student Lead	Oleg Khalimonov	oleg.khalimonov@spaceconcordia.ca	5149510810
Faculty Advisor	Krzysztof Skonieczny	kskoniec@encs.concordia.ca	(514) 848-2424 ext. 3122
Alt. Faculty Adviser			

For Mailing Awards:

Payable To:	Engineering & Computer Science Student Association
Address Line 1:	1455 de Maisonneuve Ouest, H838
Address Line 2:	Montreal, QC, H3G 1M8
Address Line 3:	
Address Line 4:	
Address Line 5:	

Demographic Data

This is all members working with your project including those not attending the event. This will help ESRA and Spaceport America promote the event and get more sponsorships and grants to help the teams and improve the event.

Number of team members

High School	0	Male	20
Under grad	22	Female	2
Masters	0	Veterans	0
PhD	0	NAR or Tripoli	5

Just a reminder the you are not required to have a NAR, Tripoli member on your team. If your country has an equivelant organization to NAR or Tripoli, you can cant them in the NAR or Tripoli box. CAR from Canada is an example.

STEM Outreach Events

If you perform any STEM related outreach events, please place a brief description here.
STEM stands for Science, Technology, Engineering, and Mathematics.
Presentation for FIRST Robotics Competition to promote STEM Education

Rocket Information

Overall rocket parameters:

	Measurement	Additional Comments (Optional)
Airframe Length (inches):	120	

Airframe Diameter (inches):	6	
Fin-span (inches):	5	
Vehicle weight (pounds):	36.49	
Propellent weight (pounds):	32.69	
Payload weight (pounds):	8.8	
Liftoff weight (pounds):	77.98	
Number of stages:	1	
Strap-on Booster Cluster:	No	
Propulsion Type:	Solid	
Propulsion Manufacturer:	Commercial	
Kinetic Energy Dart:	No	

Propulsion Systems: (Stage: Manufacturer, Motor, Letter Class, Total Impulse)

```
1st Stage: Cesaroni Pro 98, 20146N5800-P, N Class, 20145.7 Ns
```

Total Impulse of all Motors:	20145.7	(Ns)

Predicted Flight Data and Analysis

The following stats should be calculated using rocket trajectory software or by hand.

Pro Tip: Reference the Barrowman Equations, know what they are, and know how to use them.

	Measurement	Additional Comments (Optional)
Launch Rail:	ESRA Provide Rail	
Rail Length (feet):	17	
Liftoff Thrust-Weight Ratio:	15.55877461	
Launch Rail Departure Velocity (feet/second):	160.7	
Minimum Static Margin During Boost:	3	*Between rail departure and burnout
Maximum Acceleration (G):	21.4	
Maximum Velocity (feet/second):	1901	
Target Apogee (feet AGL):	30K	
Predicted Apogee (feet AGL):	30420	

Payload Information

Payload Description:

This year's payload submission is a functional fluid slosh experiment. It is designed to simulate a liquid fuel rocket engine, where the mixing of oxidizer and fuel will be observed qualitatively with the eventually objective of constructing a student built, liquid fuel engine. There will be two upper tanks both filled with isopropyl alcohol. One of the tanks will contain baffles designed to limit fluid slosh, while the second upper tank will not have baffles to act as a control. To help observe mixing, both tanks will be dyed different flourescent colours. At the moment of motor ignition, the upper tanks will be drained into a single lower tank with a small pump. The tanks and the tubing will be clear, so that the fluid may be observed during the whole process. The payload will remain in the rocket forward section during rocket launch and recovery.

Recovery Information

The recovery device is dual parachute system which will be deployed at apogee using a barometric sensor and at 700 ft. AGL. At apogee, the drogue parachute will be released by decoupling the rocket via chamber pressurization with a CO2 canister. The main parachute deployment is triggered via barometric sensor from the avionics system. It is deployed by ejecting the bulkhead cap via chamber pressurization with another CO2 canister.

An E-Match will ignite a 0.2 grams of black powder to puncture a CO2 canister. The gases released will generate pressure on the bulkheads causing a breach for the parachutes to evacuate.

This design features 2 parachute deployments, but with only one decoupling. This allows all avionics to be installed in one location, and improved safety. All components are designed with a minimum factor of safety of 2.

Planned Tests

* Please keep brief

Date	Type	Description	Status	Comments
11-26-17	Ground	Recovery System Activation Test	Successful	Activate E-match to test piercing of canister
12-28-17	Ground	Avionics Deployment Activation Testing	TBD	Trigger avionics system deployment using vacuum sealed chamber
12-1-17	Ground	Payload Leak Testing	Minor Issues	Flowrate was constricted due to lack of air intake
1-10-18	Ground	Glass/PET fuselage bending/Compression test	Successful	Test fuselage thermoplastic sample in bending and compression

4-1-18	Ground	Ground Deployement Test	Minor Issues	Test deployments of parachute from within the fuselage, on the ground
2-15-18	Ground	Payload Waterpump testing	Successful	Minor leaks were found and are being worked on
2-16-18	Ground	Avionics GPS Tracking Test	Successful	test gps accuracy and data feed
4-4-18	Ground	Ultrasonic Inspection on AFP Nosecone Fuselage	TBD	Test advanced composite component for damage
4-10-18	Ground	Payload Modal Testing	TBD	Test assembly on a shaker table to define natural frequencies

APPENDIX B: PROJECT TEST REPORTS

Test Report Subject
Recovery Ground Test

Approvals:

Function	Signature	Date
Prepared by:	M. Hoang-Cao	5/24/2018
Approved by:	O. D'angelo	5/24/2018

Revision History

Date	Revision #	Change
5/24/2018	0	Initial Release

Abstract

As part of the Supersonice Rocket technical package, this report outlines a vertical stationary ground test of the drogue deployment's fuselage separation, as well as the deployment of the main parachute. Both deployments were a success. The tests confirm the functionality of the system and gives confidence in the design.

1 Introduction

This report summarizes observations and analysis of the recovery system ground testing which occurred on the 7 & 23 May 2018. This test is part of the technical package for the ESRA 2018 competition.

2 Test Configuration

This test was done in parts A & B: a pull test for the main parachute deployment, and an ejection test for the drogue parachute deployment.

Part A – Main Parachute Pull Test

The parachute assembly was packed as per SR18-FW-RE-03, Parachute Assy [1], minus the pyrotechnics, and ejection components of the assembly. The FWD shock cord was fixed in place and the AFT shock cord was manually pulled in order to simulate the deployment sequence of the parachute.

Figure 1 - Part A Test Set Up

Part B – Ejection Test

For the ejection test, the FWD and AFT held together by 6 shear pins, and inside the fuselage, was the SR18-FW-RE-01, Recovery Bulkhead Assy [2] and the SR18-FW-RE-03, Parachute Assy [1]. The ejector was activated via command wire detonation.

The recovery preflight checklist (see Annex) was followed for this test.

Figure 2 - Part B Test Set Up

3 Resutls

The tests were captured by videos (see Ref [3] & [4]). The tests are summarized below:

Table 5 – Test Results

TEST	RESULT	PICTURE
PART A – MAIN PARACHUTE PULL TEST	SUCCESS	
PART B – EJECTION TEST	SUCCESS	

4 Conclusions and Recommendations

These tests have allowed us to confirm that the recovery system is functional, and suitable for flight on Supersonice.

5 References

[1] Space Concordia, "SR18-FW-RE-03, Parachute Assy," 2018.
[2] Space Concordia, "SR18-FW-RE-01, Recovery Bulkhead Assy," 2018.
[3] Space Concordia, *SR18-FW-RE-RPT01A, Main Parachute Pull Test,* 2018.
[4] Space Concordia, *SR18-FW-RE-RPT01B, Ejection Test,* 2018.

6 Annex

RECOVERY PREFLIGHT CHECKLIST

PARACHUTE ASSY			
		ASSY	
	FOLD PARACHUTES		
	PACK PARACHUTE BAGS		
	PACK SHOCK CHORDS TO BAG		
	ENSURE QUICK LINKS ARE LOCKED		
	CLOSE PARACHUTE BAGS		
	SECURE SHOCK CHORDS TO HOIST RINGS		
TENDER DESCENDER			
		PRM	SEC
	CHECK E-MATCH RESISTANCE 1.4Ω AND CONTINUITY		
	REMOVE E-MATCH GUARD		
	CUT TO 9 INCHES AND EXPOSE LEADS		
	FEED THROUGH TENDER DESCENDER		
	SOLDER TERMINAL LUGS		
	SHORT E-MATCH LEADS		
	FILL TENDER DESCENDER WITH BLACK POWDER		
	ASSEMBLE WITH QUICK LINKS AND CAP		
	ATTACH TENDER DESCENDER TO ASSEMBLY		
EJECTOR ASSEMBLY			
		PRM	SEC
	CHECK ALL E-MATCH RESISTANCE 1.4Ω AND CONTINUITY		
	CUT TO 7 INCHES AND EXPOSE LEADS		
	TRIM E-MATCH GUARD CAP ¾ OF THE WAY		
	FEED THROUGH BUSHING AND HOUSING		
	SOLDER TERMINAL LUGS		
	SHORT E-MATCH LEADS		
	FILL BUSHING WITH BLACK POWDER		
	INSERT NEEDLE WITH BUSING IN HOUSING		
	SCREW ON TO BASE, SEAL WITH TEFLON TAPE		
	INSERT CANISTERS, SEAL WITH TEFLON TAPE		
GENERAL			
		ASSY	
	FIX TERMINAL LUGS TO TERMINAL		
	CHECK ALL E-MATCH RESISTANCE 1.4Ω AND CONTINUITY		
	CHECK HOIST SWIVEL CLEARANCE		
	SECURE WIRING		
	TEFLON TAPE AROUND RECOVERY BULKHEAD		

THIS PAGE WAS INTENTIONALLY LEFT BLANK

THIS PAGE WAS INTENTIONALLY LEFT BLANK

APPENDIX C: HAZARD & RISK ASSESSEMENT

Hazard	Possible Causes	Risk of Mishap and Rationale	Mitigation Approach	Risk of Injury after Mitigation
Explosion of Solid Rocket Propellant motor	Cracks in propellant grain	Low; Commercial motor with proven reliability is being used	Follow all instructions carefully	Very Low
	Propellant chunks breaking off and blocking the nozzle			
	Motor case fails under normal operation		Double-check steps as assembly progresses	
	Failure of motor closures			
Main parachute deploys at the maximum altitude	Failure of the shear pins by motor forces	Medium; Multiple possible modes of failure. Some features have not yet been tested by the team	Test shear pins to confirm shear strength	Low
	Payload section is pressurized by CO2 recovery system		Verify exhaustless Peregrine caps are used for deployment of Drogue	
			Place relief holes near the Peregrine systems for the Drogue	
	Shear pins damaged before launch		Avoid twisting and bending rocket during transport	
			Designate all handling points aft of the coupler that is held together with shear pins	
	Some shear pins are omitted during assembly		Use proper checklists and assembly procedures	
	Software Error		Compare software with other software	

			Test computer in a test rocket for validation	
Partial deployment of recovery system	Failure of computer after drogue deployment shock	Medium; possibility of large deployment shock if strong winds are present, Avionics bay attached to rods bearing all deployment shock loads	Careful vibration analysis of avionics bay	Low
	Failure of computer power after drogue deployment shock		Use of approved wiring and connectors only. All connections verified pre-flight for integrity	
	Wires to deployment system (Peregrine) disconnected after drogue Deployment shock			
Recovery system completely fails to deploy	Failure of computer through software error	Medium; possibility of long wait on the pad	Thoroughly test the computer with test flights	Low
	Failure computer due to mechanical failure of PCB or avionics bay		Carefully analyse the components at risk.	
	Batteries run out of power before launch		Assure that the batteries can last for a wait on the pad of at least 3 hours	
Recovery system deploys while the rocket is still being handled by team members	Static electricity builds up and fires Peregrine system	Medium; Rocket is being used in a dry and hot environment	Keep all wires shunted before complete arming	Low
			Wear proper safety apparel and follow safety regulations while arming	
	CO2 canisters heat above 50 degrees Celsius and could possibly explode		Discontinue operations if outside temperature goes above 50 degrees	
Rocket Detaches from rail during	Failure of either for or aft rail guide during	Low; relatively low forces are being	Analyzed all bolted connections.	Low. Very high factor of safety:

mounting, possibly injuring team members working at the pad (Phase 0 failure)	mounting	applied at this stage	Selected proper fasteners for given load.	71
Failure of rocket structure at ignition, potentially creating fast moving debris (Phase 1 failure)	Failure of internal motor mount	Medium; Highest flight forces are applied at this point.	FEA performed on the critically loaded components	Low: High factor of safety: 7.8
			Generous application of epoxy fillets	
			Testing the critically loaded sections at maximum flight loads	
Deviation of flight path when the rocket clears the launch rod, potentially creating a hazard to personnel and property (Phase 2 failure)	High winds cause instability at launch	Medium; Possibility of strong winds at the launch site	Limit maximum wind speed at launch to 8.33 m/s	Low: High factor of safety: 28
			Sufficiently high static margin of stability	
	Lug failure due to high moments induced by high winds		Analysis performed on the critically loaded components	
Failure of rocket fins at maximum dynamic pressure, potentially causing the destruction of the vehicle and creating dangerous debris (Phase 3 failure)	Fins fail in fin-flutter	Medium; Rocket passes through transonic region relatively quickly, reducing turbulence window	Proper analysis of fins with NACA TN 4197 (conservative estimate)	High: Low factor of safety: 1.7
			Fins reinforced with 3 carbon fiber tip-to-tip layup	

Failure of Structure at Drogue Deployment, potentially causing the destruction of the vehicle and creating dangerous debris (Phase 4 failure)	Hoop stress causes failure of fuselage	Low; Forces involved are not very large, case assumes scenario with highest possible wind and late deployment	Comprehensive analysis of all loaded components by hand and with FEA	Low; Factor of safety: 2.8
	Deployment shock causes failure of structural components		Careful selection of materials to withstand forces	
Failure of the SRAD recovery system (Phase 4 Failure)	The piston fails to pierce the CO2 canister, caused by the needle inaccurately hitting the center of the canister	Low: Force required is very small	Several tests were performed to prove the prototypes success, redundant commercial backup is installed as failsafe	Low; Factor of safety: 3.6
Failure of structure at main parachute deployment, potentially causing the destruction of the vehicle and creating dangerous debris (Phase 5 Failure)	Hoop stress causes failure of fuselage	Medium-High: Large forces are involved	Comprehensive analysis of all loaded components by hand and with FEA	Medium: acceptable, yet still not high factor of safety: 1.6
	Deployment shock causes failure of structural components		Careful selection of materials to withstand forces	

Recovery System

Possible Mode of Failure	Severity	Tests	Contingency Plan	Results & Changes
Weighted collar isn't triggered by recovery	-Pitot functions - Retraction failure	Test in rocket	-Increase collar weight and lubricity	Test Successful

Weighted Collar wedges on nosecone	-Possible retraction failure	Test in retraction in nosecone	-elongate sliding distance -reduce outer diameter of collar	Test Successful No changes necessary
3D printed Capsule is torn by tension	-Data lost - Retraction failure	Run tensile strength tests printed samples with same print settings	-improve material selection -modify geometry to be stronger	Capsule geometry was changed to account for print shrinkage (current capsule fully functional)
Rigidity of latches prevent quick release	-Pitot functions - Retraction failure	Assemble mechanism and test	-Decrease thickness of latches -Use different material	Test Successful (materials & geometry still optimised)
Latches wedge collar in place	-Pitot functions - Retraction failure	Assemble and test mechanism and test	-Increase lubricity -Increase clearance between latches and collar	Test Successful (clearance still increased)
Wires from PCB Capsule wedge capsule in place	-Possible retraction failure	Test in retraction in nosecone	-Arrange ribbon cable in coil around sensor shaft/extrusion	Wire management successful and implemented
Weighted collar triggered prematurely by rocket deceleration	-Data cut short -Pitot recovered	-Test in rocket and check data - Test rocket deceleration impulse on mechanism with jig	-Include shear pin that fails at recovery impulse	Tests Successful in jig, further tests in rocket planned
Vibrations amplified by sliding member could spoil data	-Data may be erroneous	-Test in rocket -Test in wind tunnel	-Reduce clearance between shaft and pitot tube -Use vibration dampening materials	Test Successful Data smooth
Stuctural failure (compressive or tensile)	-Possible retraction failure	Compressive and Tensile strength tests	Inspect point of failure and improve design	Tests successful at 1.5 times expected stress

Payload System

Risk	Possible cause	Consequence	Mitigation plan
Fluid Leak	Improper Sealing Tank Cracks	Damaged Avionics Camera Bay Shoutout	Compressed Sealing Gaskets Fluid: Isopropyl Alcohol Nonconductive
Structural Failure	Weak Nanobeam Structure	Damaged Avionics Damage to Rocket Interior	Additional structural support: plate mounts
Experiment Incomplete	Solenoid Valve Fails Pump Fails Power Failure	Data Loss Incomplete Experiment	Data gathered by slosh experiment in upper tanks constitutes experiment
Pressure Differential	Change in temperature and pressure at 30000 feet	Leaking of liquid causing a short circuit of electrical components	Sealing of tanks and securing piping to structure
Electrical malfunction	Loose connection Component malfunction (pump/solenoid)	No data collection Experiment fails to run	Attach connections to structure to avoid disconnection or vibration shear

APPENDIX D: ASSEMBLY, PREFLIGHT, AND LAUNCH CHECKLISTS

1. RECOVERY

1.1. PARACHUTE ASSY

	FOLD PARACHUTES
	PACK PARACHUTE BAGS
	PACK SHOCK CHORDS TO BAG
	ENSURE QUICK LINKS ARE LOCKED
	CLOSE PARACHUTE BAGS

1.2. TENDER DESCENDER

	WEAR PROTECTIVE EYEWEAR WHEN DEALING WITH EXPLOSIVES
	CHECK E-MATCH RESISTANCE 1.4Ω AND CONTINUITY
	REMOVE E-MATCH GUARD
	CUT TO 9 INCHES AND EXPOSE LEADS
	FEED THROUGH TENDER DESCENDER
	SOLDER TERMINAL LUGS
	SHORT E-MATCH LEADS
	FILL TENDER DESCENDER WITH BLACK POWDER
	ASSEMBLE WITH QUICK LINKS AND BLASTING CAP

1.3. EJECTOR ASSY

	WEAR PROTECTIVE EYEWEAR WHEN DEALING WITH EXPLOSIVES
	CHECK ALL E-MATCH RESISTANCE 1.4Ω AND CONTINUITY
	CUT TO 7 INCHES AND EXPOSE LEADS
	TRIM E-MATCH GUARD CAP ¾ OF THE WAY
	FEED THROUGH BUSHING AND HOUSING
	SOLDER TERMINAL LUGS
	SHORT E-MATCH LEADS
	FILL BUSHING WITH BLACK POWDER
	INSERT NEEDLE WITH BUSING IN HOUSING
	SCREW ON TO BASE, SEAL WITH TEFLON TAPE
	INSERT CANISTERS, SEAL WITH TEFLON TAPE

2. PAYLOAD

	FILL COMPARTMENTS WITH LIQUID

3. CAMERA BAY

	ENSURE CAMERAS ARE FULLY CHARGED
	ENSURE CAMERAS HAVE EMPTY SD CARDS

4. STRAIN GAUGES

	ENSURE STRAIN GAUGE BATTERY ARE FULLY CHARGED
	ENSURE STRAIN GAUGE HAS EMPTY SD CARDS

5. AVIONICS

	ENSURE ALL BATTERIES ARE FULLY CHARGED

	ENSURE ALL SD CARDS ARE INSTALLED AND EMPTY
	VERIFY ALL CONNECTIONS

6. MOTOR

	INSTALL MOTOR TO AFT AS PER OEM INSTRUCTION
	INSTALL SNAP RING

7. FORWARD ASSY

	INSTALL PAYLOAD ASSY TO FRAME
	INSTALL CAMERA ASSY TO FRAME
	INSTALL AVIONICS ASSY TO FRAME
	CONNECT SHOCK CORDS TO FORWARD AND AFT
	ENSURE MASTER AVIONICS SWITCH ON RECOVERY BULKHEAD IS OFF
	CONNECT POWER TO BOARDS
	WEAR PROTECTIVE EYEWEAR WHEN DEALING WITH EXPLOSIVES
	FIX TERMINAL LUGS TO TERMINAL
	CHECK ALL E-MATCH RESISTANCE 1.4Ω AND CONTINUITY
	CHECK HOIST SWIVEL CLEARANCE
	SECURE RECOVERY WIRING
	TEFLON TAPE AROUND RECOVERY BULKHEAD
	INSTALL FRAME IN FORWARD FUSELAGE
	SET UP RBF SYSTEM
	ACTIVATE MASTER AVIONICS SWITCH ON RECOVERY BULKHEAD

8. FULL ASSEMBLY

	COUPLE FORWARD AND AFT
	INSERT SHEAR PINS
	VERIFY THE TOTAL WEIGHT OF THE ROCKET (_____G)

APPENDIX E: RESEARCH REPORT

Analysis & Validation of PET Thermoplastic Composite Rocket Fuselage Manufactured by Automated Fibre Placement

Final Report

Honours Research Project – ENGR 412

By:

Olivier D'Angelo #26729916

Submitted to:

Dr. S.V. Hoa

&

Jeffrey Fortin-Simpson

Revision: 2

Date of report submission: April 16th, 2018

45

Experimental Sounding Rocket Association

Abstract

This report presents the honours research project on the analysis and validation of a glass fibre reinforced polyethylene terephthalate (PET) thermoplastic composite fuselage manufactured by automated fibre placement (AFP) machine in tandem with Concordia's Center for Composites (CONCOM) research laboratory. A buckling analysis due to pure bending and axial compression was conducted by finite element analysis (FEA) using ANSYS. The results were verified using a MATLAB script implementing a strength of materials approach and further validated by testing cylindrical shell samples in axial compression. Results indicate that the theoretical and experimental modulus agree, although the tested samples would likely fail compression due to maximum stress is more likely than non-linear buckling.

Table of Contents

List of Figures

List of Tables

List of Symbols

E_m	Matrix Elastic Modulus, Pa
G_m	Matrix Shear Modulus, Pa
E_f	Fibre Elastic Modulus, Pa
G_f	Fibre Shear Modulus, Pa
ζ	Tsai-Hill Shape Parameter
η	Correction Factor for the theoretical transverse modulus
V_f	Fibre volume fraction
E_1	Lamina elastic modulus in longitudinal direction, Pa
E_2	Lamina elastic modulus in transverse direction, Pa
G_{12}	Lamina shear modulus in longitudinal-transverse direction, Pa
ν_{12}	Lamina Poisson's Ratio in longitudinal-transverse direction
$[Q]$	Reduced stiffness matrix
$[T]$	Transformation matrix
$[\bar{Q}]$	Transformed reduced stiffness matrix
$[A]$	In-plane stiffness matrix
n	total number of laminate layers
$\bar{E}_x$	Laminate elastic modulus in x-direction, Pa
$\bar{E}_y$	Laminate elastic modulus in y-direction, Pa
$\bar{G}_{xy}$	Laminate shear modulus in xy-direction, Pa
ν_{xy}	Laminate Poisson's ratio in xy-direction
M_{cr}	Critical Bending Load, Nm
R	Inner Radius of Cylinder, m
L	length of cylinder, m
t	Thickness of laminate, m
σ_x^{cr}	Critical buckling stress, with transverse shear effects along axial direction, Pa
σ_{Euler}^{cr}	Critical Euler buckling stress for orthotropic materials, Pa
σ'	Effective stress, after knockdown factor, Pa
γ	Empirical knockdown factor derived in NASA SP-8007
P_{cr}	Critical buckling load for cylindrical shell, N
D	Drag force, N
ρ	density of flow, kg/m^3
V_∞	Flow velocity before impacting object, m/s
A	Reference area, (frontal cross-sectional area), m^2

1. Introduction

1.1. Background

Automated fibre placement (AFP) machines have increased the ease and reliability of manufacturing for composite components of complex, closed-shaped geometry while achieving accurate fibre angles and improved quality than traditional hand layup processes, common in sounding rockets [1]. For this reason, Space Concordia's sounding rocket is manufactured with the help of this advanced manufacturing technology. Previously, the fuselage was composed of APC-2 polyether ether ketone (PEEK) and AS4 carbon fibre laminated, 12 layers thick in the following sequence $[90_2 / 45 / -45 / 0_2]_S$. This resulted in a lightweight yet strong fuselage with a safety factor of 22 in buckling due to axial compression, which is conservative [2].

An alternative thermoplastic, glass fibre reinforced polyethylene terephthalate (PET), was proposed for the forward fuselage section of the sounding rocket. This material requires lower processing temperatures, allows for radio wave permeability, and results in a more affordable product when compared to PEEK thermoplastic composites. Note that for the suggested research, thermal loads due to heat transfer on the composite will be neglected, as the rocket does not spend sufficient time flying at speeds greater than Mach one to consider aerodynamic heating [3]. Given that PET/glass fibre composite have not been used before for such a structurally demanding application according to the authors knowledge, the analysis of the airframe and validation using a manufactured sample is evaluated. The scope of the analysis will consider buckling due to bending and axial compression, respectively.

1.2. Scope of Work

- Literature studies on classical lamination theory, thin-walled composite cylindrical shells subjected to axial compressive loading and pure bending, non-linear buckling analysis.
- Estimate acting loads on forward fuselage section.
- Define theoretical critical buckling and bending loads using the strength of materials approach.
- Simulate non-linear buckling in bending and axial compression.
- Test sample cylindrical specimen in axial compression.
- Compare test results to theoretical and numerical results.
- Determine the factor of safety of the component.

1.3. Limitations

To conduct the research within reasonable time and cost, several limitations were imposed. The following consists of a list of points that have not been considered.

- Vibration effects of the rocket motor are unknown, nor are the effects of the vibrations known.
- Possible manufacturing induced defects.
- Thermal loads and moisture effects.

1.4. Theory

A general overview of the concepts and theory used in the research follows. The following equations and analysis were implemented in a MATLAB script to aid in the calculation. The code itself can be found in the Appendix B. Results can be found in section 3.

1.4.1. Prediction of Lamina Engineering Properties

The data sheet provided by the PET/GF manufacturer is limited in the reported material properties. To predict the proper response of the composite, the modified rule of mixtures and Halpin-Tsai semi-empirical formulations were used to calculate the unknown mechanical properties of the lamina based on properties of the fibre and matrix.

The transverse modulus is given by

$$E_2 = \frac{E_m\left(1 + \xi\eta V_f\right)}{1 - \eta V_f} \tag{1}$$

where

$$\eta = \frac{\frac{E_f}{E_m} - 1}{\frac{E_f}{E_m} + \xi} \tag{2}$$

Here, ξ is a parameter that accounts for packing, fibre geometry and loading condition. For fibres with circular cross-sectional area, $\xi = 2$ is used [4].

The in-plane shear modulus is given by

$$G_{12} = \frac{G_m\left(1 + \xi\eta V_f\right)}{1 - \eta V_f} \tag{3}$$

Where η is previously defined in equation 2. For G-modulus, $\xi = 1$ is used [4].

The Poisson's ratio in the longitudinal-transverse direction and vice-versa are defined using the rule of mixtures as

$$\nu_{12} = \nu_f V_f + \epsilon_{Tm} V_m \tag{4}$$

$$\nu_{21} = \frac{E_2}{E_1}\nu_{12} \tag{5}$$

1.4.2. Effective Laminate Properties

To calculate a laminate's effective properties, it is important to first understand the basic equations governing classical lamination theory. The assumptions used in the theory are briefly stated below:

- The laminate consists of perfectly bonded layers. There is no slip between the adjacent layers. In other words, it is equivalent to saying that the displacement components are continuous across layer interfaces.
- Each lamina is considered as a homogeneous layer such that its effective properties are known.
- Each lamina is in a state of plane stress.
- The individual lamina can be isotropic, orthotropic or transversely isotropic.
- The laminate deforms according to the Kirchhoff - Love assumptions for bending and stretching of thin plates (as assumed in classical plate theory). The assumptions are:
    - The normals to the mid-plane remain straight and normal to the midplane even after deformation.
    - The normals to the mid-plane do not change their lengths.

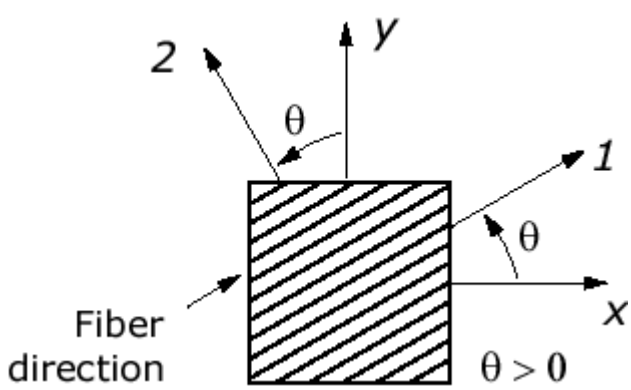

Figure 3 - Global and Principal Lamina Element Directions

Generally, the laminate global direction is defined in x and y coordinates, while the 1 and 2 directions describe the longitudinal and transverse directions of the lamina, as shown in Figure 3. The direction of the fibre within a laminate will dictate its properties. As such, each layer must be transformed to the global coordinate system following the calculation of the transformed reduced stiffness matrix.

$$\overline{[Q]} = [Q] \times [T]$$

$$[\bar{Q}] = \begin{bmatrix} Q_{11} & Q_{12} & 0 \\ Q_{12} & Q_{22} & 0 \\ 0 & 0 & Q_{66} \end{bmatrix} \begin{bmatrix} m^2 & n^2 & 2mn \\ n^2 & m^2 & -2mn \\ -mn & mn & m^2 - n^2 \end{bmatrix} \tag{6}$$

where

$$Q_{11} = \frac{E_1}{1 - \nu_{12}\nu_{21}} \tag{7}$$

$$Q_{12} = \frac{\nu_{12}E_2}{1 - \nu_{12}\nu_{21}} \tag{8}$$

$$Q_{22} = \frac{E_2}{1 - \nu_{12}\,\nu_{21}} \tag{9}$$

$$Q_{66} = G_{12} \tag{10}$$

$$m = \cos^2\theta \tag{11}$$

$$n = \sin^2\theta \tag{12}$$

The ABD matrix, a 6x6 matrix which represents the elastic properties of the laminate, can then be built using the transformed reduced stiffness matrix. This is done by summing the $\bar{Q}$ for n layers while accounting for the thickness of each layers. The effective engineering properties of a laminate can then be computed using the in-plane stiffness matrix [5]:

In-plane Stiffness matrix:

$$[A] = \sum_{k=1}^{n} [\bar{Q}]^k (h_k - h_{k-1}) \tag{13}$$

Effective engineering properties:

$$\bar{E}_x = \frac{A_{11}A_{22} - A_{12}^2}{A_{22}H} \tag{14}$$

$$\bar{E}_x = \frac{(A_{11}A_{22} - A_{12}^2)}{A_{11}H} \tag{15}$$

$$\bar{G}_{xy} = \frac{A_{66}}{H} \tag{16}$$

$$\bar{\nu}_{xy} = \frac{A_{12}}{A_{22}} \tag{17}$$

$$\bar{\nu}_{xy} = \frac{A_{12}}{A_{11}} \tag{18}$$

1.4.3. Buckling of Composite Cylindrical Shells

1.4.3.1. Pure Bending

Buckling is a critical failure condition by which the fuselage is likely to fail. To estimate composite failure of fuselage section, the load case of pure bending is studied.

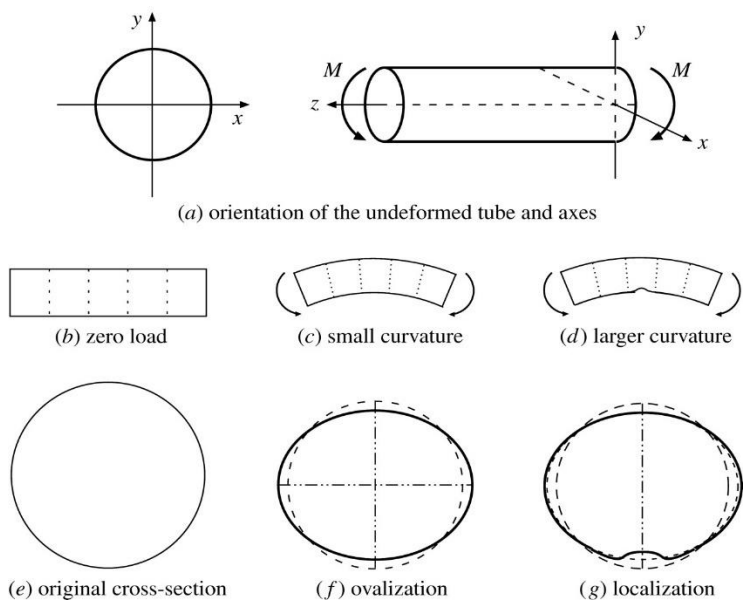

Figure 4 - Pure Bending of Thin-Walled Cylindrical Shell [6]

The common modes of failure of long cylinders in bending is determined by the cross-section instability leading to the flattening of the cross section as shown in Figure 2-f and 2-g. This phenomenon was first derived by Brazier leading to the following equation for the critical bending moment [7]:

$$M_{cr} = \frac{2\sqrt{2}}{9}\pi R t^2 \left[\frac{\bar{E}_x \times \bar{E}_y}{1-\bar{\nu}_{xy}\bar{\nu}_{yx}}\right]^{\frac{1}{2}} \tag{19}$$

1.4.3.2. Axial Compression

Cylindrical shells loaded axially in compression will buckle under the following critical stress [8].

$$\sigma_x^{cr} = \sigma_x^{Euler}\left[1 + \frac{2}{3}\left(\frac{\pi R}{L}\right)^2\left(\frac{\bar{E}_x}{\bar{G}_{xy}}\right)\right]^{-1} \tag{20}$$

Note that the equation includes the effects of transverse shear flexibility of a thin-walled cylinder. The Euler buckling stress, modified for orthotropic materials, is given as

$$\sigma_x^{Euler} = \frac{\pi^2}{2}\left(\frac{R}{L}\right)^2 \bar{E}_x \tag{21}$$

Considering the NASA SP-8007 empirical knockdown factor, which considers the shape factor. The corrected maximum stress is given by [9]

$$\sigma_x' = \sigma_x^{cr}\gamma \tag{22}$$

where

$$\gamma = 1 - 0.901\left(1 - e^{-\frac{1}{16}\sqrt{\frac{R}{t}}}\right) \tag{23}$$

For the above stress, the maximum loading for a cylindrical shell can be defined as

$$P_{cr} = \sigma_x'\pi\left(\left(\frac{d_0}{2}\right)^2 - \left(\frac{d_i}{2}\right)^2\right) \tag{24}$$

It should be noted that the knockdown factor γ is considered a lower bound within the 99% range to an empirical data set, and therefore yields conservative results. A nonlinear buckling analysis by FEA will more accurately define a critical buckling load.

2. Methodology

2.1. Model Geometry

The forward section consists of a 63 in. long glass fibre reinforced PET thin-walled tube consisting of a combined 40 in. straight section and 23 in. nosecone. The design of the forward fuselage section with respect to the rockets overall assembly is shown in Figure 3.

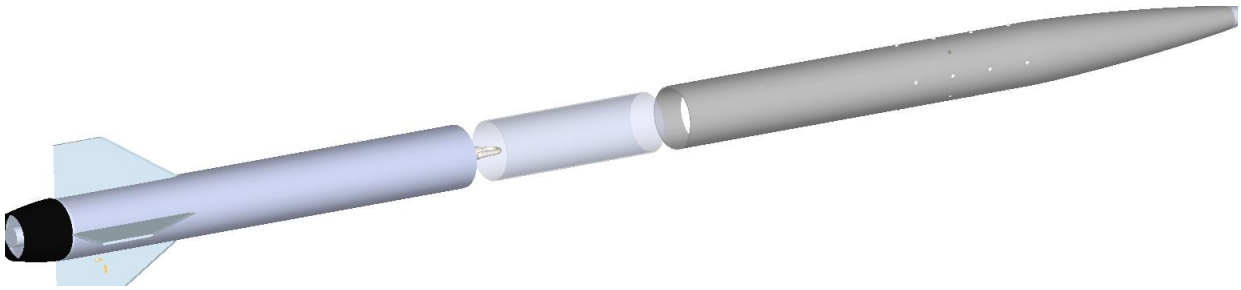

Figure 5 - Rocket Exploded Assembly View

The array of rails represents a structural mounting interface between the internal bulkhead assemblies and the fuselage shell. A set of screws secure the rail structure to the outer shell. The coupler acts as a joint between the forward and aft components, stiffening the rocket at its weakest point. Figure 6 details the placement of the above-mentioned components.

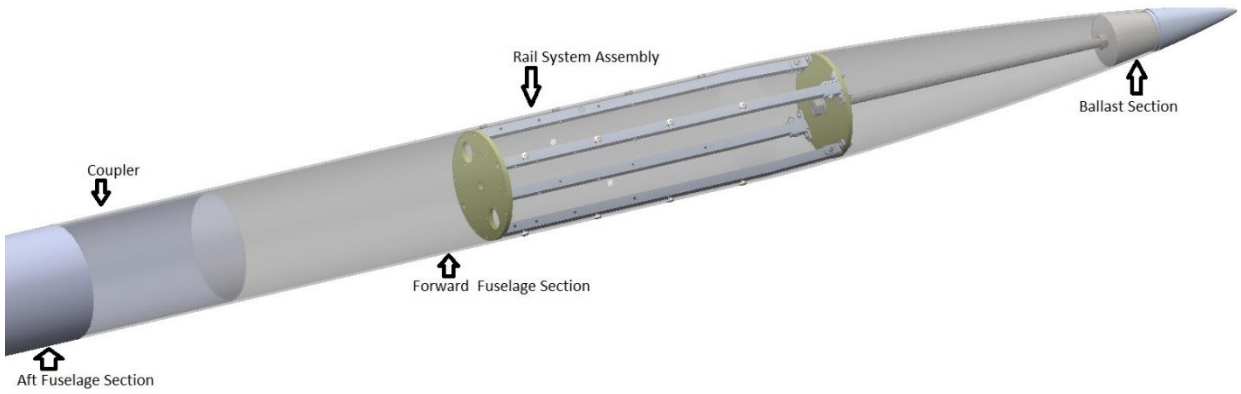

Figure 6 - Forward Section Structural Components

2.2. Loads

During the powered flight of the rocket, the fuselage section will be subjected to an axial compression impulse from initial take-off. Next, an increase in dynamic pressure at relatively constant thrust along with an oscillatory damping motion about its center of gravity causes the rockets corrective aerodynamic forces, acting at the center of pressure (cp in Figure 7), to realign the rocket with respect to its trajectory. To simulate the flight's

loading conditions within a greater accuracy, an aerodynamic flight simulation software, RASAero was utilized. Details on the simulation model can be found in APPENDIX E-C.

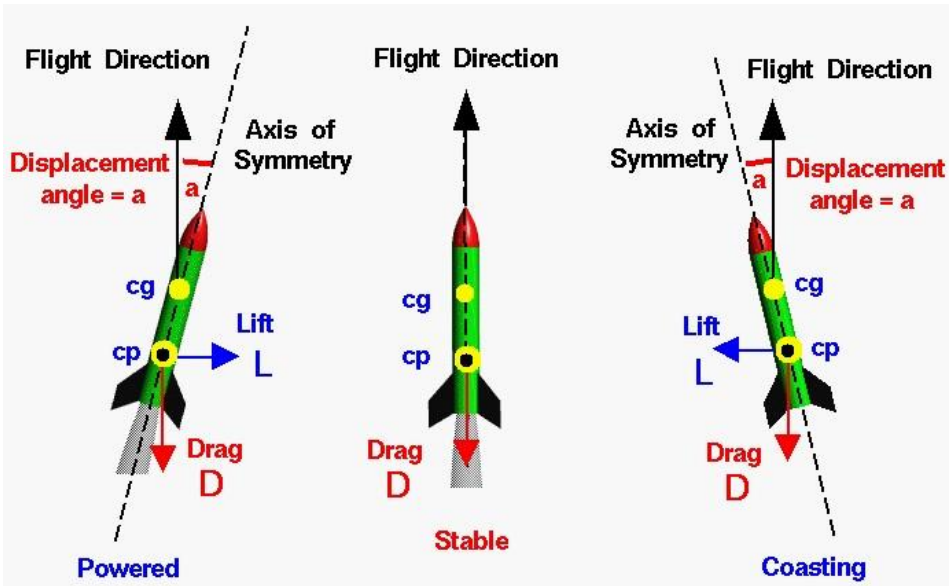

Figure 7 - Rocket Free Body Diagram

2.2.1. Axial Loading

Transient axial loads associated with an elastic wave moving up the rocket from the thrust chamber at launch were investigated. The loads at launch are applied onto the forward fuselage edge axially. The shock force can be clearly identified in the Figure 8 as the blue curve. The maximum thrust peaks at 8034 N. Given this load is applied as an impulse, a design safety factor greater than 10 is recommended for composite laminates [7]. This loading condition will be analyzed as the second loading condition on the rocket and considered as a steady state axial load, considering the higher safety factor to account for the transient shock wave.

2.2.2. Bending

Bending in a rocket is the result of aerodynamic corrective forces acting on the center of pressure to realign itself with its flight path. The resulting moment then becomes a function of the normal force coefficient, $C_{N,\alpha}$, which defines the strength of the normal corrective force. This force is influenced by conditions such as the thrust misalignment, wind gusts, rocket center of gravity offset. This will be used to more accurately define the rockets maximum bending loads [10]. To define the point along the flight with maximum loading conditions, the thrust and drag given by the equation below were plotted as a function of time (see Figure 8). The point with the maximum drag and thrust was found at 1.8 seconds to be 7295 N.

$$D = \frac{C_d \rho V_\infty^2 A}{2} \tag{25}$$

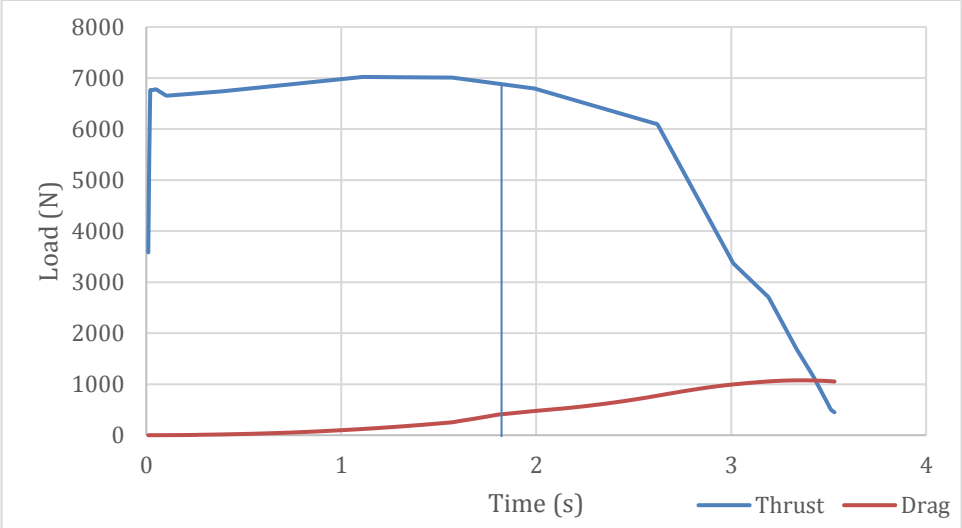

Figure 8 - Load versus Time Graph

Using the simulation data output at 1.8 seconds describing the flight conditions, found in APPENDIX E-C, the bending loads on the rocket were calculated. The system of equations from reference [10] used to derive the bending moment are further described in APPENDIX E-C. These equations are applied to each body element, as shown in Figure 9, and solved numerically.

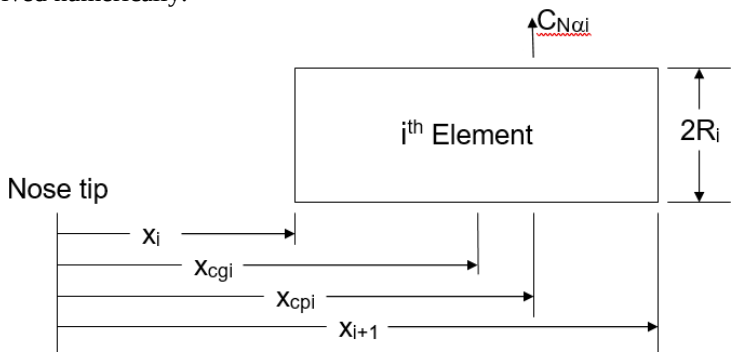

Figure 9 - Body Element Dimensions

Figure 10 represents the bending load along the fuselage. The maximum bending load is 210.6 Nm. The load found here will be compared to the critical bending loads found theoretical to determine the safety factor of the component.

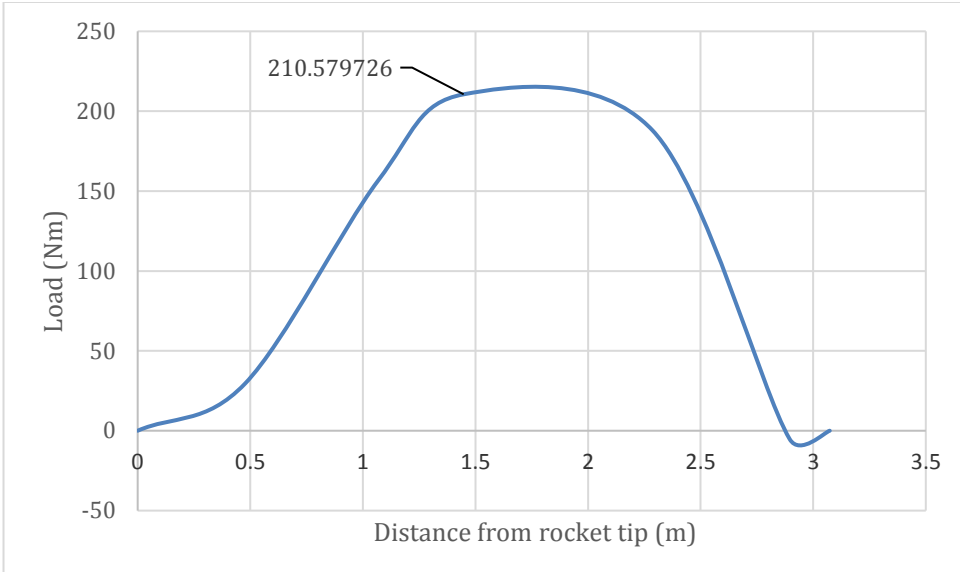

Figure 10 - Bending Loads along Body Tube starting from the nose

2.3. Finite Element Analysis

The finite element analysis was used to compare the analytical closed formed solution of the Euler buckling equation to a numerical nonlinear buckling analysis. The analysis performed utilizes the maximum length of the fuselage within the rocket which is unsupported. This consists of an 18 in. long section found between the coupler and start of the rail system. An additional analysis was conducted with a length equal to the test specimen length.

2.3.1. Mechanical Properties

The material properties of each layer of fibreglass reinforced PET were obtained from the Tencate (TC940) datasheet. The unknown material properties were derived using the micromechanics equations described in section 1.4.2 Effective Laminate Properties. The properties for fibre glass and PET individually were obtained from reference [5, 11], respectively.

Parameter	Value	Unit
V_f	0.55	
ν_m	0.37	
E_m	0.7	GPa
G_m	0.05	GPa
ν_f	0.21	
E_f	72.3	GPa
G_f	30	GPa

Table 6 - Mechanical Properties of PET and Glass Fibre Individually

Parameter	Value	Unit
Density	1890	Kg/m^3
Orthotropic Elasticity		
E_1	32	GPa
E_2	3.11	GPa
G_{12}	0.1713	GPa
ν_{12}	0.282	
t	0.125	mm

Table 7 - Material Properties of Glass Fibre/PET

The stacking sequences selected are shown below:

1. $[90 / 45 / -45 / 25 / -25 / 0_2]_s$

2. $[0 / 25 / -25 / 45 / -45 / 90]_s$
3. $[90_2 / 45 / -45 / 0_2]_s$

The change in layer orientation from 45 to 25 degrees resulted, as seen in Table 8, in an increase in shear modulus, and decrease in elastic modulus in both x and y directions, along the tube and hoop wound, respectively. Additionally, the selected layup sequences were made quasi-isotropic, balanced and symmetric because the loading in bending experienced by the fuselage will never be along the same bending axis. The last layup was selected for testing given that the optimal results for buckling and critical loading were greater for this layup sequence.

Table 8 - Effective Laminate Properties of Selected Layup Sequences

Parameter	$[90_2/45/-45/0_2]_s$	$[0/25/-25/45/-45/90]_s$	$[90/45/-45/25/-25/0_2]_s$
$\bar{E}_x$(GPa)	17.58	16.96	16.96
$\bar{E}_y$(GPa)	17.58	10.28	10.28
$\bar{G}_{xy}$(GPa)	7.063	11.10	11.10
$\bar{\nu}_{xy}$	0.2367	0.52	0.52

2.3.2. Meshing

The mesh used for the FEM uses QUAD4 elements, generally for analysis of shell structures. A mesh convergence study verified the quality of the mesh and assuring convergence of the stresses. The maximum stress is compared to the increase in mesh quality until the stress converges. Figure 11 represents the mesh chosen for which stress values were found to converge.

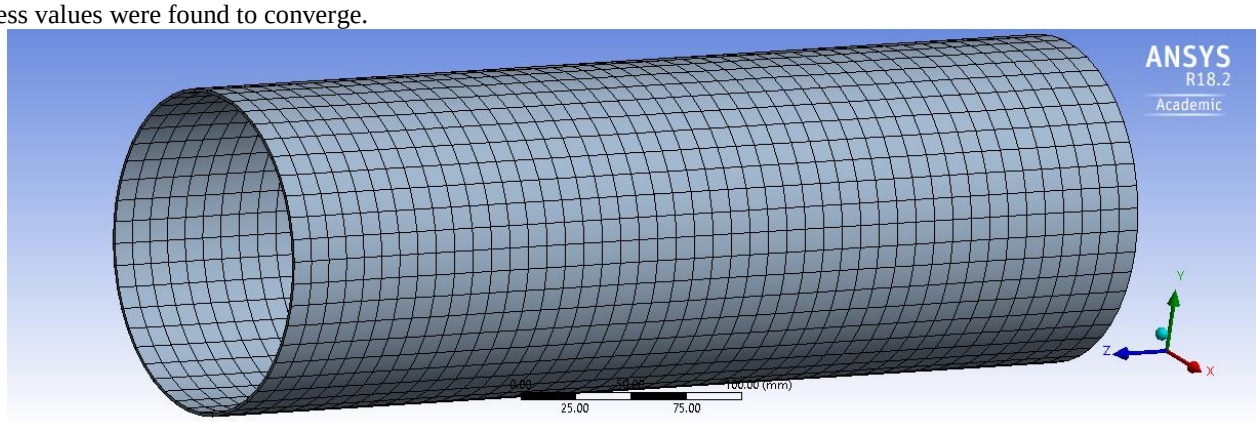

Figure 11 - Shell Mesh Density

2.3.3. Boundary Conditions

The conditions used for the numerical analysis of the tubes defines the imperfection which will cause nonlinear buckling. An induced transverse force under compressive loads were input as shown as a 0.5 N force in the y-direction to trigger nonlinear buckling. This is achieved by applying a load acting as an imperfection (non-symmetric) in the load distribution, causing the shape to deform in a non-linear fashion. Next, displacement boundaries are set at a single end. One edge is completely constrained, while the other is used to apply the coupled bending and compression loads.

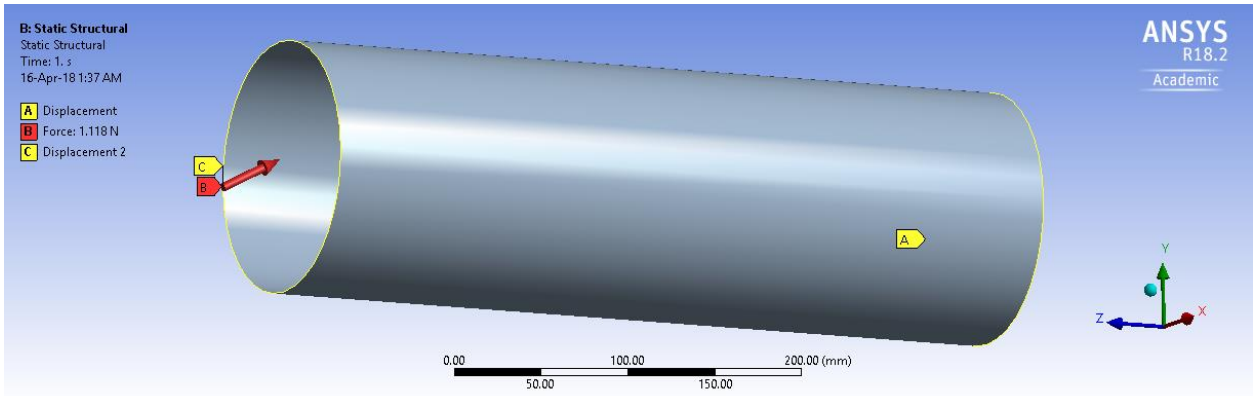

Figure 12 - Tube Constraints and Initial Loading

2.4. Experimental Setup

The test specimens were manufactured by AFP using the same inner diameter as the rocket using the following layup sequence $[90_2 / 45 / -45 / 0_2]_s$ as this yielded improved resistance to bending when observing the theoretical critical bending loads. The specimen ends were wrapped with additional 90° layers to prevent failure close to the loading fixture.

2.4.1. AFP Manufacturing Parameters

The process parameters for the material were noted for repeatability. These parameters have been determined by producing a set of rings with varying process parameters that were subsequently sectioned and subjected to a short beam shear test to determine the interlaminar shear stress. The optimum process parameters for manufacturing of GF/PET which resulted in the highest interlaminar shear stress are given as:

- Nozzle Temperature = 590 °C;
- Process Rate = 50 mm/s;
- Compaction Force = 70 lbf
- Gas Flow Rate = 80 SLPM

Two end plates were machined from aluminum to within 0.002” to keep the load aligned with the tube axial direction. To achieve results comparable to the analysis, premature failure due to edge defects must be avoided. This was accomplished using a low melting point alloy (LMPA). The LMPA is placed within the slot before the sample is slid in place to act as additional shear surface and to keep ends grounded. Figure 13 demonstrates the grounded end of a sample in the alloy.

Figure 13 - Sample Edge Secured in LMPA

Four strain gauges were mounted onto the outer wall of the tube at 180° in pairs with one sensor directed axially, and the other in the hoop direction. Figure 12 shows the experimental setup of a specimen before testing.

Figure 14 - Sample Setup in Uniaxial Testing Machine

3. Results

3.1. Analysis

The finite element analysis yielded conservative results when comparing the short cylindrical test sample. Table 8 compares the theoretical, finite element method and experimental results. The longer 18 in. simulation results fall within 10% error margin of the analytical solution to buckling as shown in Tables 9. Although the results are not far off from one another, additional samples of longer length should be tested in compression, and in bending, to validate the analytical model.

Table 9 - Critical Buckling Load Results for 5.19 in specimen, Layup 1

Critical Load Type	Analytical	FEM	Experiment
P_{cr} ($\gamma = 0.6816$) (kN)	120	80.16	>96
M_{cr}(Nm)	2882	NA	NA
Safety Factor	13.65 (Bending)	10.01	>12

Table 10 - Results for 18 in. Specimen

Layup	Critical Load Type	Analytical	FEM	Error (%)
1	P_{cr} (kN)	82.02	83.1	1.3
	M_{cr}(Nm)	2341	NA	
2	P_{cr} (kN)	82.02	88.1	6.9
	M_{cr}(Nm)	2341	NA	
3	P_{cr} (kN)	74.21	80.16	7.4
	M_{cr}(Nm)	2882	NA	

3.2. Experiment

The test was performed on 2 samples of 5.19 in. length, giving an aspect ratio smaller than 1. At the time of the manufacturing of the components, the effect of specimen aspect ratio on the buckling of the cylinder was not known. Further research has shown that short cylinders are more likely to fail due to the compressive stress rather than buckling [12]. As the compression test results show in Figure 13, no failure, either in buckling or compression was perceived as the sample reached the maximum achievable compressive load of the machine. Following the stress-strain relationship from the linear portion below, the elastic modulus along the axial direction can be determined. The average modulus $\bar{E}_x$, was 17.89 GPa, which agrees with theoretical calculations, giving an error margin of 1.71%.

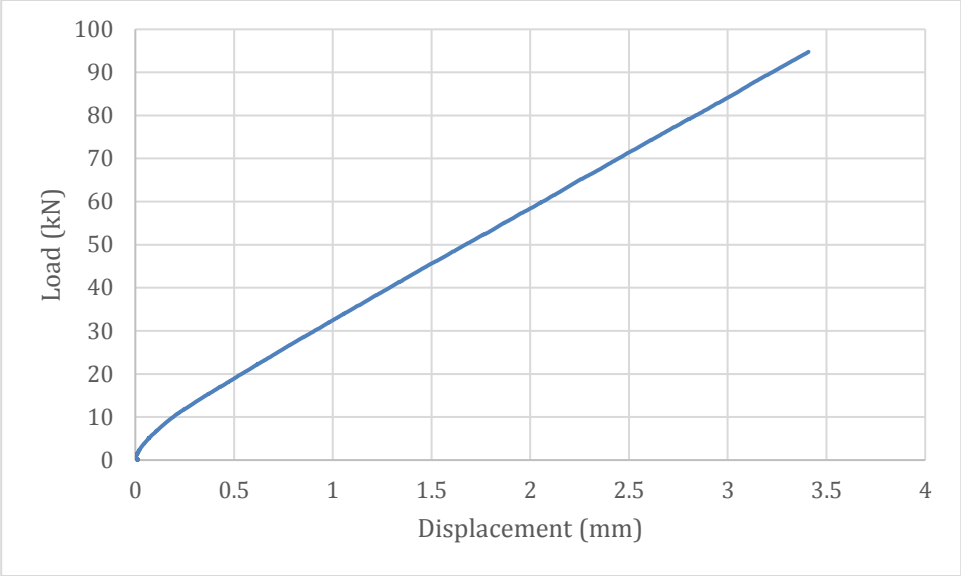

Figure 15 - Load versus Displacement Graph

4. Conclusion

The critical bending moment and compression loads were calculated for 3 separate composite laminated cylindrical PET/GF shells for a sounding rocket fuselage manufactured by automated fibre placement. The loads experienced by the rocket during flight were calculated to determine the safety factor. A non-linear buckling analysis by FEA using ANSYS was conducted on the longest unsupported cylindrical specimen with the launch vehicle to validate the determined loading conditions. Cylindrical samples were manufactured and tested following the selection of the layup sequence resulting in the highest critical loads.

The results demonstrated similar values for the elastic modulus. The samples did not fail when tested in axial compression due to a low length to diameter ratio. The analytical and numerical solutions for axial compressive loads result in safety factors within operation limits of the material. Further testing in bending should be conducted to generate conclusive evidence for the analytical bending calculations.

5. Recommendations for future work

To further validate the simulation results, a pure bending test should be conducted on samples, following the same approach used in axial compression. Additionally, material failure properties, such as σ_2^{UC}, σ_2^{UT} should be determined through standard test methods ASTM D5450, D5449. This will lead to a more thorough analysis by determining the failure criteria and more accurately simulating FEA models. Finally, an ultrasonic inspection should be conducted on the nosecone section, as it consists of the section which will contain the most defects due to its complex geometry. The ultrasonic inspection will serve to identify the weakest points on the shell structure. Further considerations should also be taken regarding the manufacturing induced defects, such as voids and high resin concentration areas.

References

[1] G. O. J. M. D. H. Zachary August, "Recent Developments in Automated Fiber Placement of Thermoplastic Composites," Automated Dynamics, Schenectady, NY, 2014.

[2] N. Woodcock, "Critical Design Review Report," Space Concordia Rocketry Division, Montreal, 2015.

[3] P. B. Adam Roslowicz, "Analysis of Heat Transfer in a Supersonic Rocket Head," Transactions of the Institute of Aviation, Warsaw, 2017.

[4] J. L. K. J. C. Halpin, "The Halpin-Tsai Equations: Aa Review," Polymer Engineering and Science, 1976.

[5] M. W. Hyer, Stress Analysis of Fiber-Reinforced Composite Materials, Lancaster: DEStech Publication Inc., 2009.

[6] M. A. W. A. P. B. A. A. A. M. Khurram Wadee, "Longitudinally inhomogeneous deformation patterns in isotropic tubes under pure bending," The Royal Society, 2006.

[7] S. V. H. S. W. T. Daniel Gay, Composite Materials Design and Applications, Paris: CRC Press Web, 2003.

[8] M. M. M. J. Michael P. Nemeth, "Simple Formulas and Results for Buckling Resistance and Stiffness Design of Compression-Loaded Laminated-Composite Cylinders," NASA, Hampton, Virgina, 2009.

[9] P. S. V. I. Weingarten, "Buckling of Thin-Walled Circular Cylinders," NASA, Washington, D.C., 1965.

[10] C. P. Hoult, "Sounding Rocket Structural Design Loads," California State University Los Angeles, Los Angeles, 2014.

[11] MatWeb, LLC, Overview of materials for Polyethylene Terephthalate (PET), Unreinforced, 2014.

[12] D. C. Charles E. Rogers, "Rogers Aeroscience RASAero Aerodynamic Analysis and Flight Simulation Program," Rogers Aeroscience, Lancaster, 2011.

[13] G. A. C. Sr., "THE DESCRIPTIVE GEOMETRY OF NOSE CONES," Institute of Physics of São Carlos, São Carlos, 1996.

[14] M. H.-C. C. B.-T. Juan S. Prieto, "Recovery System Design," Space Concordia Rocketry Division, Montreal, 2018.

[15] Tencate Performance Composites, "TenCate Cetex TC940," Tencate Performance Composites, Camarillo.

[16] "Standard Test Method for In-Plane Shear Response of Polymer Matrix Composite Materials by Tensile Test of a 45° Laminate," ASTM International, West Conshohocken, 2001.

[17] I.-J. S. Dong-Joo Lee, "Effects of vacuum, mold temperature and cooling rate on mechanical properties of press consolidated glass fiber/PET composite," Journal of Composites Part A: Applied Science and Manufacturing, 2002.

[18] "Standard Test Method for Enthalpies of Fusion and Crystallization of Polymers by Differential Scanning Calorimetry," ASTM International, West Conshohocken, 1999.

APPENDIX E-A

Polar properties of PET/Glass Fibre:

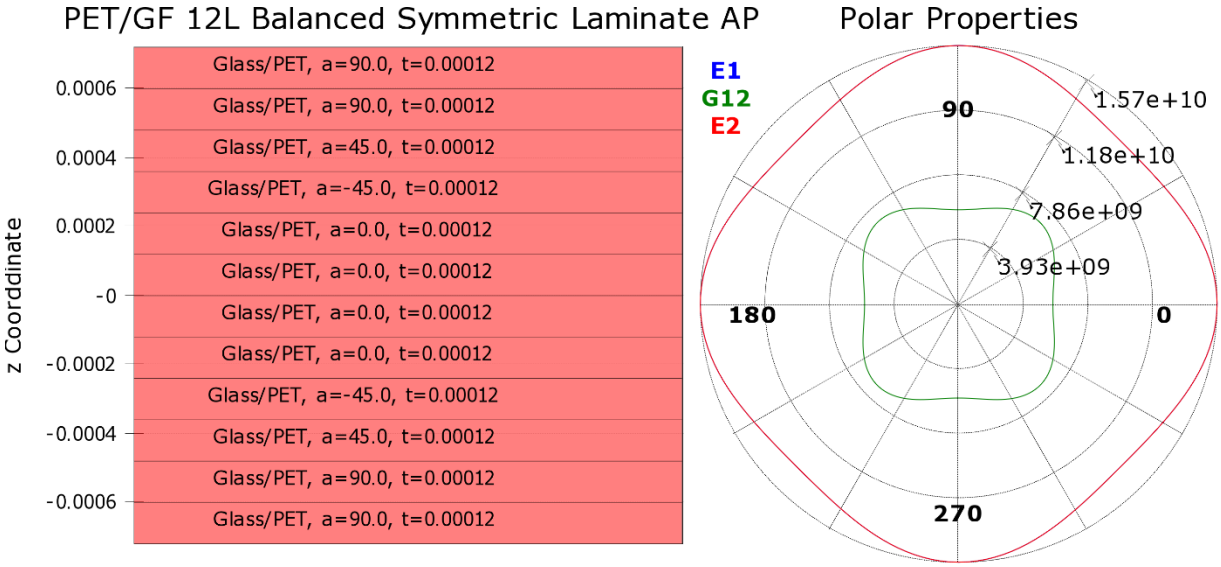

APPENDIX E-B

```
%Sounding Rocket Fuselage Analysis
clc;
clear;
%%%%%%%%%%%%%% MICROMECHANICS %%%%%%%%%%%%%%%%%%

%Material Properties of PET/Glass Fibre(Tencate TC940):
Vf = 0.4343; %(Tencate TC940 TDS)

%PET Resin Material Properties Source:
http://www.goodfellow.com/E/Polyethylene-terephthalate.html
NUm = 0.37;
Em = 700e+06; %Pa (Tencate TC940 TDS)
Gm = 50e+06; %Pa Source:
%Fibre Material Properties (E-Glass) Source: MATWeb, E-Glass Fibre, Generic
NUf = 0.21;
Ef = 72.3e+09; %Pa
Gf = 30e+09; %Pa
%Elasticity
E1 = E1(Vf,Ef,Em); %MPa (E1_Theoretical < E1_Datasheet **)
zeta = 2;
eta = (Ef/Em-1)/(Ef/Em+zeta);
E2 = Em*((1+zeta*eta*Vf)/(1-eta*Vf)); %MPa Source: Halpin-Tsai Formula Eq4.31
Barbero
E3 = E2;    %MPa
%Poisson's Ratio
NU12 = NU12(Vf,NUf,NUm);

% Shear Modulus
G12 = G12(Vf, Gf,Gm,0,3); %MPA PMM: Eq4.41, E. Barbero 2nd Ed.
G13 = G12;
% G23 = 2.714e+03; %MPa NOT NEEDED

% Laminate Engineering Constants (Example: [90_2/45/-45/0_2]s)
Q = ReducedStiffness(E1,E2,NU12,G12);
Qbar_0 = Q;
Qbar_neg45 = Qbar(Q,-45);
Qbar_45 = Qbar(Q,45);
Qbar_90 = Qbar(Q,90);
A = zeros(3,3);
z1 = 0;
z2 = 0.125e-03; %m
%Laminate Thickness
H = (z2-z1)*12;
% 0 layers
A = Amatrix(A,Qbar_0,z1,z2);
A = Amatrix(A,Qbar_0,z1,z2);
A = Amatrix(A,Qbar_0,z1,z2);
A = Amatrix(A,Qbar_0,z1,z2);
% 90 layers
A = Amatrix(A,Qbar_90,z1,z2);
A = Amatrix(A,Qbar_90,z1,z2);
A = Amatrix(A,Qbar_90,z1,z2);
A = Amatrix(A,Qbar_90,z1,z2);
% +45 layers
```

```
A = Amatrix(A,Qbar_45,z1,z2);
A = Amatrix(A,Qbar_45,z1,z2);
% -45 layers
A = Amatrix(A,Qbar_neg45,z1,z2);
A = Amatrix(A,Qbar_neg45,z1,z2);

% Engineering Constants
Ebarx = Ebarx(A,H);
Ebary = Ebary(A,H);
NUbaryx = NUbaryx(A,H);
NUbarxy = NUbarxy(A,H);
Gbarxy = Gbarxy(A,H);

% Geometry Parameters
r_0 = 73.025e-03;   %m Inner Radius
t = H;              %m thickness
L = 131.83e-03;     %m Length

% Critical Buckling Moment due to Bending of Composite Tubes:
M_crit = 2*sqrt(2)/9*pi*r_0*t^2*sqrt(Ebarx*Ebary/(1-NUbarxy*NUbaryx));

% Critical Buckling Stress due to Axial Compression
sigma_cr  =  pi^2/2*(r_0/L)^2*Ebarx*(1+(2/3*(pi*r_0/L)^2*(Ebarx/Gbarxy)))^(-
1);

% Empirical Knockdown Factor
KDF = 1-(0.901*(1-(exp(-1/16*sqrt(r_0/t)))));

% Effective maximum critical axial compressive load
P_cr = sigma_cr*KDF*pi*((r_0+t)^2-(r_0)^2);

function y = E1(Vf,E1f,Em)
%E1   This function returns Young's modulus in the
%     longitudinal direction. Its input are three values:
%     Vf  - fibre volume fraction
%     E1f - longitudinal Young's modulus of the fibre
%     Em  - Young's modulus of the matrix
%     This function uses the simple rule-of-mixtures formula
%     of equation (3.2)
Vm = 1 - Vf;
y = Vf*E1f + Vm*Em;

function y = E2(Vf,E2f,Em,Eta,NU12f,NU21f,NUm,E1f,p)
%E2   This function returns Young's modulus in the
%     transverse direction. Its input are nine values:
%     Vf    - fibre volume fraction
%     E2f   - transverse Young's modulus of the fibre
%     Em    - Young's modulus of the matrix
%     Eta   - stress-partitioning factor
%     NU12f - Poisson's ratio NU12 of the fibre
%     NU21f - Poisson's ratio NU21 of the fibre
%     NUm   - Poisson's ratio of the matrix
%     E1f   - longitudinal Young's modulus of the fibre
%     p     - parameter used to determine which equation to use:
```

```
%             p = 1 - use equation (3.4)
%             p = 2 - use equation (3.9)
%             p = 3 - use equation (3.10)
%     Use the value zero for any argument not needed
%     in the calculations.
Vm = 1 - Vf;
if p == 1
    y = 1/(Vf/E2f + Vm/Em);
elseif p == 2
    y = 1/((Vf/E2f + Eta*Vm/Em)/(Vf + Eta*Vm));
elseif p == 3
    deno = E1f*Vf + Em*Vm;
    etaf = (E1f*Vf + ((1-NU12f*NU21f)*Em + NUm*NU21f*E1f)*Vm)/deno;
    etam = (((1-NUm*NUm)*E1f - (1-NUm*NU12f)*Em)*Vf + Em*Vm)/deno;
    y = 1/(etaf*Vf/E2f + etam*Vm/Em);
end

function y = G12(Vf,G12f,Gm,EtaPrime,p)
%G12   This function returns the shear modulus G12
%      Its input are five values:
%      Vf         - fibre volume fraction
%      G12f       - shear modulus G12 of the fibre
%      Gm         - shear modulus of the matrix
%      EtaPrime   - shear stress-partitioning factor
%      p          - parameter used to determine which equation to use:
%                   p = 1 - use equation (3.5)
%                   p = 2 - use equation (3.13)
%                   p = 3 - use equation (3.14)
%      Use the value zero for any argument not needed
%      in the calculations.
Vm = 1 - Vf;
if p == 1
    y = 1/(Vf/G12f + Vm/Gm);
elseif p == 2
    y = 1/((Vf/G12f + EtaPrime*Vm/Gm)/(Vf + EtaPrime*Vm));
elseif p == 3
    y = Gm*((Gm + G12f) - Vf*(Gm - G12f))/((Gm + G12f) + Vf*(Gm - G12f));
end

function y = NU12(Vf,NU12f,NUm)
%NU12   This function returns Poisson's ratio NU12
%       Its input are three values:
%       Vf    - fibre volume fraction
%       NU12f - Poisson's ratio NU12 of the fibre
%       NUm   - Poisson's ratio of the matrix
%       This function uses the simple rule-of-mixtures
%       formula of equation (3.3)
Vm = 1 - Vf;
y = Vf*NU12f + Vm*NUm;


function y = NUxy(E1,E2,NU12,G12,theta)
%NUxy   This function returns Poisson's ratio
%       NUxy in the global
%       coordinate system. It has five arguments:
```

```
%       E1    - longitudinal elastic modulus
%       E2    - transverse elastic modulus
%       NU12  - Poisson's ratio
%       G12   - shear modulus
%       theta - fibre orientation angle
%       The angle "theta" must be given in degrees.
%       NUxy is returned as a scalar
m = cos(theta*pi/180);
n = sin(theta*pi/180);
denom = m^4 + (E1/G12 - 2*NU12)*n*n*m*m + (E1/E2)*n*n;
numer = NU12*(n^4 + m^4) - (1 + E1/E2 - E1/G12)*n*n*m*m;
y = numer/denom;

function y = NUyx(E1,E2,NU21,G12,theta)
%NUyx   This function returns Poisson's ratio
%       NUyx in the global
%       coordinate system. It has five arguments:
%       E1    - longitudinal elastic modulus
%       E2    - transverse elastic modulus
%       NU21  - Poisson's ratio
%       G12   - shear modulus
%       theta - fibre orientation angle
%       The angle "theta" must be given in degrees.
%       NUyx is returned as a scalar
m = cos(theta*pi/180);
n = sin(theta*pi/180);
denom = m^4 + (E2/G12 - 2*NU21)*n*n*m*m + (E2/E1)*n*n;
numer = NU21*(n^4 + m^4) - (1 + E2/E1 - E2/G12)*n*n*m*m;
y = numer/denom;

function y = ReducedStiffness(E1,E2,NU12,G12)
%ReducedStiffness   This function returns the reduced stiffness
%                   matrix for fibre-reinforced materials.
%                   There are four arguments representing four
%                   material constants. The size of the reduced
%                   stiffness matrix is 3 x 3.
NU21 = NU12*E2/E1;
y = [E1/(1-NU12*NU21) NU12*E2/(1-NU12*NU21) 0 ; NU12*E2/(1-NU12*NU21) E2/(1-
NU12*NU21) 0 ; 0 0 G12];

function y = Qbar(Q,theta)
%Qbar   This function returns the transformed reduced
%       stiffness matrix "Qbar" given the reduced
%       stiffness matrix Q and the orientation
%       angle "theta".
%       There are two arguments representing Q and "theta"
%       The size of the matrix is 3 x 3.
%       The angle "theta" must be given in degrees.
m = cos(theta*pi/180);
n = sin(theta*pi/180);
T = [m*m n*n 2*m*n ; n*n m*m -2*m*n ; -m*n m*n m*m-n*n];
Tinv = [m*m n*n -2*m*n ; n*n m*m 2*m*n ; m*n -m*n m*m-n*n];
y = Tinv*Q*T;

function y = Amatrix(A,Qbar,z1,z2)
```

```
%Amatrix   This function returns the [A] matrix
%          after the layer k with stiffness [Qbar]
%          is assembled.
%          A     - [A] matrix after layer k
%                  is assembled.
%          Qbar  - [Qbar] matrix for layer k
%          z1    - z(k-1) for layer k
%          z2    - z(k) for layer k
for i = 1 : 3
    for j = 1 : 3
        A(i,j) = A(i,j) + Qbar(i,j)*(z2-z1);
    end
end
y = A;

function y = Ebarx(A,H)
%Ebarx   This function returns the average laminate modulus
%        in the x-direction. Its input are two arguments:
%        A  - 3 x 3 stiffness matrix for balanced symmetric
%             laminates.
%        H - thickness of laminate
a = inv(A);
y = 1/(H*a(1,1));

function y = Ebary(A,H)
%Ebary   This function returns the average laminate modulus
%        in the y-direction. Its input are two arguments:
%        A  - 3 x 3 stiffness matrix for balanced symmetric
%             laminates.
%        H - thickness of laminate
a = inv(A);
y = 1/(H*a(2,2));

function y = Gbarxy(A,H)
%Gbarxy   This function returns the average laminate shear
%         modulus. Its input are two arguments:
%        A  - 3 x 3 stiffness matrix for balanced symmetric
%             laminates.
%        H - thickness of laminate
a = inv(A);
y = 1/(H*a(3,3));
```

APPENDIX E-C

Table 11 - Parameters for rocket at maximum loading condition

Altitude, ft AGL	Launch Altitude, ft	Launcher Length, ft	Mach Number	Flight Speed, fps	Dynamic pressure, lb/ft^2
1050	5500	17	1.04	1200	1397
Aerodynamic reference area, ft^2	**Max Body Diameter, in**	**Axial Acceleration, ft/sec^2**	**Thrust, lb**	**C.G. Lateral Offset, ft**	**Thrust misalignment angle, rad.**
0.1875	5.868	706	1548	0.003	0.015

Body Station: location along longitudinal direction of the rocket starting from the nose tip.

Table 12 - Rocket Elements Input Data

Element Counter	Element Contents	x_i, Element, inches from nose	R_i, Element body external radius at body station x_i, in	w_i, Element weight (finless), lb	Element $C_{N\alpha i}$ (finless), per radian	Element Xcpi, (finless) from element front, in	Element $C_{N\alpha i}$, per radian	Element Xcpi, from nose tip, in
1	Nose Cone	18.764	2.39	11	2	13.957	2	13.957
2	NC + Forward	42	6	14	0	0	0	18.764
3	Body Tube	57	6	11	0	0	0	42
4	Aft Fuselage	90	6	18	0	0	0	57
5	Fins	114	6	19	0	0	9.07	112
6	Boattial	121	6	2	-1.1	0	-1.1	114

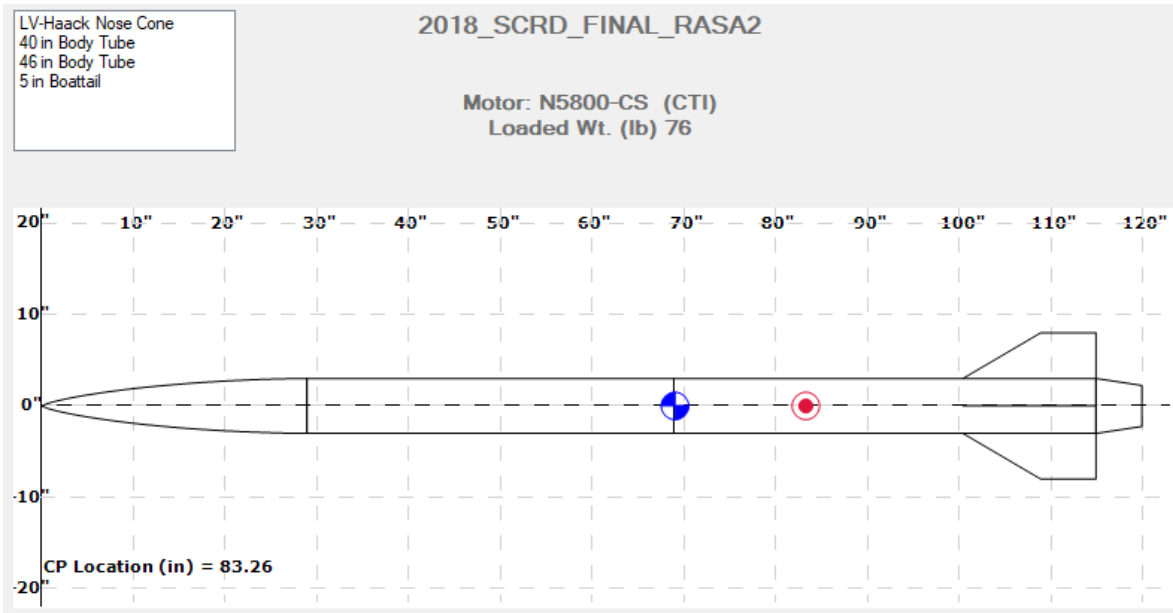

Figure 16 - RASAero 2 Flight Simulation

System of equations used to calculate the bending loads from Reference [10]:

Summing the forces acting on the element in the +z direction gives

$$S_{i+1} - S_i - qS_{ref}C_{N\alpha i}\alpha = m_i\left(A_z - \left(X - x_{cgi}\right)\frac{d^2\alpha}{dt^2}\right), \text{ where} \qquad (1)$$

$X =$ The total rigid body center of mass given by

$$X = \frac{\sum m_i x_{cgi}}{\sum m_i}, \text{ and} \qquad (2a)$$

$A_z =$ The normal acceleration given by

$$A_Z = -\frac{qS_{ref}\alpha\sum C_{N\alpha i}}{\sum m_i} \qquad (3)$$

Similarly, summing the y axis torques (right hand rule) about the element center of mass gives

$$M_i - M_{i+1} + \left(x_{cgi} - x_i\right)S_i + \left(l_i + x_i - x_{cgi}\right)S_{i+1} + qS_{ref}C_{N\alpha i}\alpha\left(x_{cgi} - x_{cpi}\right) = J_i\frac{d^2\alpha}{dt^2} \qquad (4)$$

The nose tip initial conditions are that

$$S_1 = M_1 = 0 \qquad (5)$$

A marching solution of these difference equations is straightforward. Starting with the known value of S_1, eq. (1) can be used to find S_2. Then, given M_1, S_1 and S_2, eq. (4) can be used to find M_2. This marching process can be used for the second element, and so on.

Finally, it must be emphasized that the air load acting on a body element is composed of contributions from both the body itself and any attached fins. For a discussion of the latter, see Appendix F.

Rigid Body Motion

Equations (1) and (4) have terms in A_z, α and $\frac{d^2\alpha}{dt^2}$. The rigid body moment equation relates the latter two. First, the total moment of inertia can be found from the parallel axis theorem:

$$I_{YY} = \sum J_i + m_i\left(X - x_{cgi}\right)^2. \qquad \text{(2b)}$$

Then,

$$I_{YY}\frac{d^2\alpha}{dt^2} = qS_{ref}\alpha\sum C_{N\alpha i}\left(X - x_{cpi}\right). \qquad \text{(6)}$$

As noted in the Introduction, α can be one of the major BENDIT inputs, or one can estimate it in BENDIT from first principles as described in Appendix D.. Using eq's (3) and (6) to find A_z and $\frac{d^2\alpha}{dt^2}$ enables the marching solution of eq's. (1) & (4).

Static Aeroelastic Effects

Up until now, the rocket body has been assumed to be perfectly rigid. But, sometimes rockets have slender upper stages or darts much more susceptible to bending than the main vehicle. At angle of attack their nose curls up increasing the normal force loading. And, the increased normal force causes additional deflection, and so on. In theory this cycle of air load and deflection can continue until divergence occurs. In practice this cannot happen because the increased loads cause structural failure first.

Our point of departure is equations (1), (3), (4) and (6). The way to look at this problem is to consider that the $C_{N\alpha}$ for the nose is increased by a factor F to allow for flexibility effects. Equations (3) and (6) show that the rigid body motions, A_z and $\frac{d^2\alpha}{dt^2}$, are slightly affected by the increase in nose normal force. Then, to estimate F model the flexible nose as a uniform beam with a concentrated load at its tip. Reference (10) describes this process in detail. The slope $\frac{dy}{dx}$ of the bent nose at its tip is

$$\frac{dy}{dx} = (qS_{ref}C_{N\alpha N}(\alpha + \frac{dy}{dx}) + m_N(A_z - (X - x_{CGN})\frac{d^2\alpha}{dt^2}))l_N^2 / 2EI. \qquad \text{(7a)}$$

After substituting from eq's. (3 and 6), this can be solved for $\frac{dy}{dx}$, and then for the total nose tip angle of attack,

$$\alpha_{TOT} = \alpha + \frac{dy}{dx} = \alpha \left[\frac{2EI - qS_{ref}\left[\frac{m_N}{m} C_{N\alpha} + \frac{m_N (X - x_{CGN})}{I_{YY}} \sum C_{N\alpha i}(X - x_{CPi})\right] l_N^2}{2EI - qS_{ref} C_{N\alpha N} l_N^2} \right] \quad \text{(7b)}$$

Note that the dynamic pressure which will make the denominator vanish in eq. (7b) is the divergence dynamic pressure:

$$q_D = \frac{2EI}{S_{ref} C_{N\alpha N} l_N^2}$$

Next, to incorporate this effect in BENDIT7, it is only necessary to increase the nose tip normal force slope to

$$C_{N\alpha N} \left[\frac{2EI - qS_{ref}\left[\frac{m_N}{m} C_{N\alpha} + \frac{m_N (X - x_{CGN})}{I_{YY}} \sum C_{N\alpha i}(X - x_{CPi})\right] l_N^2}{2EI - qS_{ref} C_{N\alpha N} l_N^2} \right] = F C_{N\alpha N} \,.$$

(7c)

That is, in eq. (7c) the term in brackets is the amplification factor, F, applied to all elements forward of x_N.

When eq. (7c) is substituted into eq's. (3) and (6) the result is we still have two linear equations with two unknowns giving solutions for A_z and $\frac{d^2\alpha}{dt^2}$, both proportional to α.

Finally, note that the bending stiffness is the product of the material Young's modulus, E, and the cross section moment of inertia, I. For a beam of circular cross section,

$$I = \frac{\pi}{4}(R_o^4 - R_i^4),$$

where R_o and R_i are the outer and inner radii respectively.

APPENDIX F: ENGINEERING DRAWINGS

ITEM NO.	PART NUMBER	DESCRIPTION	NOTES	QTY.
1	SR18-FW	FORWARD		1
2	SR18-AF	AFT		1
3	SR18-FW-RE-03-010	SHEAR PIN	MCMASTER P/N 97263A709	6

NOTES
1. INTERPRET DWG AS PER ANSI Y14.5
2. COUPLE SUCH THAT PAINT PATTERN IS ALIGNED

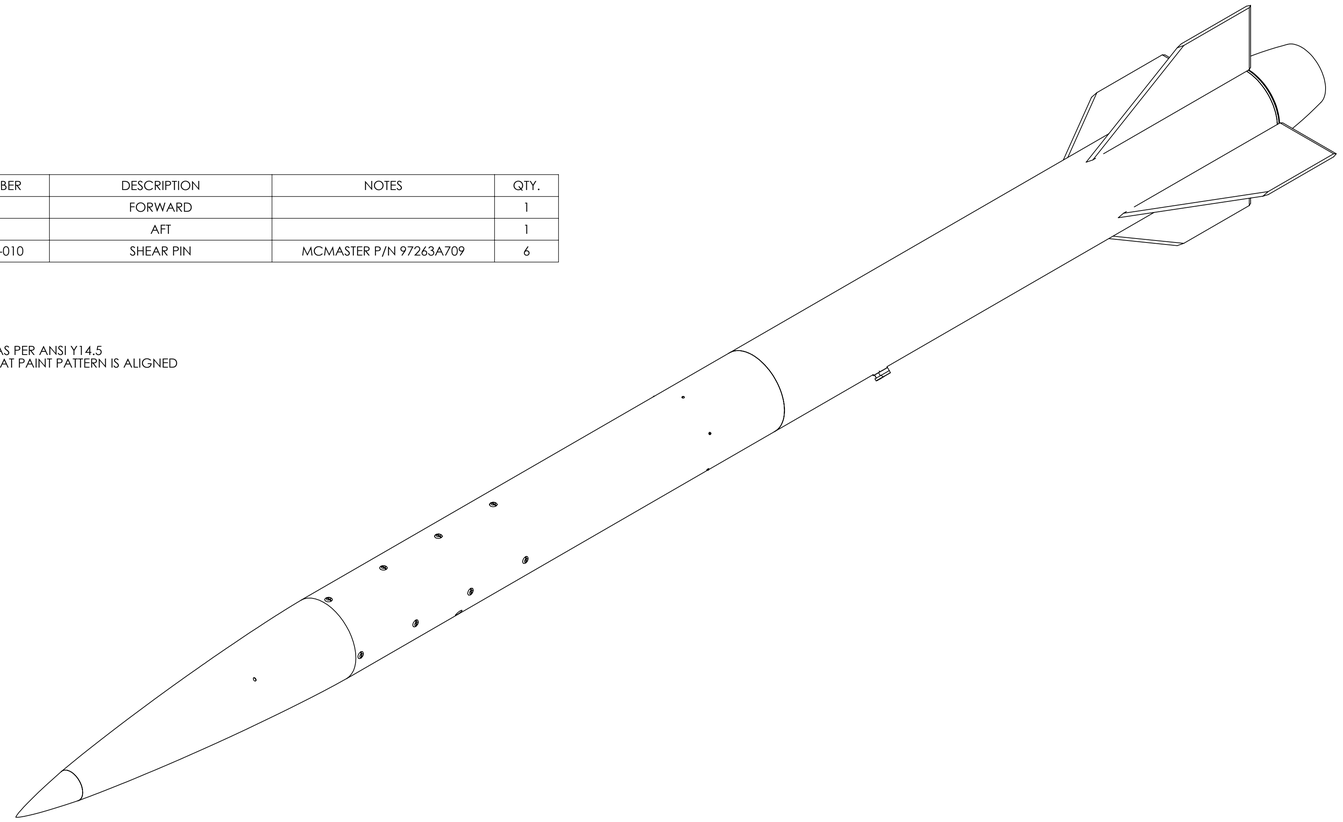

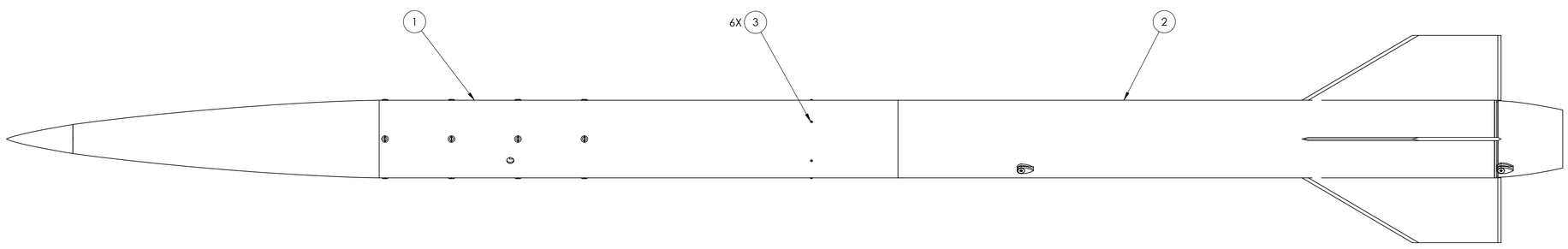

Concordia UNIVERSITY	MATERIAL	SURFACE ROUGHNESS √	TITLE SUPERSONICE
	FINISH	TOLERANCES X ± .1 X ± .01 X ± .005 XXX ± .005 ANGLE ± .5°	
PROPRIETARY INFORMATION NOT TO BE REPRODUCED WITHOUT AUTHORIZATION FROM CONCORDIA UNIVERSITY	DESIGNER O.KHALIMONOV	ALL DIMENSIONS IN INCHES UNLESS OTHERWISE SPECIFIED	SIZE D DATE 5/27/2018 USED ON SR18
	DRAFTER M.HOANG-CAO	APPROVED O.D'ANGELO	SCALE 1:5 SHEET 1 / 1 DWG NO. SR18 REV NO. 00

ITEM NO.	PART NUMBER	DESCRIPTION	NOTES	QTY.
1	SR18-FW-FR-00	FRAME ASSY		1
2	SR18-FW-AV-11	AVIONICS ASSY		1
3	SR18-FW-PA-05	PAYLOAD ASSY		1
4	SR18-FW-BA	BALLAST	NOT ILLUSTRATED	1
5	SR18-FW-RE-00	RECOVERY ASSY		1

NOTE

1. INTERPRET DWG AS PER ANSI Y14.5
2. MOUNT FRAME TO FUSELAGE SUCH THAT CAMERA & RBF HOLES ALIGN

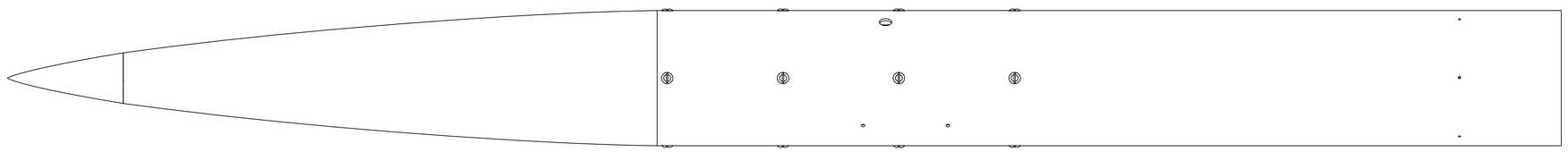

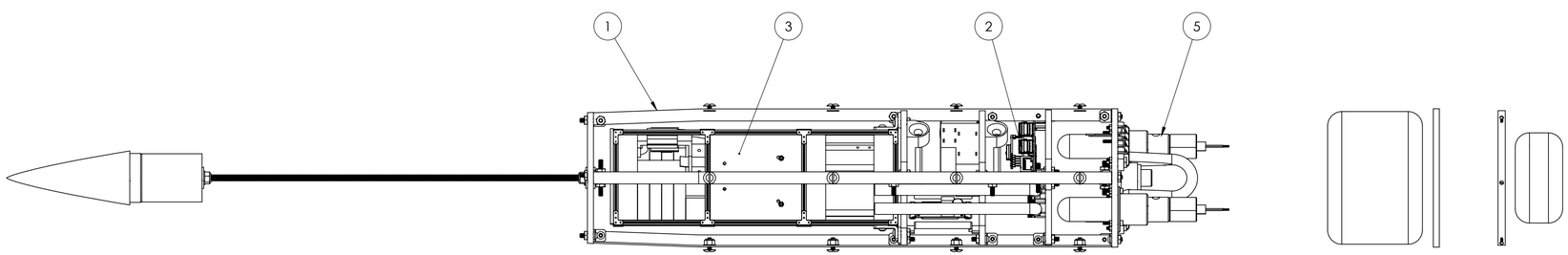

INTERNAL VIEW

Concordia UNIVERSITY	MATERIAL	SURFACE ROUGHNESS √	TITLE **FORWARD**
	FINISH	TOLERANCES X ± .1 X ± .05 .XX ± .005 .XXX ± .002 ANGLE ± .5°	
PROPRIETARY INFORMATION NOT TO BE DISCLOSED OR REPRODUCED WITHOUT AUTHORIZATION FROM CONCORDIA UNIVERSITY	DESIGNER **O.KHALIMONOV**	ALL DIMENSIONS IN **INCHES** UNLESS OTHERWISE SPECIFIED	SIZE DATE **5/27/2018** USED ON **SR18**
	DRAFTER **M.HOANG-CAO**	APPROVED **O.D'ANGELO**	SCALE **1:3** SHEET **1 / 1** DWG NO. **SR18-FW** REV NO. **00**

ITEM NO.	PART NUMBER	DESCRIPTION	NOTES	QTY.
1	SR18-FW-FR-00-001	RAILS		4
2	SR18-FW-FR-00-007	NOSECONE TIP		1
3	SR18-FW-FR-00-010	FORWARD FUSELAGE		1
4	90015A308	LOCKNUT	MCMASTER P/N	16
5	90322A657	THREADED ROD	MCMASTER P/N	1
6	93286A049	LOCKNUT	MCMASTER P/N	3
7	93298A115	LOCKNUT 1/4"-28	MCMASTER P/N	3
8	SR18-FW-FR-00-002	BULKHEAD		1
9	90480A009	HEXNUT 8-32	MCMASTER P/N	8
10	92949A196	MACHINESCREW 8-32	MCMASTER P/N	8
11	SR18-FR-00-05	BALLAST	2LBS	1
12	SR18-FW-FR-01-01	L-BRACKET		4
13	93298A109	SCREW	MCMASTER P/N	16

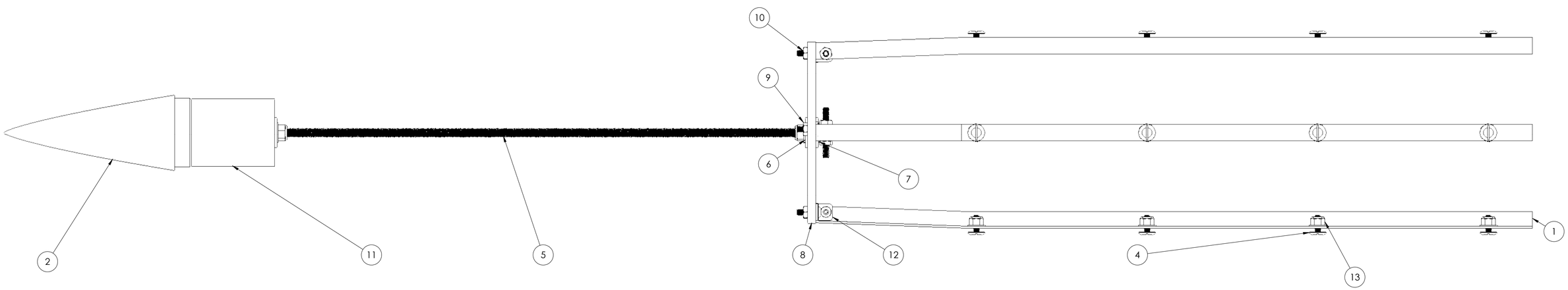

Concordia UNIVERSITY	MATERIAL	SURFACE ROUGHNESS	TITLE **FRAME ASSY**
	FINISH	TOLERANCES X ± .1 X.X ± .05 X.XX ± .005 X.XXX ± .002 ANGLE ± .5°	
PROPRIETARY INFORMATION NOT TO BE DISCLOSED WITHOUT WRITTEN PERMISSION FROM CONCORDIA UNIVERSITY	DESIGNER **O.KHALIMONOV**	ALL DIMENSIONS IN **INCHES** UNLESS OTHERWISE SPECIFIED	SIZE D DATE **2018-05-27** USED ON **SR18-FW-RA**
	DRAFTER **M.HOANG-CAO**	APPROVED **O.D'ANGELO**	SCALE **1:2** SHEET **1 / 1** DWG NO. **SR18-FW-FR-00** REV NO. **00**

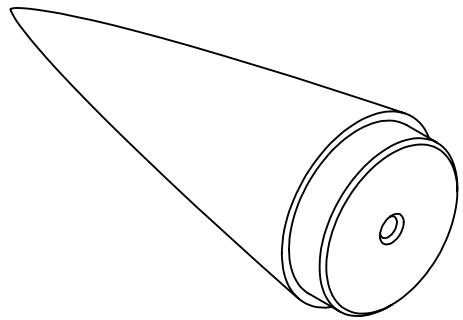

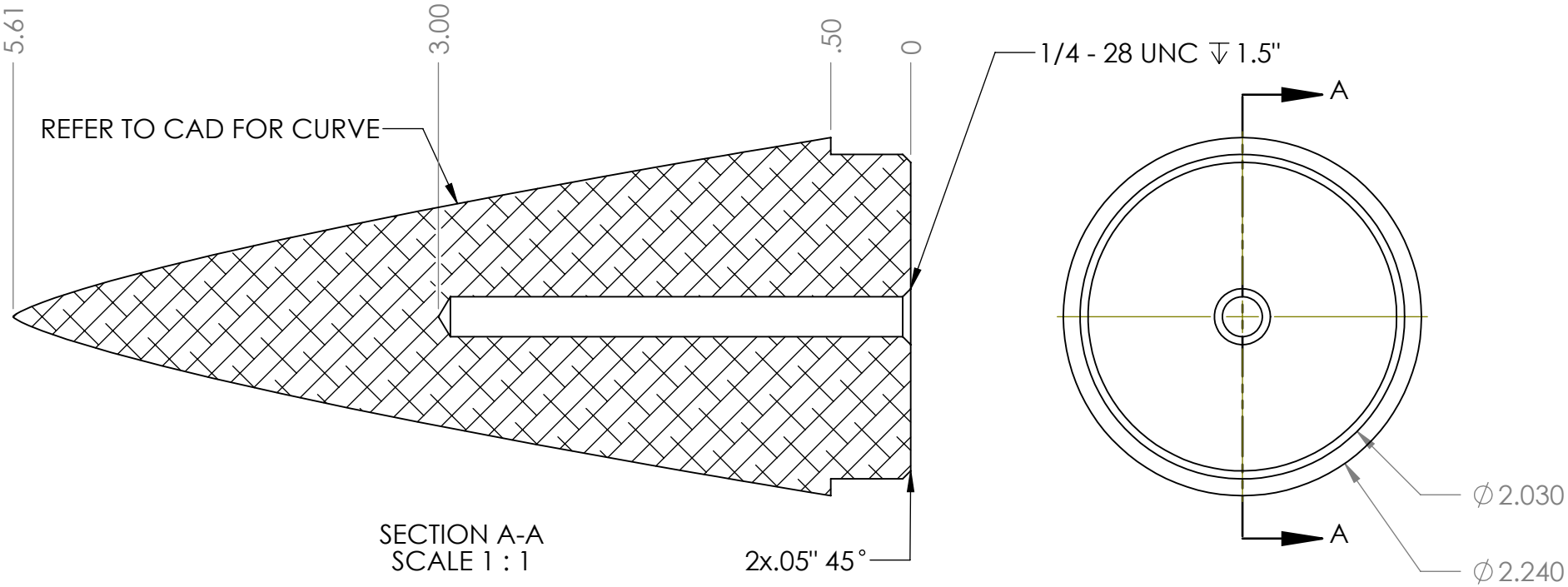

Concordia	MATERIAL **Aluminum 60601 T6 ∅2.5"x6"**	UNLESS OTHERWISE SPECIFIED	SURFACE ROUGHNESS √32	TITLE **Nosecone Tip**	
	FINISH **Clean**		TOLERANCES X ± .1 .X ± .05 .XX ± .005 .XXX ± .002 ANGLE ± .5°		
PROPRIETARY INFORMATION NOT TO BE RELEASED WITHOUT WRITTEN AUTHORIZATION FROM CONCORDIA UNIVERSITY	DESIGNER **O.Khalimonov**	ALL DIMENSIONS IN **INCHES** UNLESS OTHERWISE SPECIFIED		A SIZE	DATE **25-May-2018**	USED ON **SC- Rocketry**
	DRAFTER **O.Khalimonov**	APPROVED **O.Khalimonov**	SCALE **1:1**	SHEET **1 / 1**	DWG NO. **00025**	REV NO. **00**

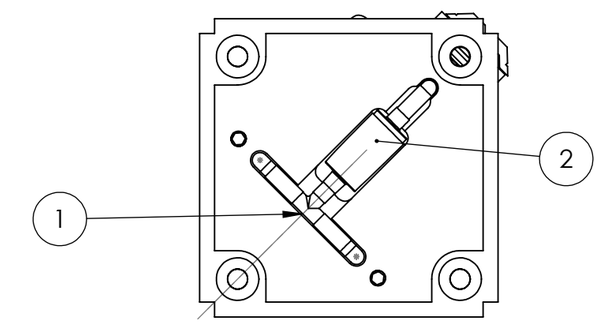

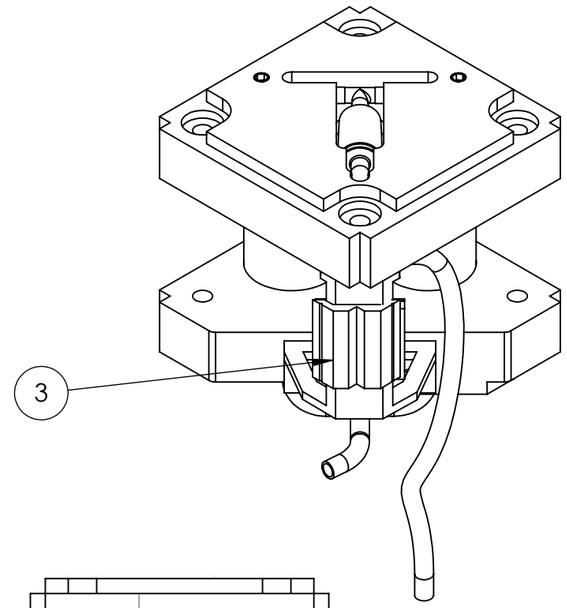

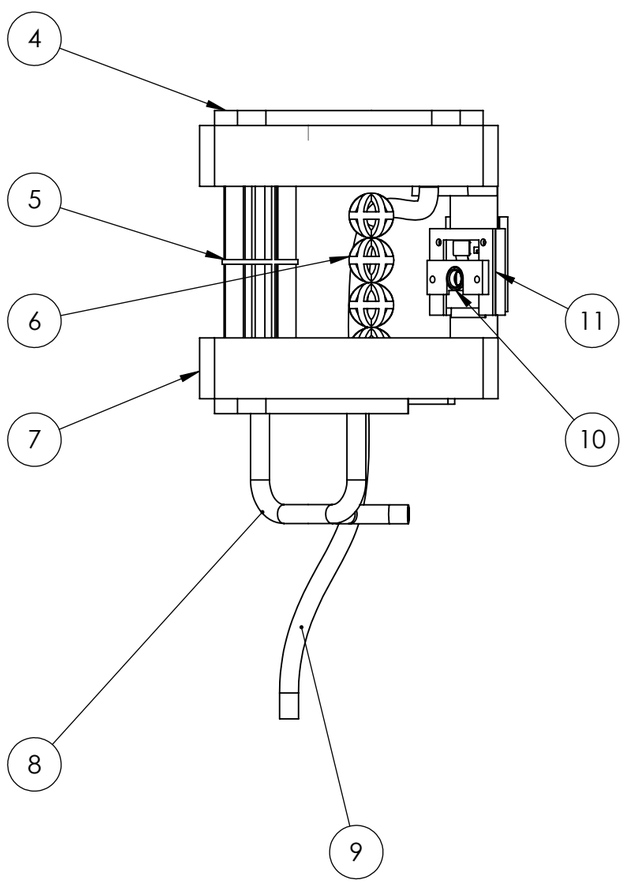

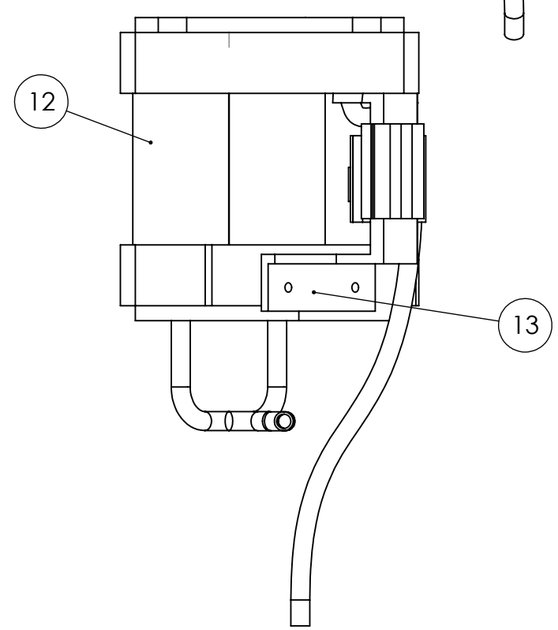

ITEM NO.	PART NUMBER	Description	QTY.
1	SR18-FW-PA-05-001	Three Way Link	1
2	SR18-FW-PA-05-003	One Way Valve	1
3	SR18-FW-PA-02-010	Camera Mount Back Plate	1
4	SR18-FW-PA-02-000	Tank Block A	1
5	SR18-FW-PA-02-003	Baffle 1	1
6	SR18-FW-PA-02-004	Baffle 2	4
7	SR18-FW-PA-02-001	Tank Block B	1
8	SR18-FW-PA-01-001	T-junction	1
9	SR18-FW-PA-02-006	Air Tube	1
10	SR18-FW-CM-00-004	Pi Camera	1
11	SR18-FW-CM-00-013	Pi camera Mount	1
12	SR18-FW-PA-02-002	Small Tank	2
13	SR18-FW-PA-02-009	Upper Camera Mount	1

BAFFLES 1 AND 2 ARE IN SEPERATE TANKS

PROPRIETARY INFORMATION NOT TO BE RELEASED WITHOUT WRITTEN AUTHORIZATION FROM CONCORDIA UNIVERSITY

MATERIAL **N/A**
FINISH **N/A**
DESIGNER **K.BOLUSI**
DRAFTER **J.CANIZALES**
ALL DIMENSIONS IN **INCHES** UNLESS OTHERWISE SPECIFIED
APPROVED **O.KHALIMONOV**
SURFACE ROUGHNESS √XX
TOLERANCES X ± .1, .X ± .05, .XX ± .005, .XXX ± .002, ANGLE ± .5°
TITLE **TOP UNIT ASSEMBLY**
B SIZE
DATE **2018-05-27**
USED ON **ROCKETRY**
SCALE **1:4**
SHEET **1 / 1**
DWG NO. **1**
REV NO. **00**

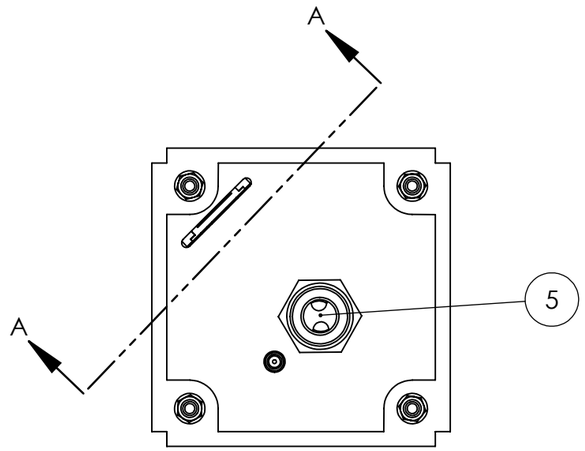

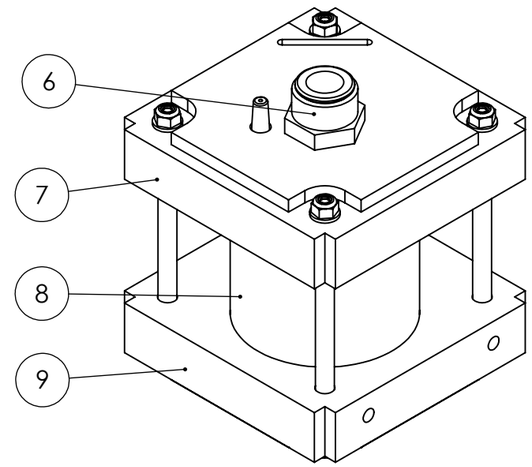

ITEM NO.	PART NUMBER	Description	QTY.
1	SR18-FW-PA-05-003	One Way Valve	1
2	94185A581	Threaded Rod	4
3	SR18-FW-PA-03-003-02	Nozzle End	1
4	94710A101	Locking Nut	8
5	SR18-FW-PA-03-003-02	Vortex Insert	1
6	SR18-FW-PA-03-003-03	Push-To-Connect Fitting	1
7	SR18-FW-PA-03-000	Tank Block C	1
8	SR18-FW-PA-03-002	Big Tank	1
9	SR18-FW-PA-03-001	Tank Block D	1
10	SR18-FW-PA-03-004	Lower Camera Mount	1
11	SR18-FW-CM-00-014	Pi Camera	1
12	SR18-FW-CM-00-013	Camera Mount	1

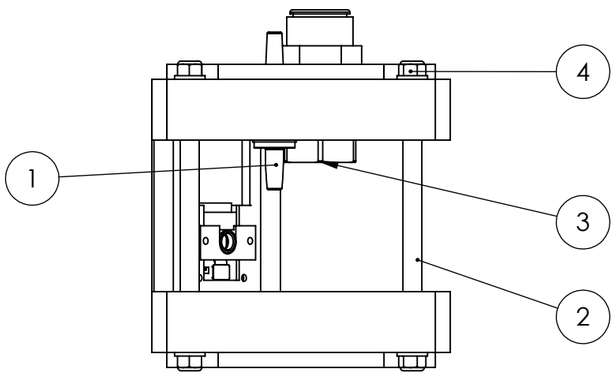

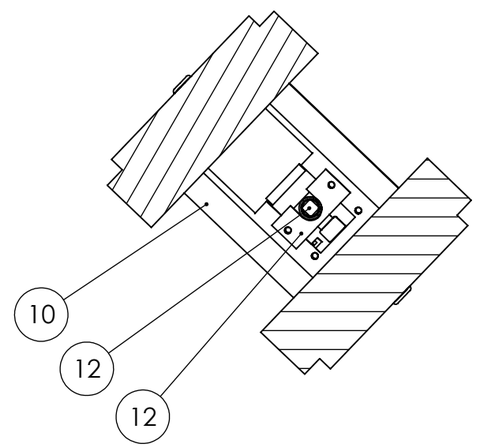

SECTION A-A

Concordia UNIVERSITY	MATERIAL **N/A**		SURFACE ROUGHNESS √XX	TITLE **BOTTOM UNIT ASSEMBLY**	
	FINISH **N/A**		TOLERANCES X ± .1 .X ± .05 .XX ± .005 .XXX ± .002 ANGLE ± .5° (UNLESS OTHERWISE SPECIFIED)		
PROPRIETARY INFORMATION NOT TO BE RELEASED WITHOUT WRITTEN AUTHORIZATION FROM CONCORDIA UNIVERSITY	DESIGNER **K.BOLUSI**	ALL DIMENSIONS IN **INCHES** UNLESS OTHERWISE SPECIFIED	B SIZE	DATE **2018-05-27**	USED ON **ROCKETRY**
	DRAFTER **J.CANIZALES**	APPROVED **O.KHALIMONOV**	SCALE **1:2**	SHEET **1 / 1**	DWG NO. **1**	REV NO. **00**

ITEM NO.	PART NUMBER	DESCRIPTION	QTY.
1	SR18-FW-PA-03-003-02	VORTEX GENERATOR	1
2	SR18-FW-PA-03-003-02	SPRAY NOZZLE	1
3	SR18-FW-PA-03-003-03	1/2" PIPE PUSH-FITTING	1

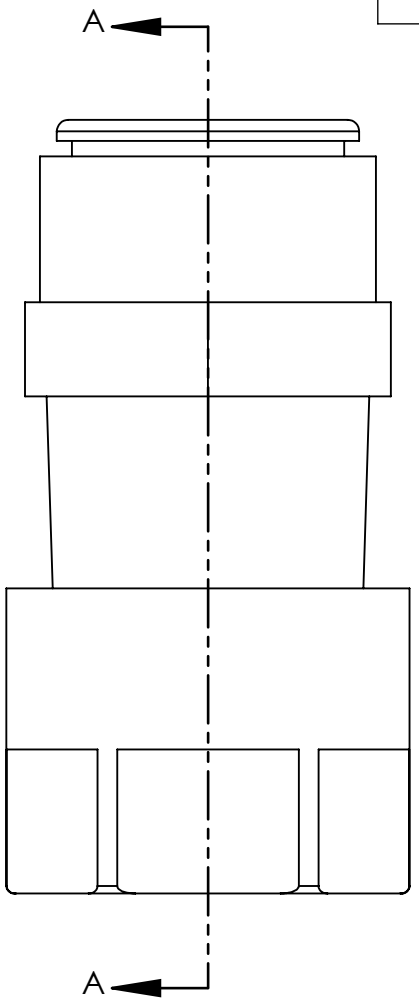

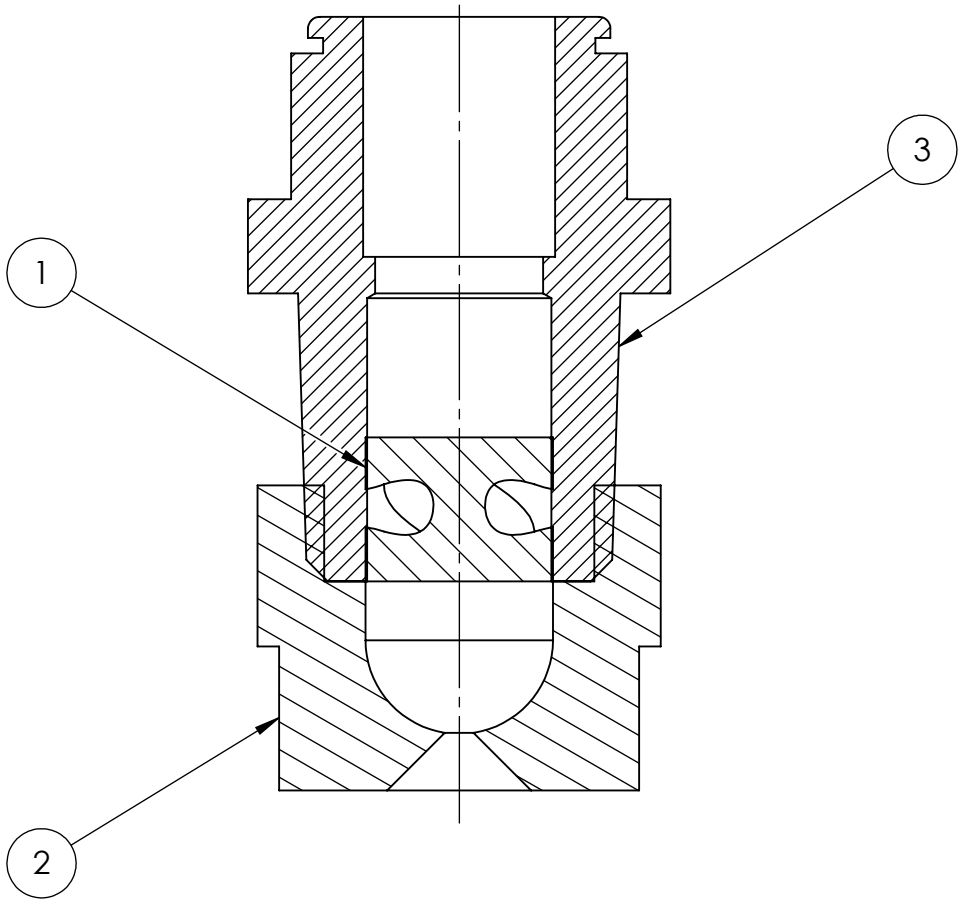

SECTION A-A

Concordia	MATERIAL -		SURFACE ROUGHNESS √63	TITLE SPRAY NOZZLE ASSY		
	FINISH -		TOLERANCES X ± .1, .X ± .05, .XX ± .005, .XXX ± .002, ANGLE ± .5°			
PROPRIETARY INFORMATION NOT TO BE RELEASED WITHOUT WRITTEN AUTHORIZATION FROM CONCORDIA UNIVERSITY	DESIGNER **D.CANIZALES**	ALL DIMENSIONS IN **INCHES** UNLESS OTHERWISE SPECIFIED		A SIZE	DATE **5/25/2018**	USED ON **SC**
	DRAFTER **D.CANIZALES**	APPROVED **K.BOLUSI**	SCALE **2:1**	SHEET **1 / 1**	DWG NO. **1**	REV NO. **00**

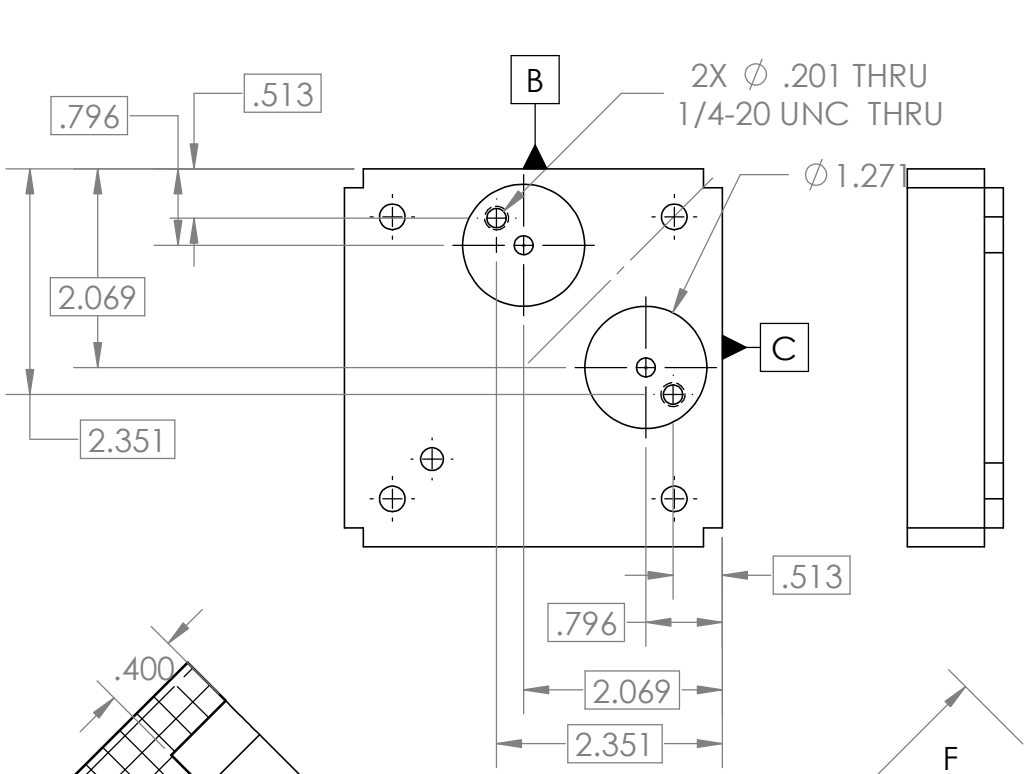

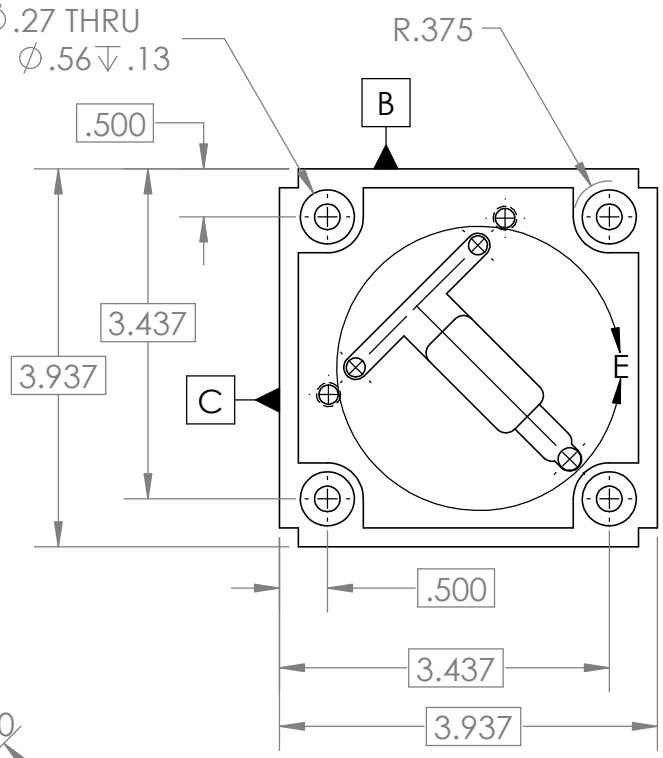

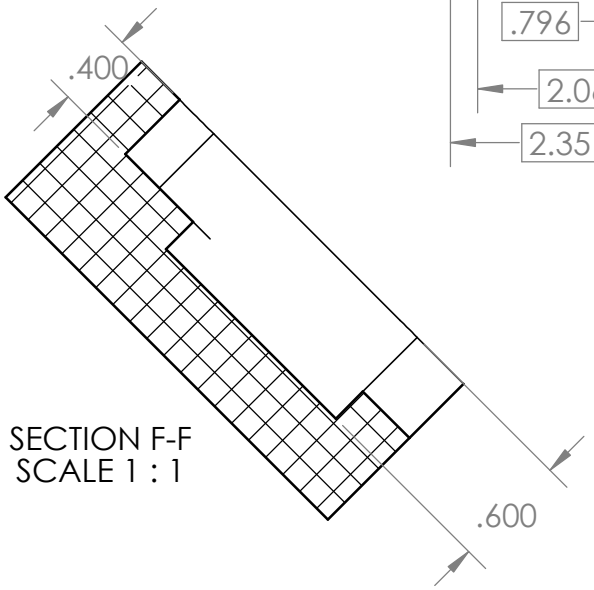

SECTION F-F
SCALE 1 : 1

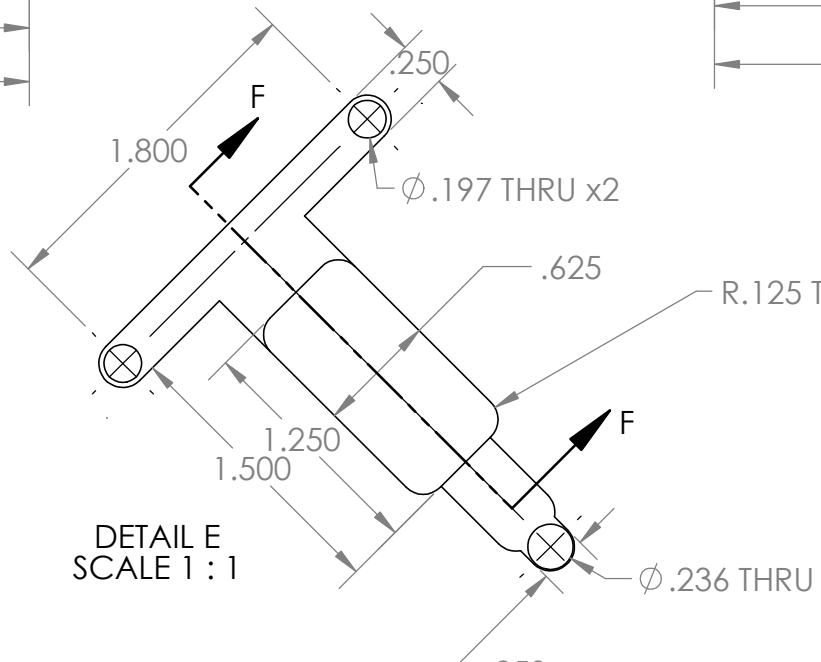

DETAIL E
SCALE 1 : 1

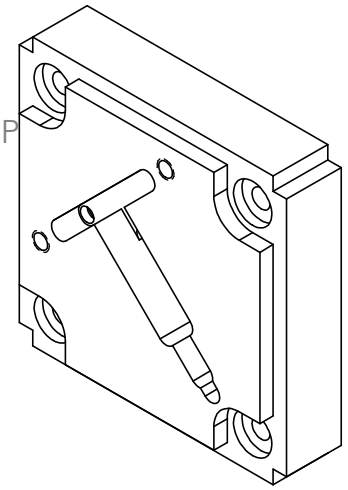

Concordia University	MATERIAL **WHITE ACETAL 4X4X1 THK**		SURFACE ROUGHNESS 63	TITLE **Tank Block A**	
	FINISH **CLEAN**		TOLERANCES X ± .1, .X ± .05, .XX ± .005, .XXX ± .002, ANGLE ± .5°		
PROPRIETARY INFORMATION NOT TO BE RELEASED WITHOUT WRITTEN AUTHORIZATION FROM CONCORDIA UNIVERSITY	DESIGNER **K.BOLUSI**	ALL DIMENSIONS IN **INCHES** UNLESS OTHERWISE SPECIFIED	A SIZE	DATE **2018-05-25**	USED ON **SC**
	DRAFTER **D.CANIZALES**	APPROVED **M.REMBACZ**	SCALE **1:2**	SHEET **1 / 1**	DWG NO. **1**	REV NO. **00**

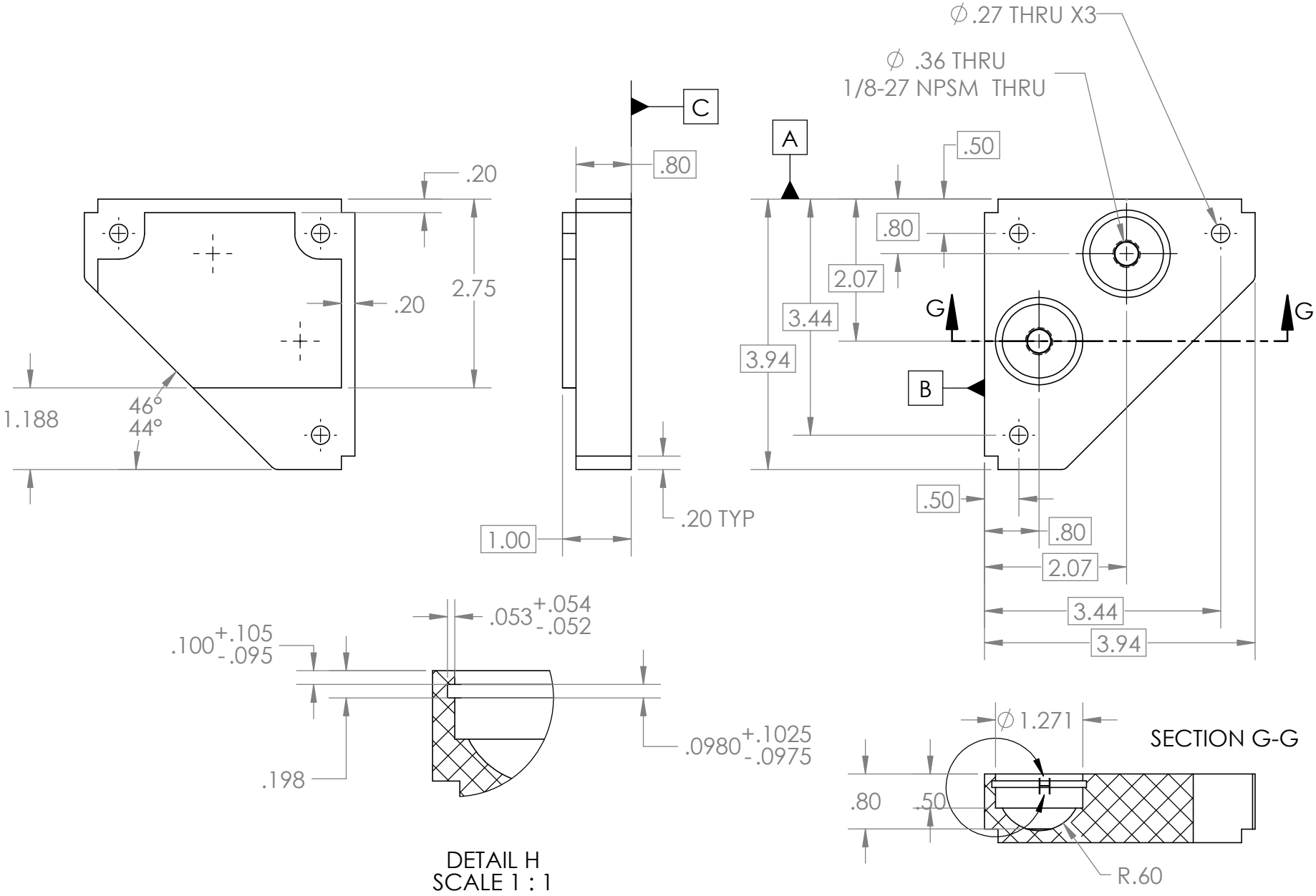

Concordia University	MATERIAL **WHITE ACETAL 4X4X1 THK**		SURFACE ROUGHNESS 63	TITLE **Tank Block B**	
	FINISH **CLEAN**		TOLERANCES X ± .1, .X ± .05, .XX ± .005, .XXX ± .002, ANGLE ± .5°		
PROPRIETARY INFORMATION NOT TO BE RELEASED WITHOUT WRITTEN AUTHORIZATION FROM CONCORDIA UNIVERSITY	DESIGNER **K.BOLUSI**	ALL DIMENSIONS IN **INCHES** UNLESS OTHERWISE SPECIFIED		A SIZE	DATE **2018-05-25** USED ON **SC**
	DRAFTER **D.CANIZALES**	APPROVED **M.REMBACZ**	SCALE **1:2**	SHEET **1 / 1** DWG NO. **1**	REV NO. **00**

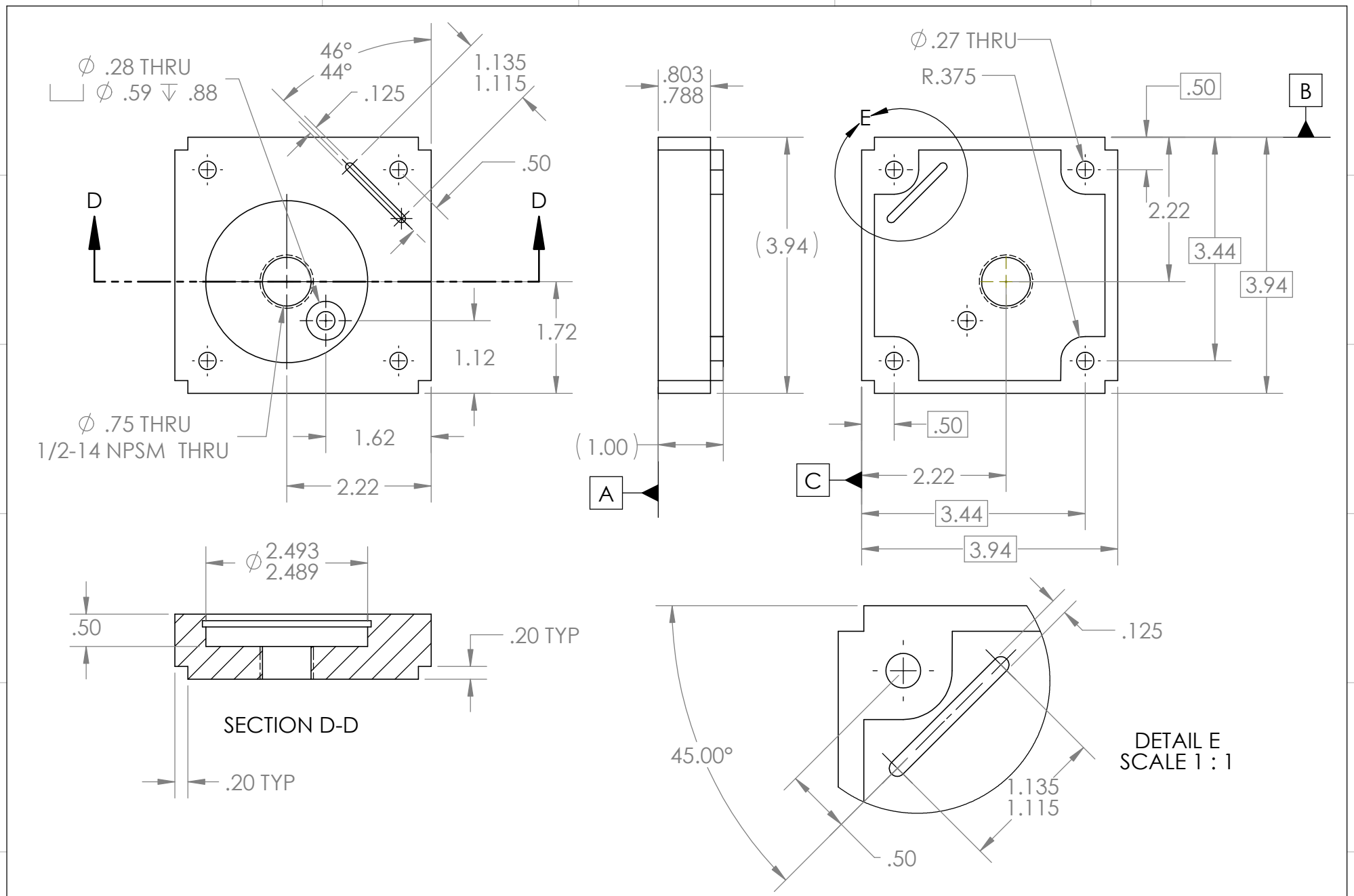

Concordia University	MATERIAL **WHITE ACETAL 4X4X1 THK**		SURFACE ROUGHNESS 63	TITLE **Tank Block C**	
	FINISH **CLEAN**		TOLERANCES X ± .1, .X ± .05, .XX ± .005, .XXX ± .002, ANGLE ± .5° (UNLESS OTHERWISE SPECIFIED)		
PROPRIETARY INFORMATION NOT TO BE RELEASED WITHOUT WRITTEN AUTHORIZATION FROM CONCORDIA UNIVERSITY	DESIGNER **K.BOLUSI**	ALL DIMENSIONS IN **INCHES** UNLESS OTHERWISE SPECIFIED		A SIZE	DATE **2018-05-25** USED ON **SC**
	DRAFTER **D.CANIZALES**	APPROVED **F.LASTNAME**	SCALE **1:2**	SHEET **1 / 1** DWG NO. **1**	REV NO. **00**

NOTES:
1 DO NOT MEASURE DRAWING
2 UOS DIMENSIONS ARE IN INCHES
3 INTERPRET AS PER ASME Y14.5M-1994
4 UOS BREAK EDGES .003-.015
5 UOS CORNERS MUST HAVE FILLETS R.005-.020

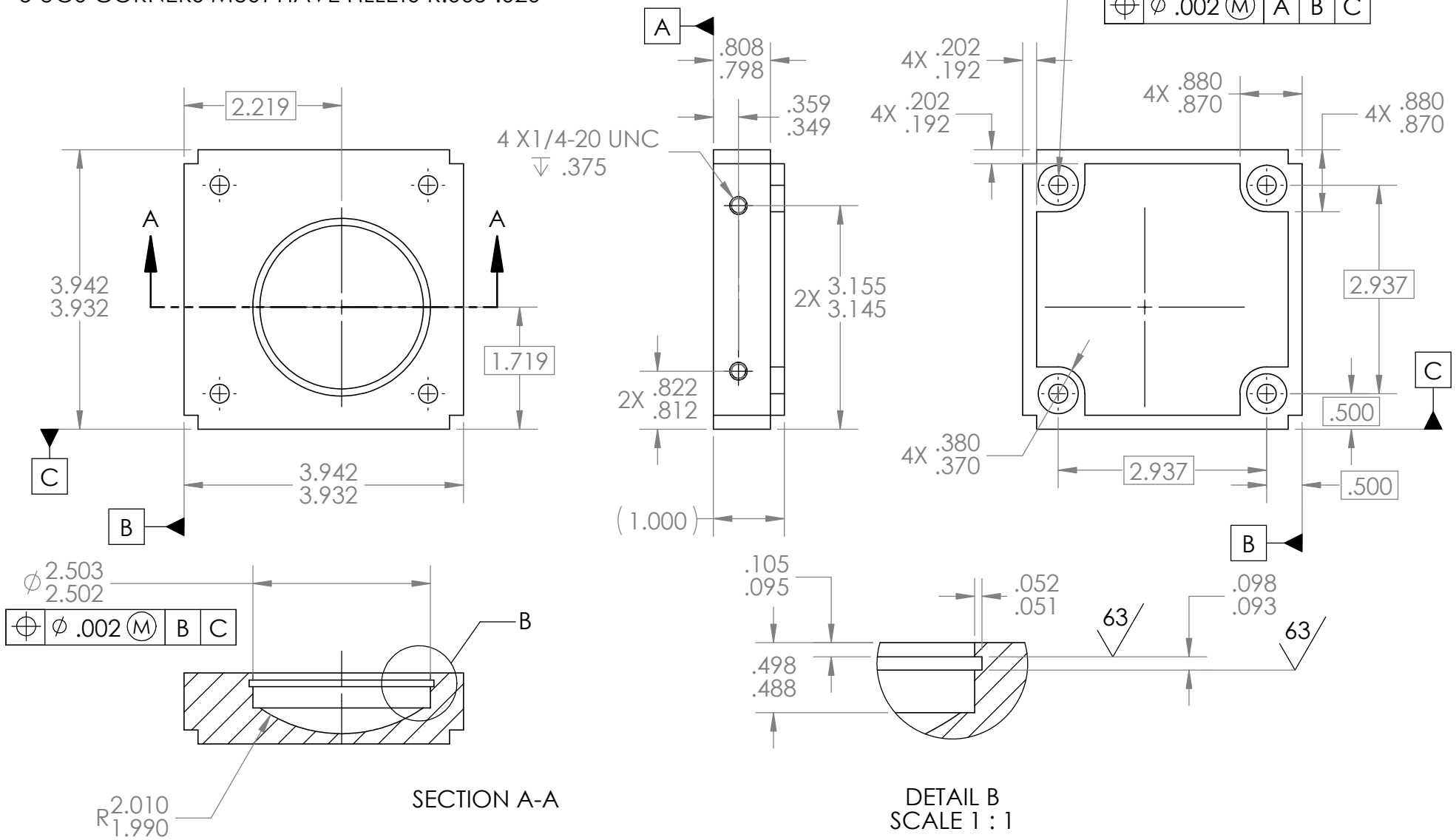

SECTION A-A

DETAIL B
SCALE 1 : 1

OMIT FOR
PROTOTYPE BUILD

Concordia University	MATERIAL **WHITE ACETAL 4X4X1 THK**	SURFACE ROUGHNESS √63	TITLE **SR18-FW-PA-03-001-Tank_Block_D**	
	FINISH **-**	TOLERANCES X ± .1, .X ± .05, .XX ± .005, .XXX ± .002, ANGLE ± .5°		
PROPRIETARY INFORMATION NOT TO BE RELEASED WITHOUT WRITTEN AUTHORIZATION FROM CONCORDIA UNIVERSITY	DESIGNER **K.BOLUSI**	ALL DIMENSIONS IN **INCHES** UNLESS OTHERWISE SPECIFIED	A SIZE	DATE **2018-05-25** USED ON **ROCKETRY**
	DRAFTER **D.CANIZALES**	APPROVED **O.KHALIMONOV**	SCALE **1:2**	SHEET **1 / 1** DWG NO. **001** REV NO. **00**

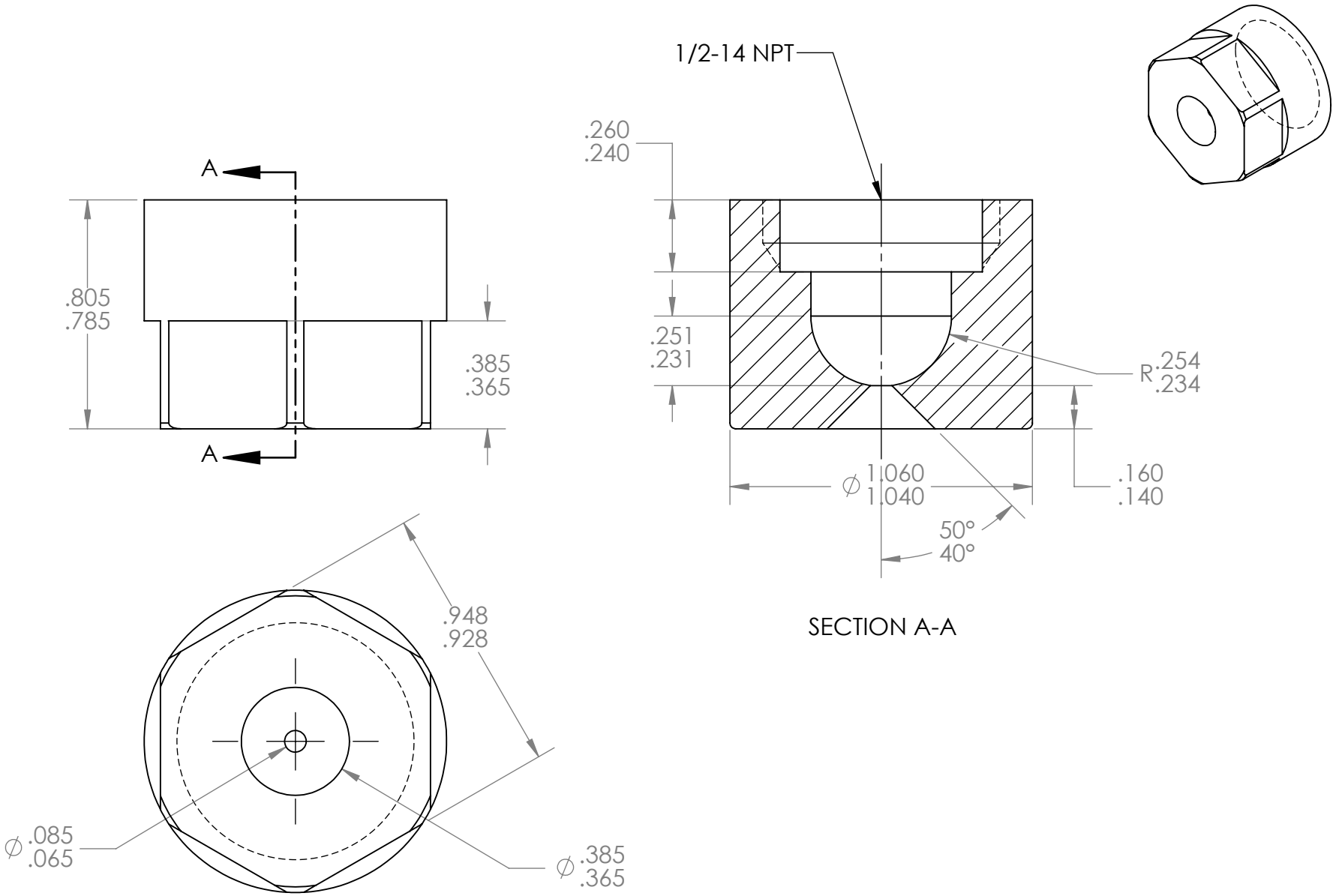

Concordia	MATERIAL **3D PRINTED BLACK PLA**		SURFACE ROUGHNESS √63	TITLE SPRAY NOZZLE ASSY			
	FINISH **MATTE 3D PRINTED**		TOLERANCES X ± .1, .X ± .05, .XX ± .005, .XXX ± .002, ANGLE ± .5°				
PROPRIETARY INFORMATION NOT TO BE RELEASED WITHOUT WRITTEN AUTHORIZATION FROM CONCORDIA UNIVERSITY	DESIGNER **D.CANIZALES**	ALL DIMENSIONS IN **INCHES** UNLESS OTHERWISE SPECIFIED		A SIZE	DATE **5/25/2018**	USED ON **SC**	
	DRAFTER **D.CANIZALES**	APPROVED **K.BOLUSI**	SCALE **2:1**	SHEET **1 / 1**	DWG NO. **1**	REV NO. **00**	

ITEM NO.	PART NUMBER	DESCRIPTION	NOTES	QTY.
1	SR18-FW-AV-10-001	AVIONICS BULKHEAD	G10 1/4" THICK	1
2	90480A009	10-32 NUT	MCMASTER P/N	16
3	92949A196	10-32 BOLT	MCMASTER P/N	16
4	SR18-FW-FR-01-01	L-BRACKET		8
5	SR18-FW-AV-02	FLIGHT COMPUTER	RASPBERRY PI PCB	1
6	SR18-FW-AV-11-005	RASPBERRY PI PCB		1
7	SR18-FW-AV-04-001	GPS BASE		1
8	SR18-FW-AV-01-001	PIN		18
9	SR18-FW-AV-01-002	PIN BODY		9
10	SR18-FW-AV-04-002	GPS CHIP		1
11	SR18-FW-AV-05-001	A&P BOARD		1
12	SR18-FW-AV-13-05	RFD900X		1
13	SR18-FW-AV-11-03	ANTENNA		2
14	SR18-FW-CM-00-001	CAMERA BAY BULKHEAD	G10 1/4" THICK	1
15	SR18-FW-CM-01-01	GOPRO HERO 4	4K CAMERA	1
16	SR18-FW-AV-12-01	SUPPORT	STRATOLOGGER/TELEMETRUM SUPPORT	1
17	SR18-FW-AV-06-001	TELEMETRUM BOARD	-	1
18	SR18-FW-AV-06-002	GPS		1
19	SR18-FW-AV-06-003	BUZZER	-	1
20	DG340-381	TERMINAL BLOCK	TERMINAL BLOCK	1
24	SR18-FW-AV-07	PERFECTFLITE STRATALOGGER	-	1
25	91115A502	4-40 STANDOFF	4-40 STANDOFF	8
26	SR18-FW-AV-14-01	SWTICHES	SINGLE POLE DOUBLE THROW SNAP ACTION SWITCH	2
27	SR18-FW-AV-14-02	RBF SUPPORT	3D PRINTED PLA SUPPORT	2
28	93505A472	4-40 STANDOFF	4-40 STANDOFF	7
29	-	LIPO		1
30	-	9V BATTERY		2

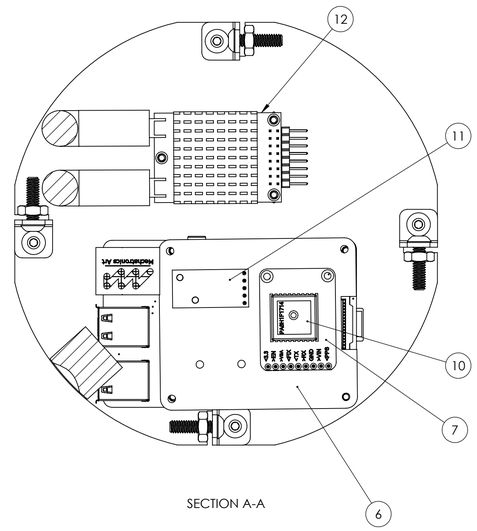

SECTION A-A

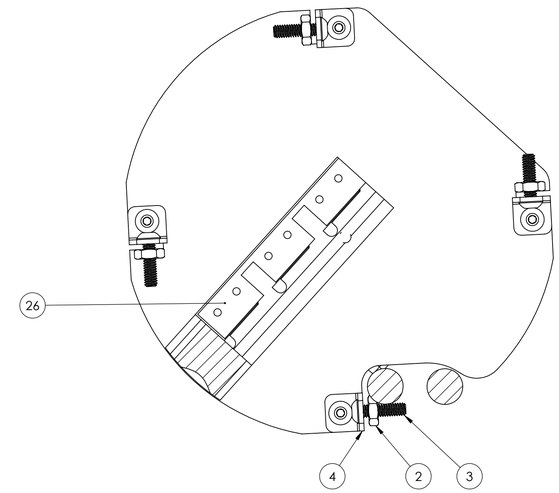

SECTION B-B

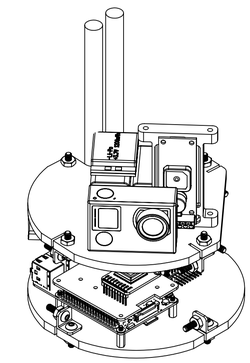

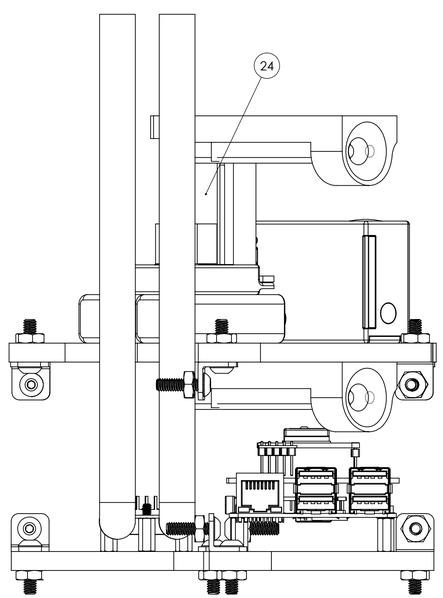

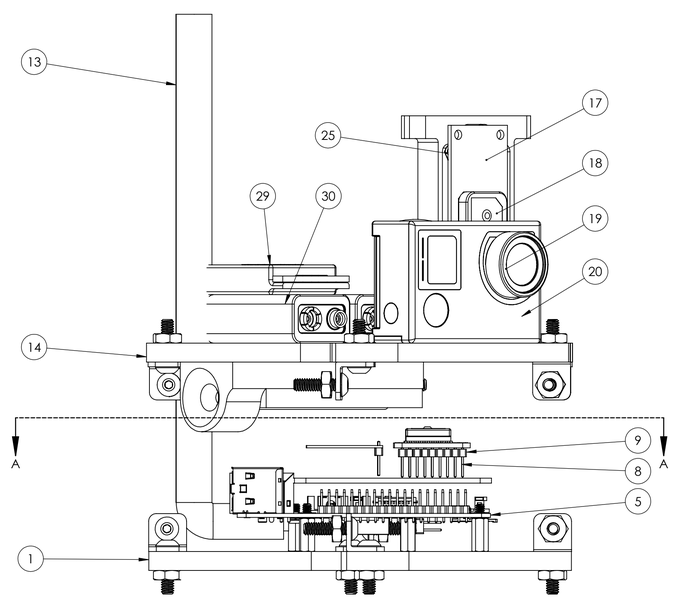

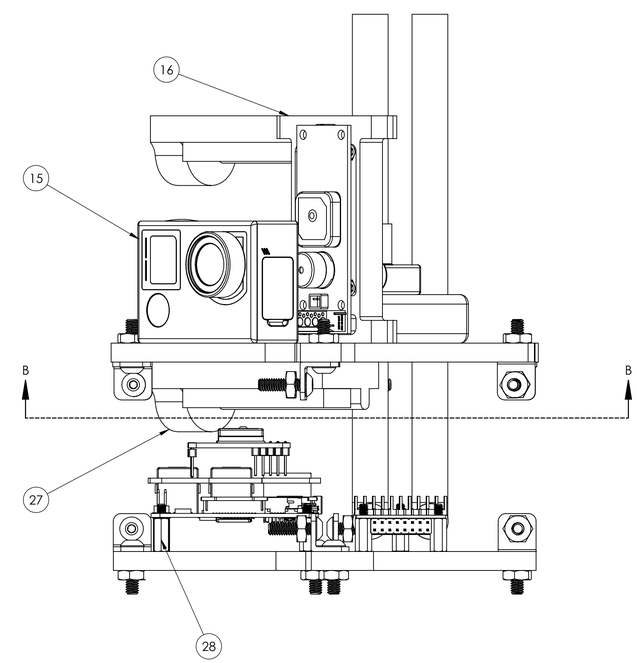

Concordia UNIVERSITY	MATERIAL AINSI 4130	SURFACE FINISH	TITLE SR18-FW-AV-11-Avionics_Assembly
	FINISH SEE NOTE 3	TOLERANCES X ± .1 X ± .05 .XX ± .005 .XXX ± .001 ANGLE ± 2°	
CONFIDENTIAL INFORMATION. NO PART OF THIS DOCUMENT MAY BE REPRODUCED, TRANSMITTED, TRANSLATED, OR DISCLOSED WITHOUT PRIOR WRITTEN CONSENT OF CONCORDIA UNIVERSITY	DESIGNER F.LASTNAME	ALL DIMENSIONS IN INCHES UNLESS OTHERWISE SPECIFIED	SIZE DATE 5/28/2018 USED ON PROJECT NAME
	DRAFTER F.LASTNAME	APPROVED F.LASTNAME	SCALE 1:1 SHEET 1 / 1 DWG NO. 123456789 REV NO. 00

ITEM NO.	PART NUMBER	DESCRIPTION	NOTES	QTY.
1	SR18-FW-RE-01-001	BULKHEAD		1
2	SR18-FW-RE-01-002	HOIST SWIVEL	MCMASTER P/N 2994T64	1
3	SR18-FW-RE-01-003	WASHER	MCMASTER P/N 93744A160	1
4	SR18-FW-RE-01-004	HOIST NUT	MCMASTER P/N 95462A031	1
5	SR18-FW-RE-01-006	BULKHEAD SCREW	MCMASTER P/N 92949A199	8
6	SR18-FW-RE-01-007	BULKHEAD NUT	MCMASTER P/N 90480A009	8
9	SR18-FW-RE-01-010	TERMINAL	MCMASTER P/N 7527K44	2
10	SR18-FW-RE-01-011	SCREW	MCMASTER P/N 91292A029	14
11	SR18-FW-RE-01-012	LOCKNUT	DIN 985-3-C	14
12	SR18-FW-RE-02	EJECTOR ASSY		2
13	SR18-FW-FR-01-01	L-BRACKET		4

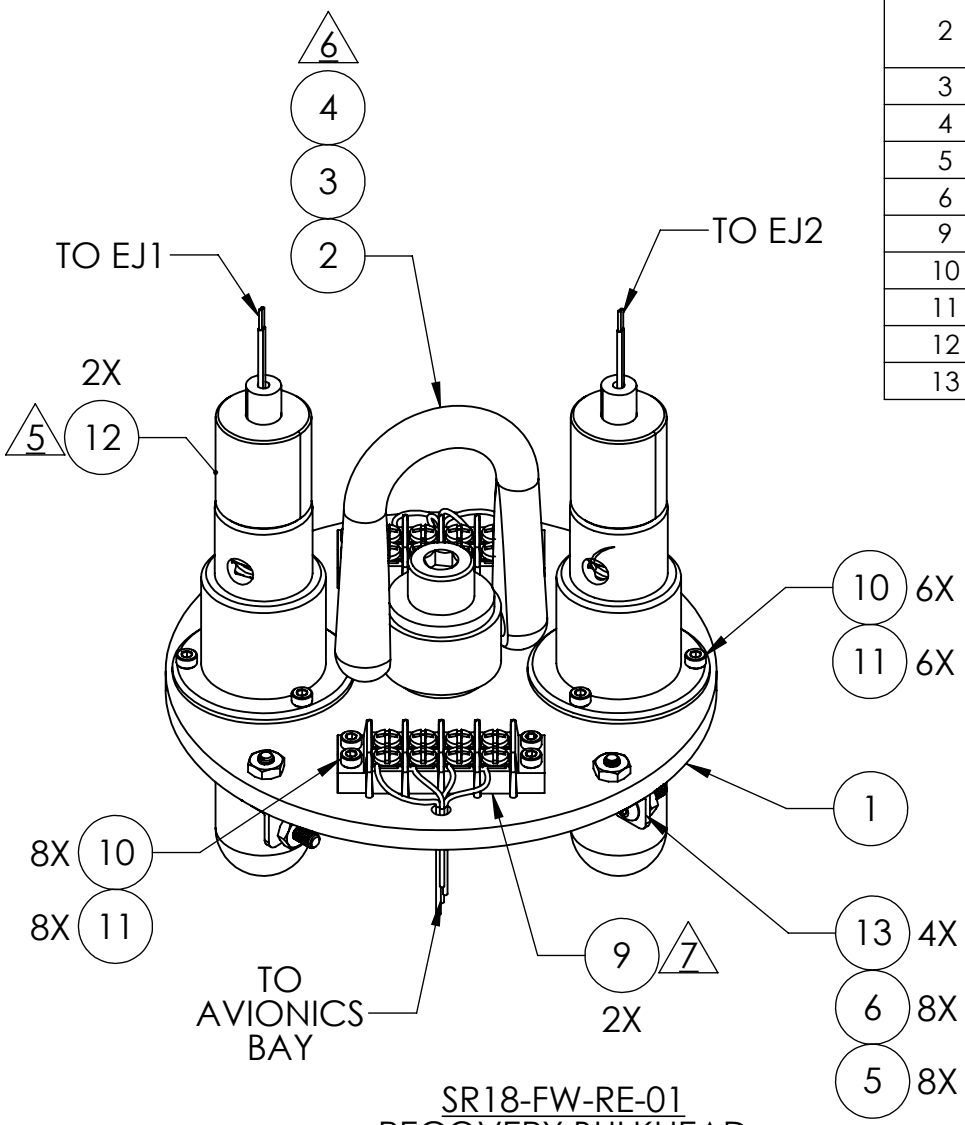

SR18-FW-RE-01
RECOVERY BULKHEAD
ISOMETRIC VIEW
LOOKING INBD FWD

NOTES

GENERAL

1 DWG TO BE INTERPRETED AS PER ANSI Y14.5
2 WIRING NOT FULLY SHOWN FOR SIMPLICITY

ASSEMBLY

3 SEAL W/ TEFLON TAPE OR ADHESIVES A/R
4 SECURE WIRING A/R
5 EJECTOR ASSY MAY BE INSTALLED IN VARIOUS CONFIGURATIONS
6 ENSURE ROTATION AREA CLEAR FROM OBSTRUCTIONS

IDENTIFICATION

7 CLEARLY MARKUP TERMINAL ZONES ON BULKHEAD AND WIRES:
- EJECTOR, MAIN - "EJ1"
- EJECTOR, SECONDARY - "EJ2"
- TENDER DESCENDER, MAIN - "TD1"
- TENDER DESCENDER, SECONDARY - "TD2"

Concordia UNIVERSITY	MATERIAL		SURFACE ROUGHNESS 63	TITLE **RECOVERY BULKHEAD ASSY**	
	FINISH		TOLERANCES X ± .1, .X ± .05, .XX ± .005, .XXX ± .002, ANGLE ± .5°		
PROPRIETARY INFORMATION NOT TO BE RELEASED WITHOUT WRITTEN AUTHORIZATION FROM CONCORDIA UNIVERSITY	DESIGNER **M.HOANG-CAO**	ALL DIMENSIONS IN **INCHES** UNLESS OTHERWISE SPECIFIED		A SIZE	DATE **5/21/2018** USED ON **SR18**
	DRAFTER **M.HOANG-CAO**	APPROVED **O.KHALIMONOV**	SCALE **1:2**	SHEET **1 / 1**	DWG NO. **SR-18-FW-RE-01** REV NO. **00**

NOTES

GENERAL

1 DWG TO BE INTERPRETED AS PER ANSI Y14.5

ASSEMBLY

2 SEAL W/ TEFLON TAPE A/R

3 CHECK FOR CONTINUITY, AND ENSURE RESISTANCE ~1.4Ω PRIOR TO INSTALLATION

4 TRIM WIRES TO 7IN. AND SOLDER ON TERMINAL LUGS

5 USE CAUTION AND WEAR PROTECTIVE EYEWEAR WHEN HANDLING EXPLOSIVES

ITEM NO.	PART NUMBER	DESCRIPTION	NOTES	QTY.
1	MJG89899	E-MATCH	CANADIAN ROCKET STORE P/N	1
2	SR18-FW-RE-02-002	HOUSING		1
3	SR18-FW-RE-02-003	BUSHING		1
4	SR18-FW-RE-02-004	NEEDLE		1
5	SR18-FW-RE-02-005	O-RING	MCMASTER P/N 1161N19	1
6	SR18-FW-RE-02-006	SPRING	MCMASTER P/N 9657K338	1
7	SR18-FW-RE-02-007	BASE		1
8	SR18-FW-RE-02-008	CANISTER	25G CO2	1
9	-	BLACK POWDER	FFFFG	A/R
10	7113K35	TERMINAL LUG	MCMASTER P/N, NI	2

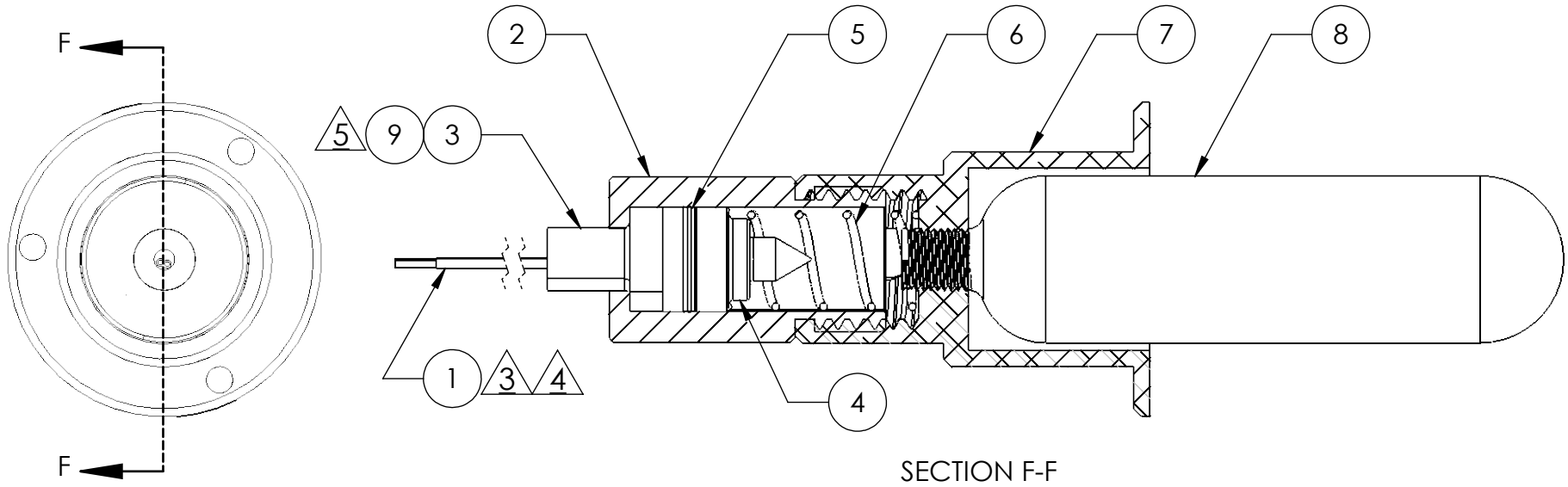

SECTION F-F

Concordia UNIVERSITY	MATERIAL		SURFACE ROUGHNESS √	TITLE **EJECTOR ASSY**	
	FINISH		TOLERANCES X ± .1, .X ± .05, .XX ± .005, .XXX ± .002, ANGLE ± .5° (UNLESS OTHERWISE SPECIFIED)		
PROPRIETARY INFORMATION NOT TO BE RELEASED WITHOUT WRITTEN AUTHORIZATION FROM CONCORDIA UNIVERSITY	DESIGNER **M.HOANG-CAO**	ALL DIMENSIONS IN **INCHES** UNLESS OTHERWISE SPECIFIED		A SIZE	DATE **5/18/2018** USED ON **SR18**
	DRAFTER **M.HOANG-CAO**	APPROVED **O.KHALIMONOV**	SCALE **1:1**	SHEET **1 / 1**	DWG NO. **SR18-FW-RE-02** REV NO. **00**

NOTES

GENERAL
1. INTERPRET DWG AS PER ANSI Y14.5

MODIFICATION
2. ZIG-ZAG STITCHES, SPACING 5
3. SIMPLE SINGLE STITCHES, SPACING 5

ASSEMBLY
4. CHECK FOR CONTINUITY, AND ENSURE RESISTANCE ~1.4Ω PRIOR TO INSTALLATION
5. TRIM WIRES TO 9IN, AND SOLDER ON TERMINAL LUGS
6. USE CAUTION AND WEAR PROTECTIVE EYEWEAR WHEN HANDLING EXPLOSIVES
7. Z-FOLD ALONG LINES
8. UNTANGLE SUSPENSION LINES
9. SEAL WITH TEFLON TAPE AND ADHESIVES
10. LOCK IN PLACE W/ PRUSIK KNOT

ITEM NO.	P/N	DESCRIPTION	NOTES	QTY
0	SR18-FW-RE-03	PARACHUTE ASSY		1
1	SR18-FW-RE-03-001	MAIN PARACHUTE	FRUITY CHUTES P/N: IFC-72	1
2	SR18-FW-RE-03-002	DROGUE PARACHUTE	FRUITY CHUTES P/N: CFC-30	1
3	SR18-FW-RE-03-003	TENDER DESCENDER	TINDER ROCKETRY L2 TENDER DESCENDER	2
4	SR18-FW-RE-03-004	MAIN BAG		1
5	SR18-FW-RE-03-005	20' SHOCK CORD W/ LOOP	MAC PERFORMANCE ROCKETRY $\frac{3}{8}$" TUBULAR KEVLAR	1
6	SR18-FW-RE-03-006	10' SHOCK CORD W/ LOOP	MAC PERFORMANCE ROCKETRY $\frac{3}{8}$" TUBULAR KEVLAR	3
7	SR18-FW-RE-03-007	QUICKLINK	1760LBS SWL	4
8	SR18-FW-RE-03-008	SPACER	3D PRINTED PLA 5% HONEYCOMB	3
11	SR18-FW-RE-03-011	SHEAR PIN HOUSING	MCMASTER P/N 92474A026	6
12	SR18-FW-RE-03-012	DROGUE BAG		1
13	SR18-FW-RE-03-015	HOUSING RING		1
14	SR18-FW-RE-03-014	PISTON BULKHEAD		1
15	NB-21	21" NOMEX BLANKET	FRUITY CHUTES	1
16	-	17" BLANKET	AS-17	1
17	-	DOUBLER		A/R
18	-	ELASTIC		13
19	-	VELCRO	.75"X3" PATCH	2
20	-	VELCRO	.75X3.75" PATCH	2
21	-	NYLON THREAD		A/R
22	-	BLACK POWDER	FFFFG BLACK POWDER	A/R
23	MJG89899	E-MATCH	CANADIAN ROCKET STORE P/N	2
24	7113K35	TERMINAL LUG	MCMASTER P/N	4
25	-	TWINE		A/R

Université Concordia University

MATERIAL	REFER TO B.O.M.	SURFACE ROUGHNESS √	TITLE PARACHUTE ASSY
FINISH		TOLERANCES (UNLESS OTHERWISE SPECIFIED) X ± .1, .X ± .05, .XX ± .005, .XXX ± .002, ANGLE ± .5°	
DESIGNER M.HOANG-CAO	ALL DIMENSIONS IN INCHES UNLESS OTHERWISE SPECIFIED		A SIZE · DATE 05/18/2018 · USED ON SR18
DRAFTER M.HOANG-CAO	APPROVED O.KHALIMONOV	SCALE NTS	SHEET 1 / 6 · DWG NO. SR18-FW-RE-03 · REV NO. 00

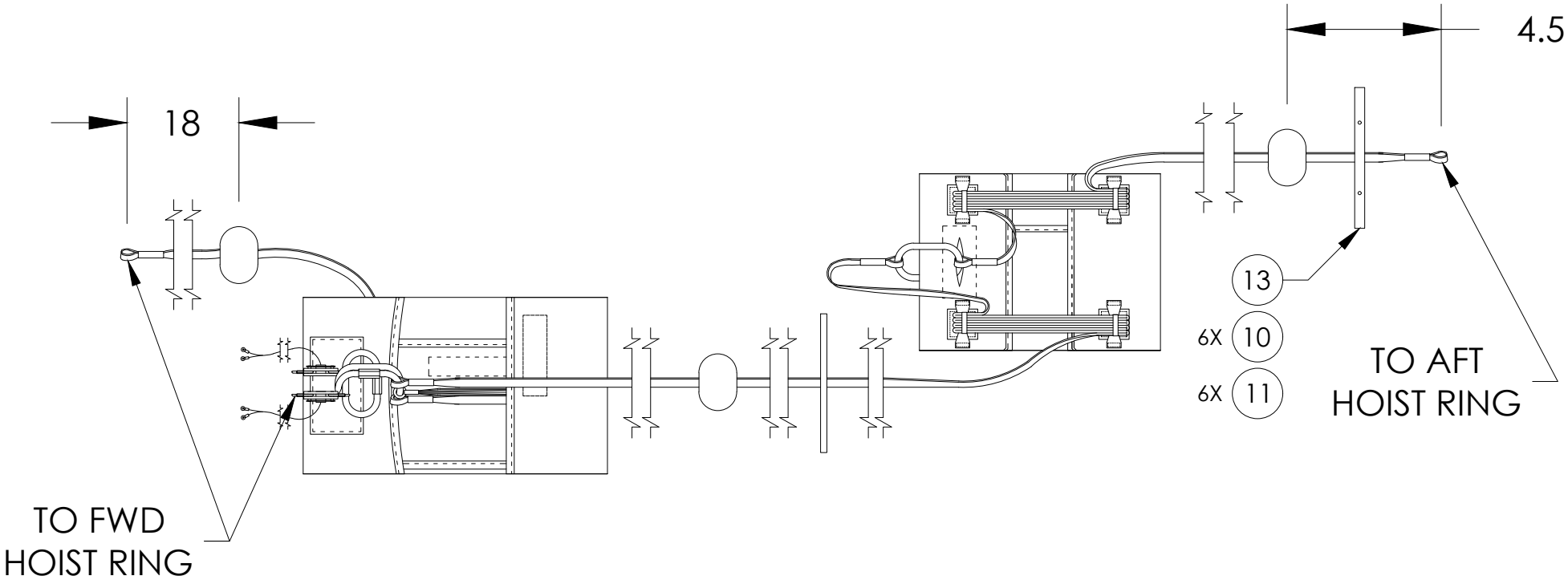

0

SR18-FW-RE-03
PARACHUTE ASSY
PACKED VIEW

Université Concordia University	MATERIAL	REFER TO B.O.M.	SURFACE ROUGHNESS √	TITLE	PARACHUTE ASSY
	FINISH		TOLERANCES X ± .1, .X ± .05, .XX ± .005, .XXX ± .002, ANGLE ± .5° (UNLESS OTHERWISE SPECIFIED)		
PROPRIETARY INFORMATION NOT TO BE RELEASED WITHOUT WRITTEN AUTHORIZATION FROM CONCORDIA UNIVERSITY	DESIGNER M.HOANG-CAO	ALL DIMENSIONS IN INCHES UNLESS OTHERWISE SPECIFIED		A SIZE	DATE 05/18/2018	USED ON SR18
	DRAFTER M.HOANG-CAO	APPROVED O.KHALIMONOV	SCALE NTS	SHEET 2 / 6	DWG NO. SR18-FW-RE-03	REV NO. 00

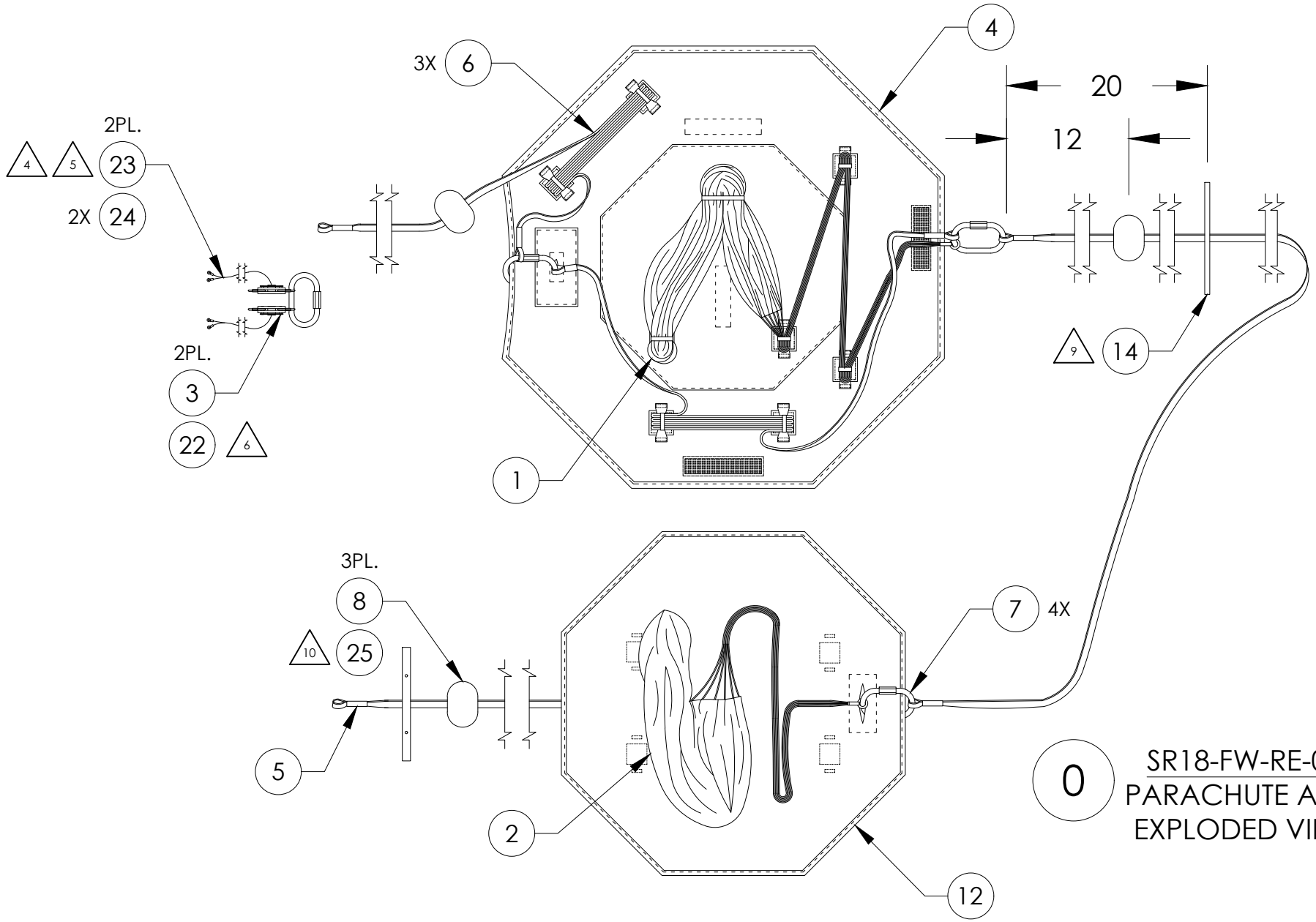

0

SR18-FW-RE-03
PARACHUTE ASSY
EXPLODED VIEW

Université Concordia University	MATERIAL **REFER TO B.O.M.**		SURFACE ROUGHNESS √	TITLE **PARACHUTE ASSY**	
	FINISH		TOLERANCES UNLESS OTHERWISE SPECIFIED X ± .1, .X ± .05, .XX ± .005, .XXX ± .002, ANGLE ± .5°		
PROPRIETARY INFORMATION NOT TO BE RELEASED WITHOUT WRITTEN AUTHORIZATION FROM CONCORDIA UNIVERSITY	DESIGNER **M.HOANG-CAO**	ALL DIMENSIONS IN **INCHES** UNLESS OTHERWISE SPECIFIED		A SIZE	DATE **05/18/2018**	USED ON **SR18**
	DRAFTER **M.HOANG-CAO**	APPROVED **O.KHALIMONOV**	SCALE **NTS**	SHEET **3 / 6**	DWG NO. **SR18-FW-RE-03**	REV NO. **00**

4

SR18-FW-RE-03-004
MAIN BAG
MODIFICATION

PRE-MODIFICATION

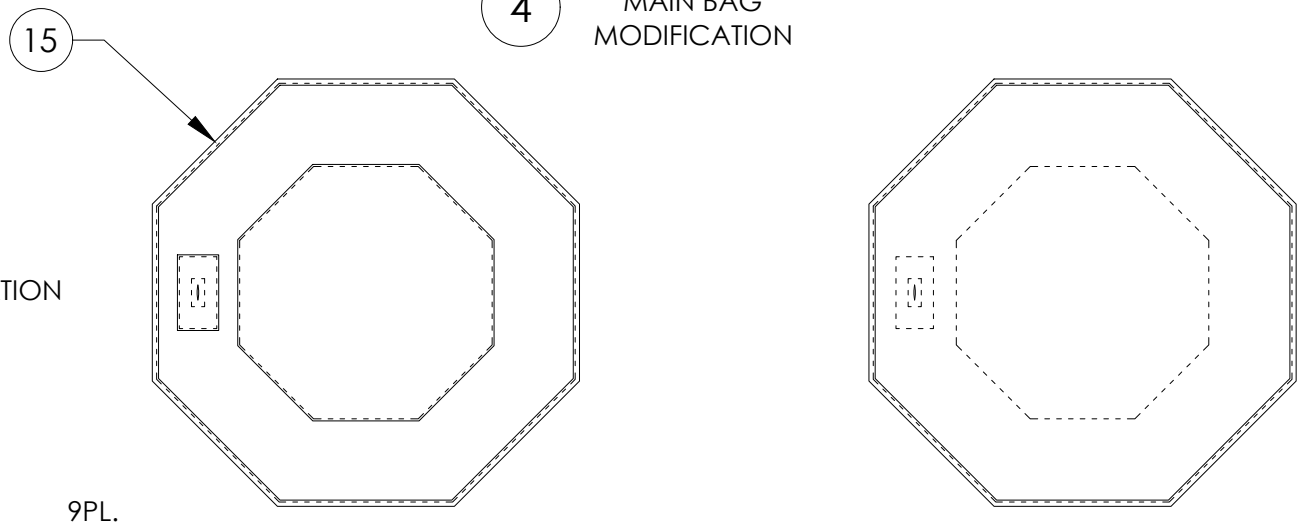

INTERNAL VIEW

EXTERNAL VIEW

POST-MODIFICATION

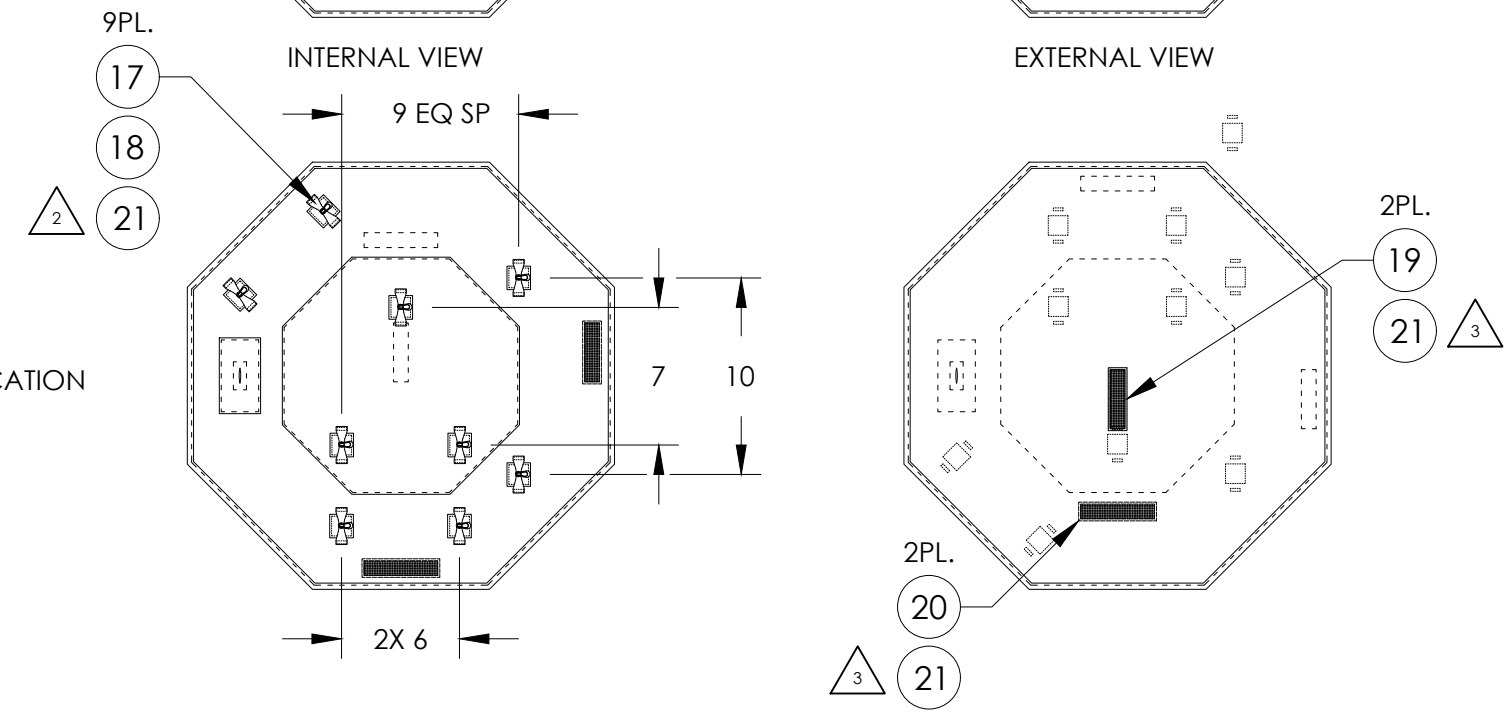

Université Concordia University	MATERIAL **REFER TO B.O.M.**		SURFACE ROUGHNESS √	TITLE **PARACHUTE ASSY**	
	FINISH		TOLERANCES X ± .1, .X ± .05, .XX ± .005, .XXX ± .002, ANGLE ± .5° (UNLESS OTHERWISE SPECIFIED)		
PROPRIETARY INFORMATION NOT TO BE RELEASED WITHOUT WRITTEN AUTHORIZATION FROM CONCORDIA UNIVERSITY	DESIGNER **M.HOANG-CAO**	ALL DIMENSIONS IN **INCHES** UNLESS OTHERWISE SPECIFIED		A SIZE	DATE **05/18/2018**	USED ON **SR18**
	DRAFTER **M.HOANG-CAO**	APPROVED **O.KHALIMONOV**	SCALE **NTS**	SHEET **4 / 6**	DWG NO. **SR18-FW-RE-03**	REV NO. **00**

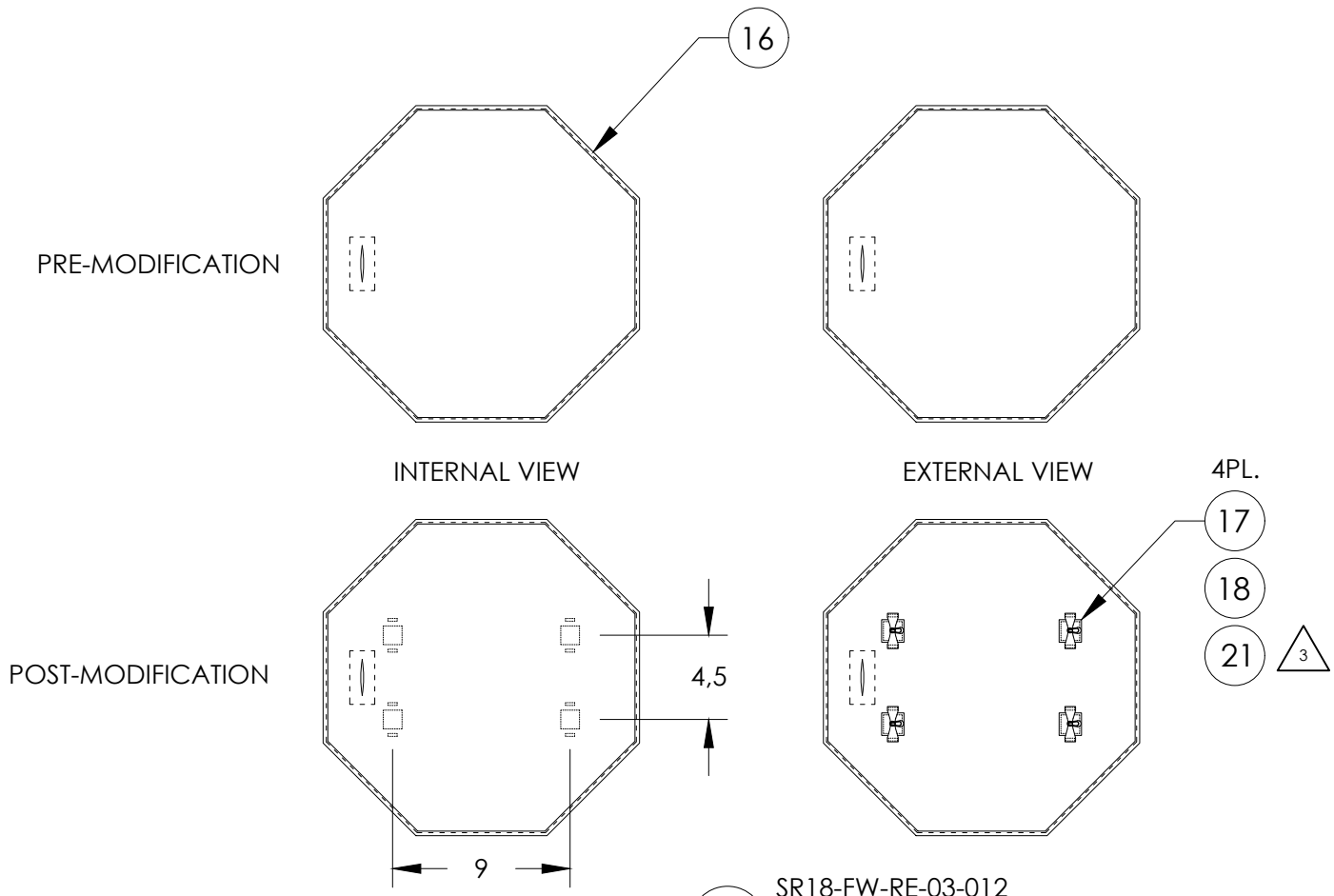

12 SR18-FW-RE-03-012
DROGUE BAG
MODIFICATION

Université Concordia University	MATERIAL **REFER TO B.O.M.**		SURFACE ROUGHNESS √	TITLE **PARACHUTE ASSY**	
	FINISH		TOLERANCES X ± .1, .X ± .05, .XX ± .005, .XXX ± .002, ANGLE ± .5° (UNLESS OTHERWISE SPECIFIED)		
PROPRIETARY INFORMATION NOT TO BE RELEASED WITHOUT WRITTEN AUTHORIZATION FROM CONCORDIA UNIVERSITY	DESIGNER **M.HOANG-CAO**	ALL DIMENSIONS IN **INCHES** UNLESS OTHERWISE SPECIFIED		A SIZE	DATE **05/18/2018**	USED ON **SR18**
	DRAFTER **M.HOANG-CAO**	APPROVED **O.KHALIMONOV**	SCALE **NTS**	SHEET **5 / 6**	DWG NO. **SR18-FW-RE-03**	REV NO. **00**

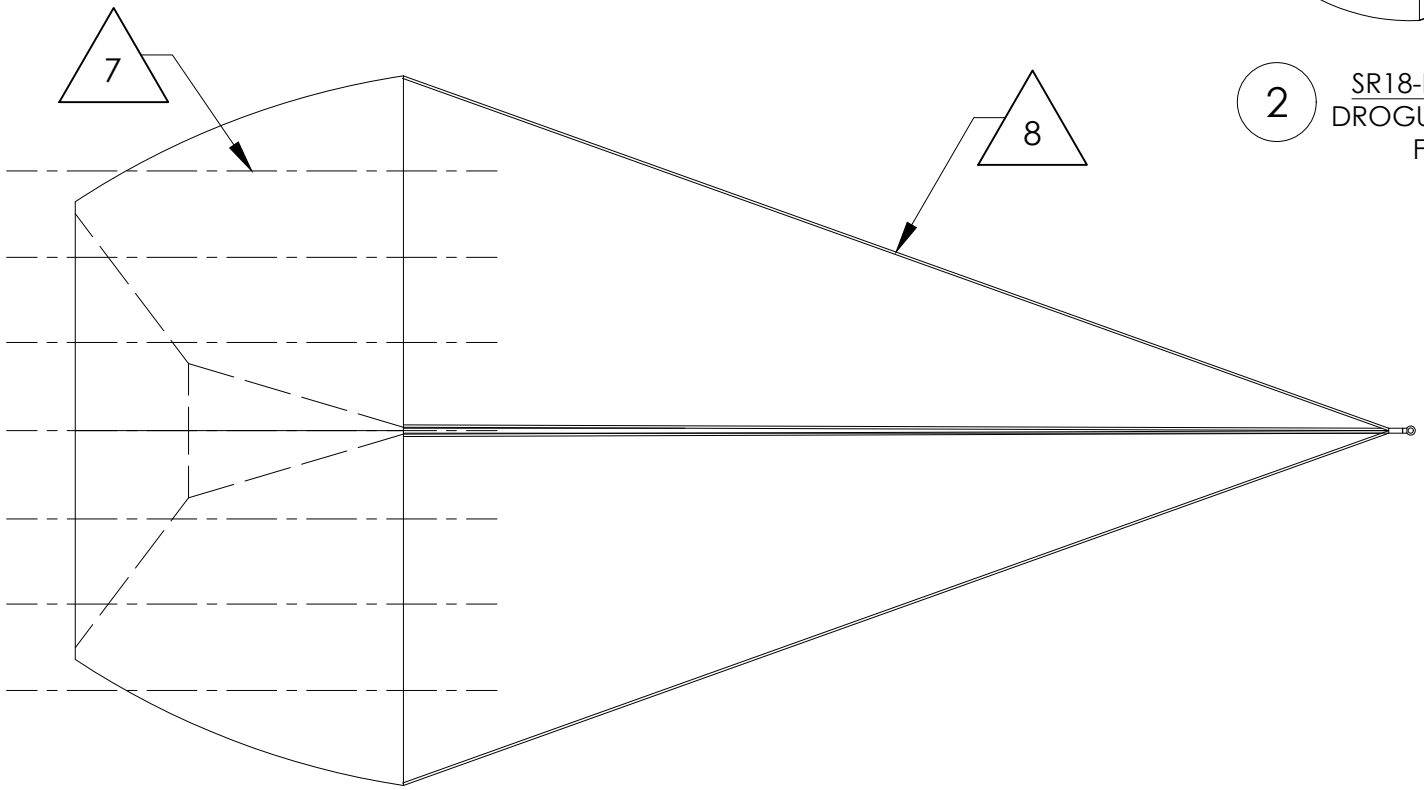

1 SR18-FW-RE-03-001
MAIN PARACHUTE
FOLDING

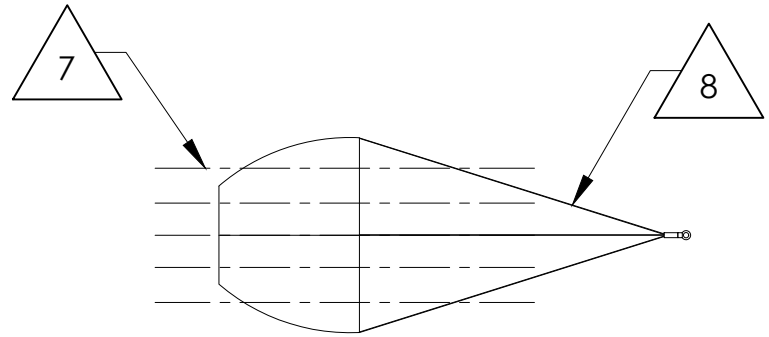

2 SR18-FW-RE-03-002
DROGUE PARACHUTE
FOLDING

Université Concordia University	MATERIAL **REFER TO B.O.M.**		SURFACE ROUGHNESS √	TITLE **PARACHUTE ASSY**	
	FINISH		TOLERANCES X ± .1, .X ± .05, .XX ± .005, .XXX ± .002, ANGLE ± .5° (UNLESS OTHERWISE SPECIFIED)		
PROPRIETARY INFORMATION NOT TO BE RELEASED WITHOUT WRITTEN AUTHORIZATION FROM CONCORDIA UNIVERSITY	DESIGNER **M.HOANG-CAO**	ALL DIMENSIONS IN **INCHES** UNLESS OTHERWISE SPECIFIED		A SIZE	DATE **05/18/2018**	USED ON **SR18**
	DRAFTER **M.HOANG-CAO**	APPROVED **O.KHALIMONOV**	SCALE **NTS**	SHEET **6 / 6**	DWG NO. **SR18-FW-RE-03**	REV NO. **00**

ITEM NO.	PART NUMBER	DESCRIPTION	NOTES	QTY.
1	SR18-AF-00-001	FUSELAGE	APC-2 PEEK CARBON FIBER TUBE, THICNKESS: 0.060	1
2	SR18-AF-00-006A	CENTERING RING	GAROLITE G10, THICKNESS: 1/4"	2
3	SR18-AF-00-006B	TOP CENTERING RING	GAROLITE G10, THICKNESS: 1/4"	1
4	SR18-AF-00-006C	CENTERING RING HOLE	GAROLITE G10, THICKNESS: 1/4"	1
5	SR18-AF-00-006D	MOTOR CENTERING RING 2		1
6	SR18-AF-00-007	COUPLER	APC-2 PEEK CARBON FIBER TUBE, THICKNESS: 1/8"	1
7	SR18-AF-00-008	RETAINING RING	MCMASTER P/N 99142A680	1
8	SR18-AF-00-014	MOTOR TUBE	S-GLASS TUBE, THICKNESS: 1/16"	1
9	SR18-AF-02-001	BOATAIL	CARBON FIBER, THICKNESS: 0.080"	1
10	SR18-AF-02-002	MOTOR CASING	CESSARONI PRO 98	1
11	SR18-AF-02-003	JESUS BULKHEAD	ALUMINUM MOTOR RETAINER	1
12	SR18-AF-02-007-	MOTOR RETAINING BULKHEAD	GAROLITE G10, THICKNESS: 1/4"	1
13	SR18-AF-02-010	BOATAIL PLUG	ALUMINUM MOTOR RETAINER	1
14	SR18-AF-03-001	STRAIN GAUGE		4
15	SR18-AF-03-002	GAUGE WIRES	NOT ILLUSTRATED	1
16	SR18-AF-03-003	STRAIN GAUGE CIRCUIT BOARD		1
17	SR18-AF-04-002	FLAT HEAD SCREW	MCMASTER P/N 91253A009	2
18	SR18-AF-04-003	RAIL GUIDE		2
19	SR18-AF-04-004	GUIDE RAIL BRACKET		1
20	SR18-AF-05-001	FIN	ALUMINUM HONEYCOMB REINFORCED WITH CARBON FIBER, THICKNESS: 1/4"	4
21	SR18-AF-06-00	HOIST RING		1

NOTES

GENERAL

1. INTERPRET DWG AS PER ANSI Y14.5

ASSEMBLY

2. BOND WITH LOCTITE H8000 A/R
3. TIP TO TIP VACUUM BAG LAYUP W/ 3 LAYERS 3K-70-P PLAIN WEAVE CARBON FIBER & AEROPOXY PR2032 + PH3665

SURFACE FINISH (ALL EXTERIOR UOS)

4. SAND SURFACE UNTIL SMOOTH
5. PRIMER: 4 LAYERS RUST-OLEUM 2X ULTRA COVER WHITE PRIMER
6. PAINT: 4 LAYERS RUST-OLEUM
7. DO NOT PAINT SURFACE

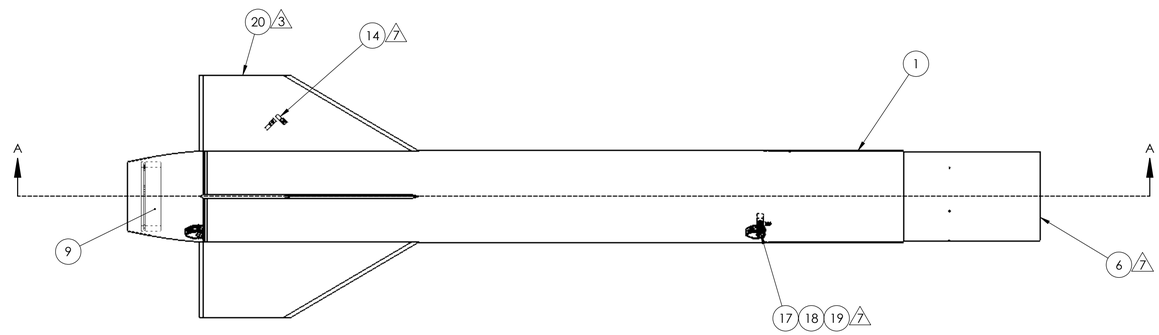

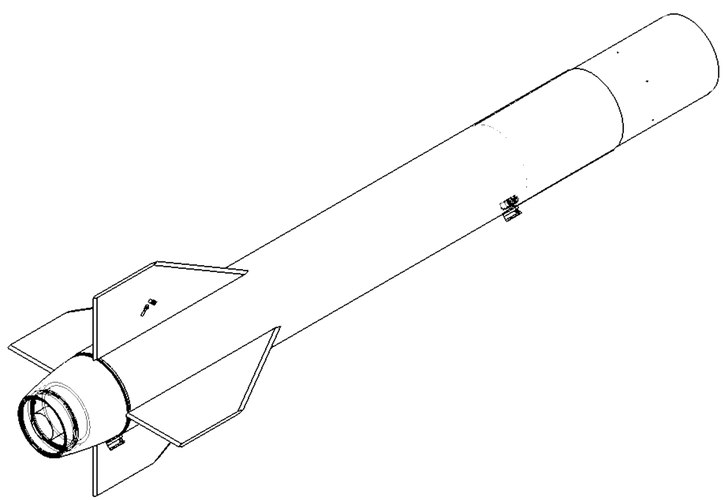

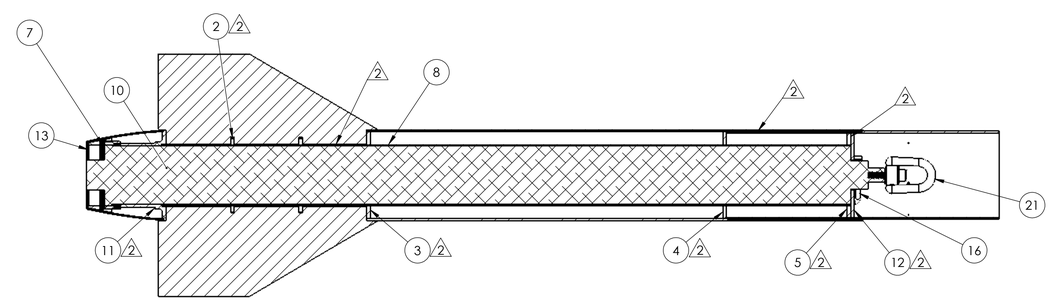

SECTION A-A

Concordia UNIVERSITY	MATERIAL SEE B.O.M.	SURFACE ROUGHNESS √	TITLE AFT	
	FINISH SEE NOTES	TOLERANCES X ± .1 X ± .05 XX ± .010 XXX ± .005 ANGLE ± 2°		
PROPRIETARY INFORMATION NOT TO BE RELEASED WITHOUT WRITTEN PERMISSION OF THE DEAN FROM CONCORDIA UNIVERSITY	DESIGNER O. KHALIMONOV	ALL DIMENSIONS IN INCHES UNLESS OTHERWISE SPECIFIED	SIZE	DATE 5/25/2018 USED ON SR18
	DRAFTER J.S.PRIETO	APPROVED O. D'ANGELO	SCALE 1:5	SHEET 1 / 1 DWG NO. SR18-AF REV NO. 00

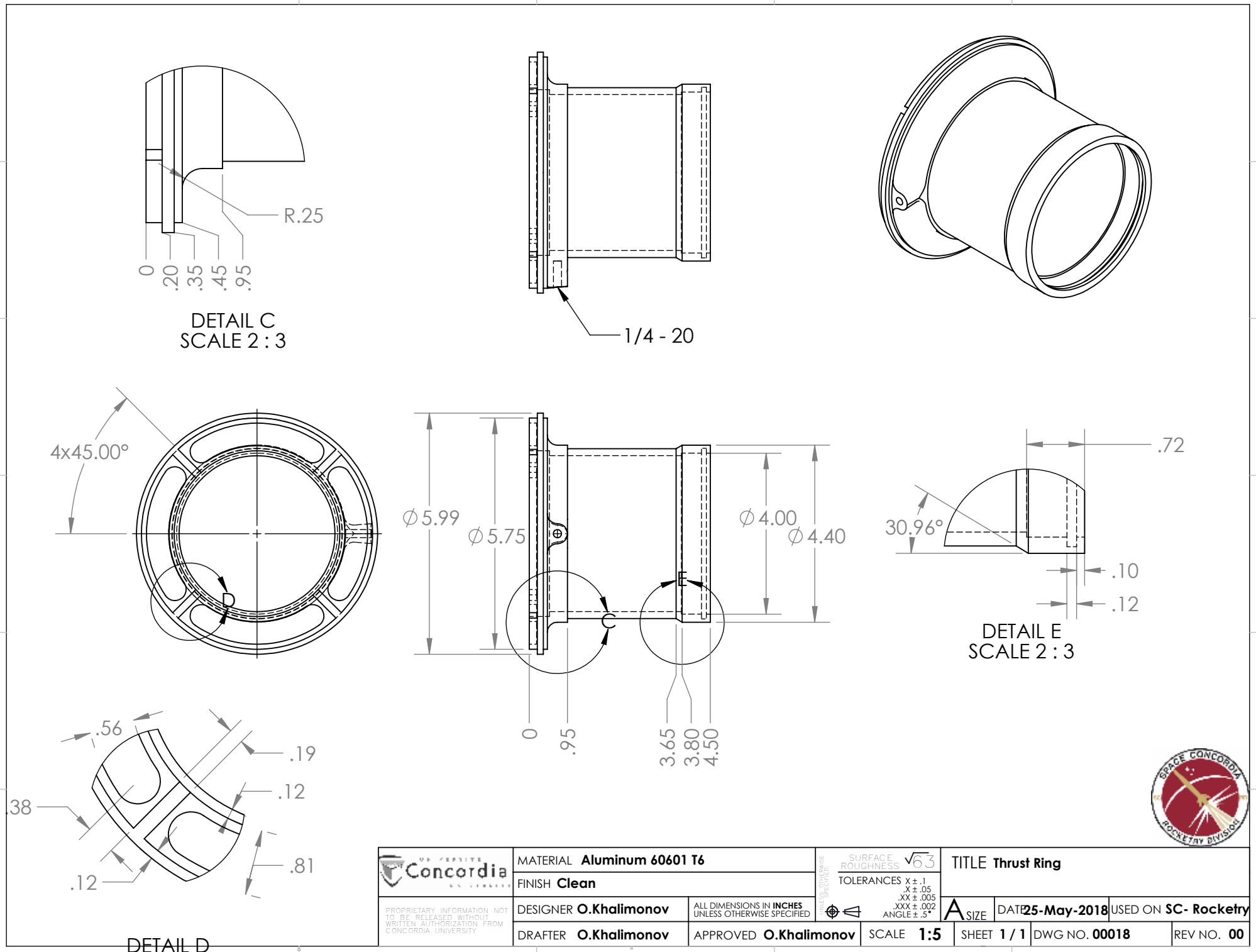

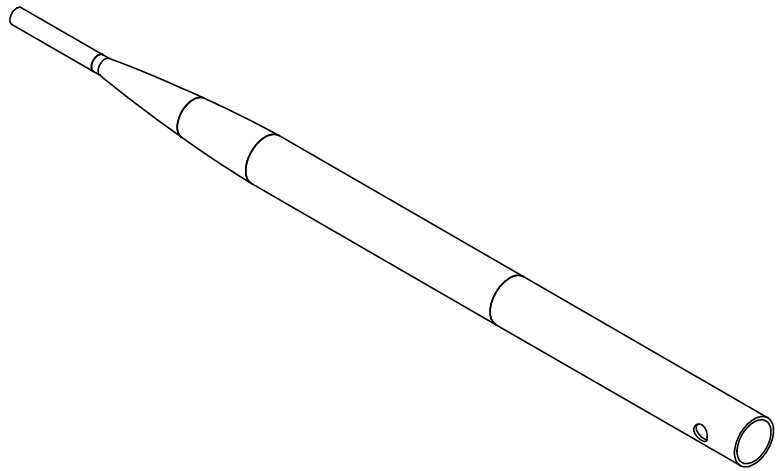

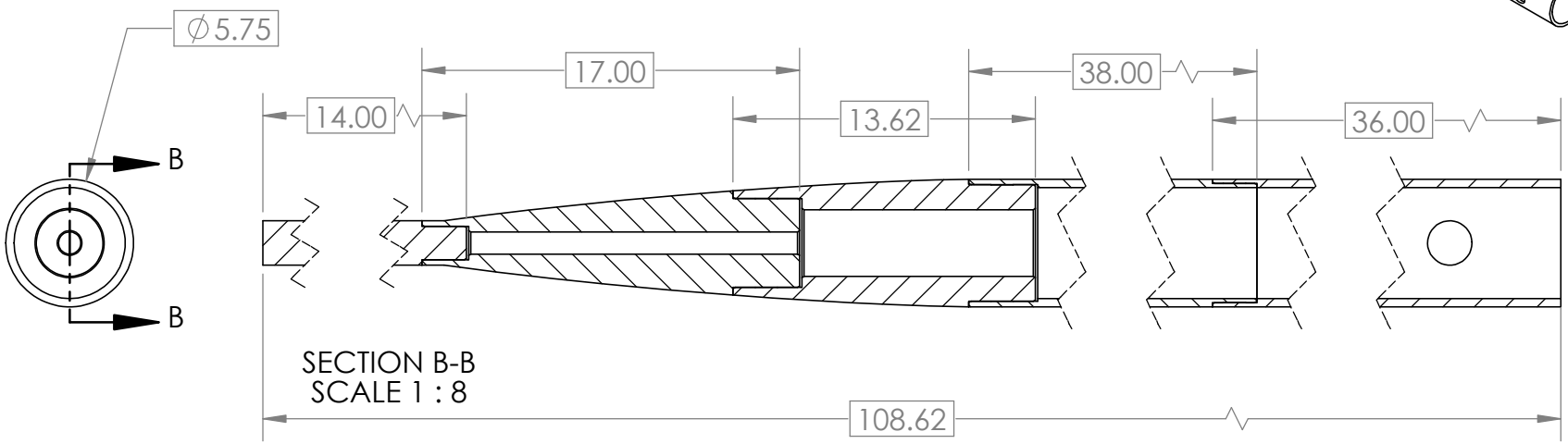

Concordia UNIVERSITY	MATERIAL **6061 T6 - ∅6"MAX x 86"**	UNLESS OTHERWISE SPECIFIED	SURFACE ROUGHNESS √63	TITLE **1000_MANDREL**	
	FINISH **CLEAN**		TOLERANCES X ± .1 .X ± .05 .XX ± .005 .XXX ± .002 ANGLE ± .5°		
PROPRIETARY INFORMATION NOT TO BE RELEASED WITHOUT WRITTEN AUTHORIZATION FROM CONCORDIA UNIVERSITY	DESIGNER **O.Khalimonov**	ALL DIMENSIONS IN **INCHES** UNLESS OTHERWISE SPECIFIED		A SIZE	DATE **10-Oct-2017**	USED ON **SC-Rocketry**
	DRAFTER **O.Khalimonov**	APPROVED **O.Khalimonov**	SCALE **1:20**	SHEET **1 / 1**	DWG NO. **0001**	REV NO. **00**

NOTES:

1- UOS. ALL DIA. ⌖ ∅ .010 Ⓜ A

2- MATERIAL AL 6061-T6

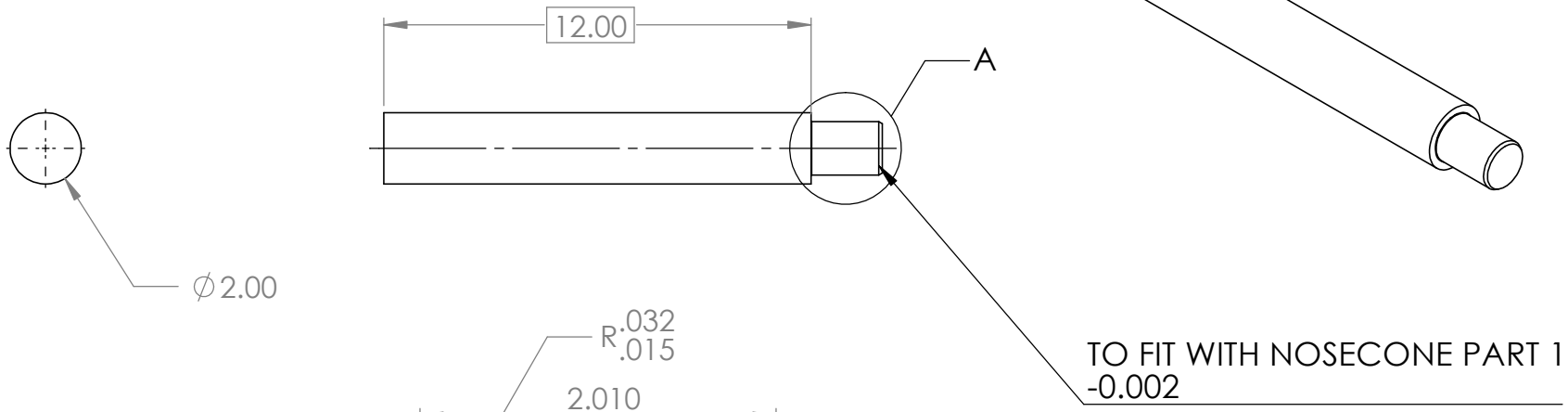

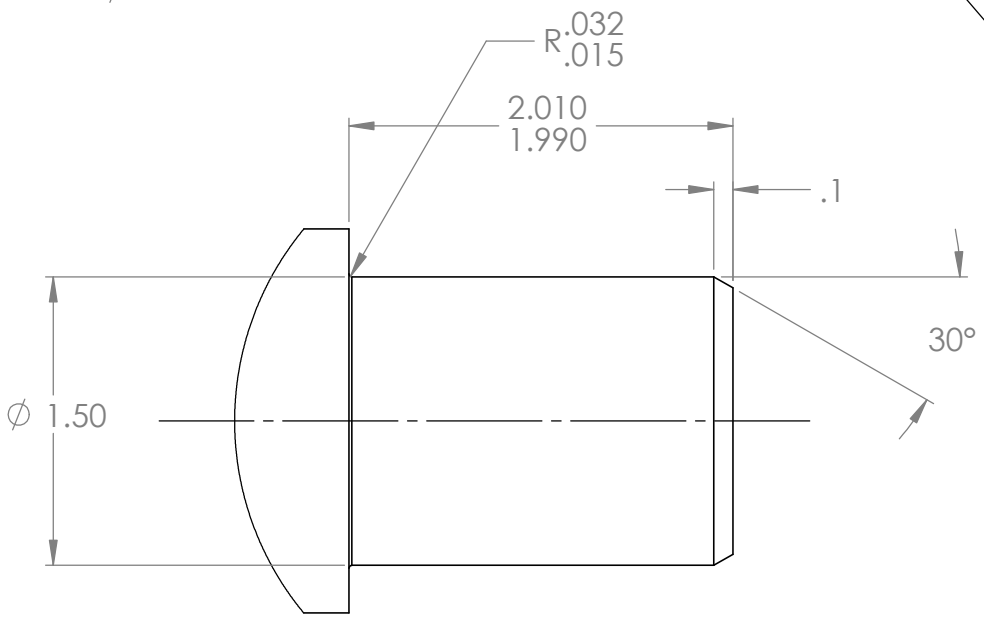

DETAIL A
SCALE 1 : 1

Université Concordia University	MATERIAL **6061 T6 - ∅2-1/8" x 14-1/4"**	UNLESS OTHERWISE SPECIFIED	SURFACE ROUGHNESS √63	TITLE **1001_NOSECONE_CLEARANCE_DIEGO**	
	FINISH **-**		TOLERANCES X ± .1 .X ± .05 .XX ± .005 .XXX ± .002 ANGLE ± .5°		
PROPRIETARY INFORMATION NOT TO BE RELEASED WITHOUT WRITTEN AUTHORIZATION FROM CONCORDIA UNIVERSITY	DESIGNER **O.KHALIMONOV**	ALL DIMENSIONS IN **INCHES** UNLESS OTHERWISE SPECIFIED		A SIZE	DATE **04-Oct-2017** USED ON **ROCKET17**
	DRAFTER **D.CANIZALES**	APPROVED **O.KHALIMONOV**	SCALE **1:5**	SHEET **1 / 1**	DWG NO. **1001** REV NO. **00**

NOTES:

1- UOS. ALL DIA. ⌖ ∅ .010 Ⓜ A

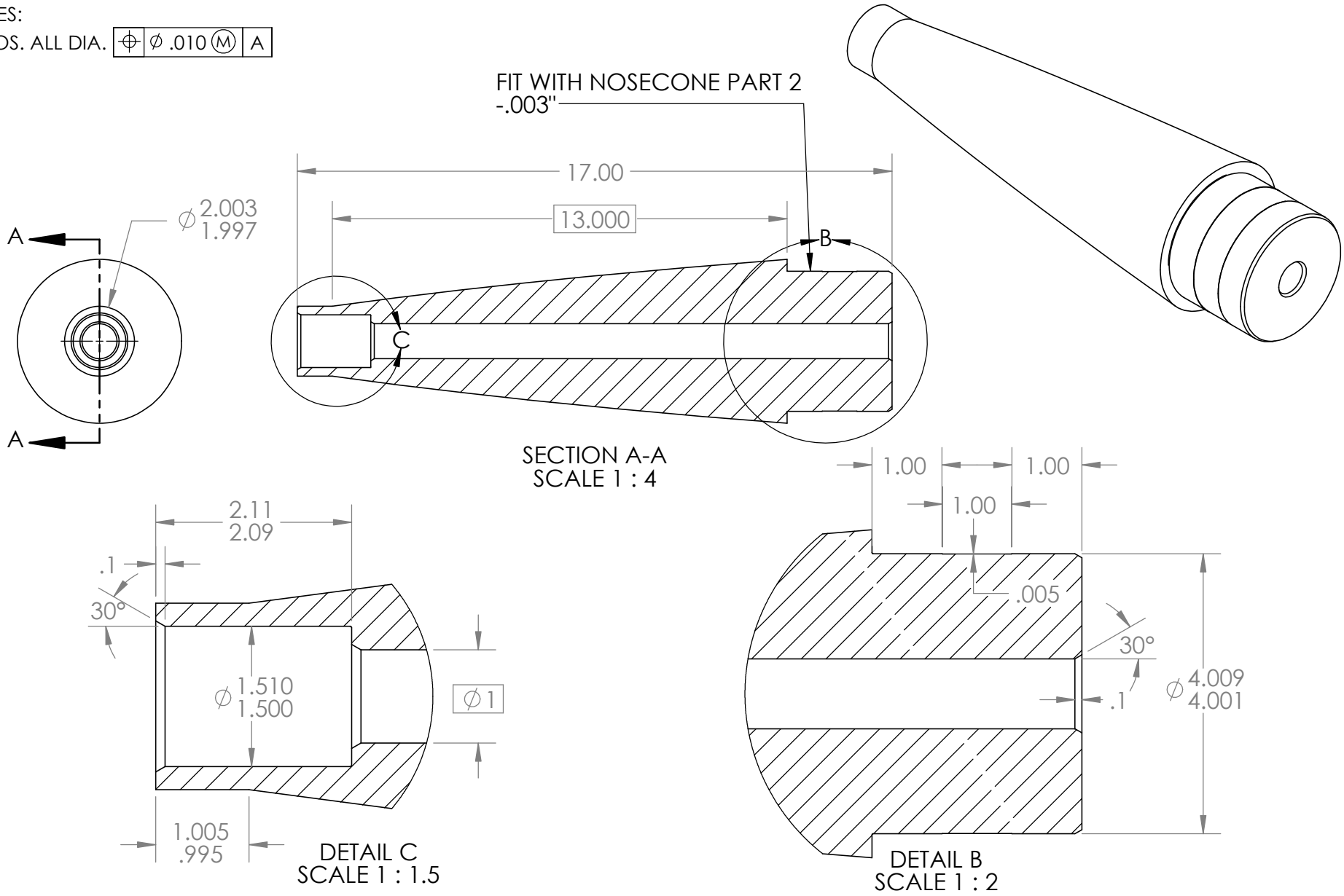

Concordia	MATERIAL **6061 T6 - ∅6"MAX x 86"**		SURFACE ROUGHNESS √63	TITLE **1002_NOSECONE_PART_ONE**	
	FINISH **CLEAN**		TOLERANCES X ± .1, .X ± .05, .XX ± .005, .XXX ± .002, ANGLE ± .5°		
PROPRIETARY INFORMATION NOT TO BE RELEASED WITHOUT WRITTEN AUTHORIZATION FROM CONCORDIA UNIVERSITY	DESIGNER **O.Khalimonov**	ALL DIMENSIONS IN **INCHES** UNLESS OTHERWISE SPECIFIED		A SIZE	DATE **10-Oct-2017**	USED ON **SC-Rocketry**
	DRAFTER **O.Khalimonov**	APPROVED **O.Khalimonov**	SCALE **1:5**	SHEET **1 / 1**	DWG NO. **0001**	REV NO. **00**

NOTES:

1- UOS. ALL DIA. ⌖ | ∅ .010 Ⓜ | A

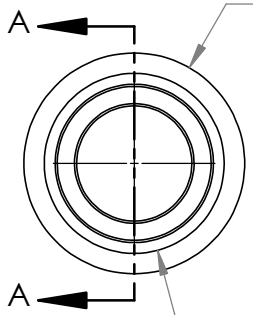

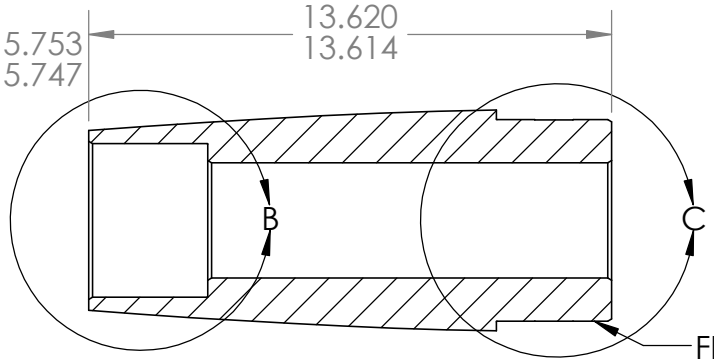

SECTION A-A

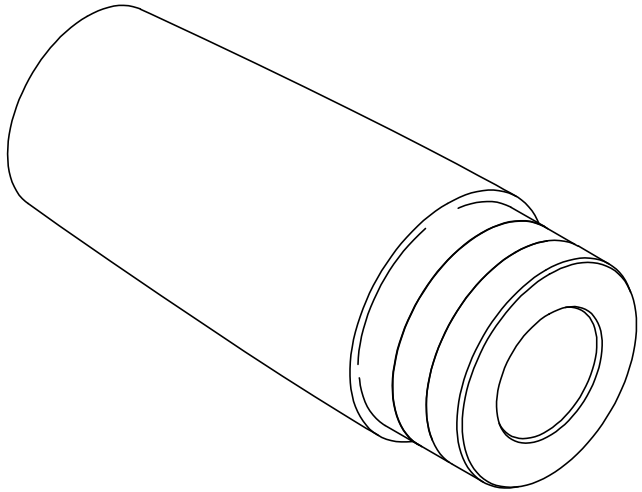

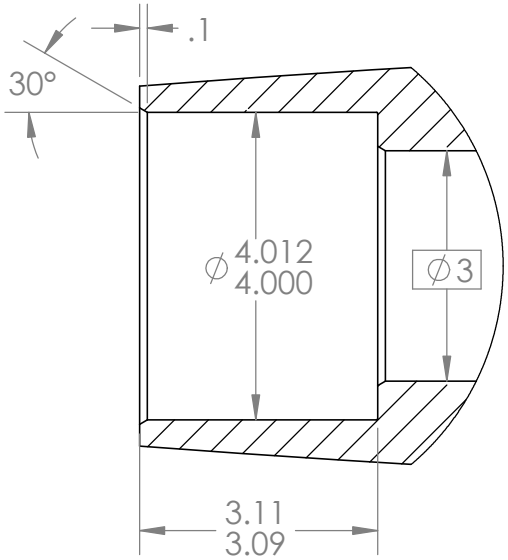

DETAIL B
SCALE 2 : 5

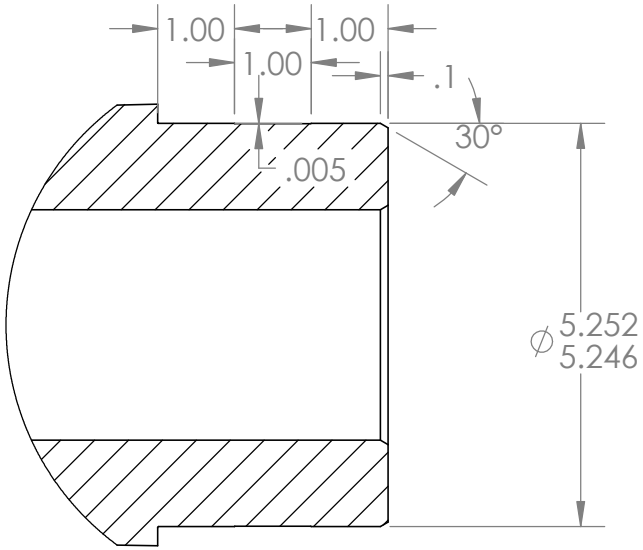

DETAIL C
SCALE 2 : 5

Concordia UNIVERSITY	MATERIAL **6061 T6 - ∅6"MAX x 86"**		SURFACE ROUGHNESS √63	TITLE **1003_NOSECONE_PART_TWO**	
	FINISH **CLEAN**		TOLERANCES X ± .1 .X ± .05 .XX ± .005 .XXX ± .002 ANGLE ± .5°		
PROPRIETARY INFORMATION NOT TO BE RELEASED WITHOUT WRITTEN AUTHORIZATION FROM CONCORDIA UNIVERSITY	DESIGNER **O.Khalimonov**	ALL DIMENSIONS IN **INCHES** UNLESS OTHERWISE SPECIFIED	ALL DIMENSIONS UNLESS OTHERWISE SPECIFIED	A SIZE	DATE **10-Oct-2017**	USED ON **SC-Rocketry**
	DRAFTER **O.Khalimonov**	APPROVED **O.Khalimonov**	SCALE **1:5**	SHEET **1 / 1**	DWG NO. **0001**	REV NO. **00**

NOTES:

1- UOS. ALL DIA. ⌖ ∅ .010 Ⓜ A

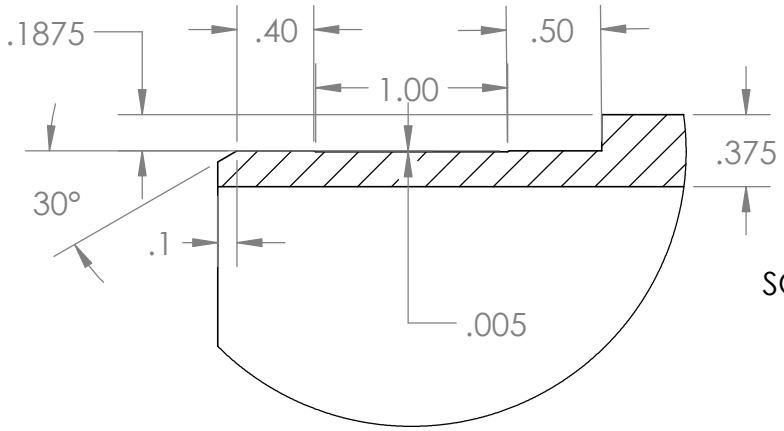

DETAIL B
SCALE 1 : 1

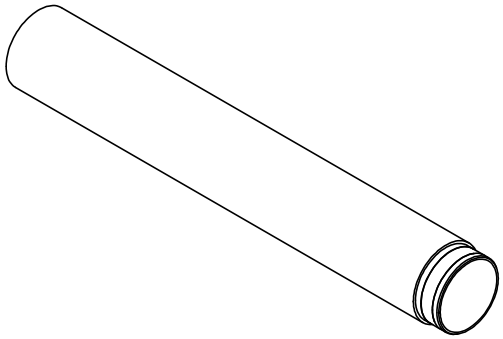

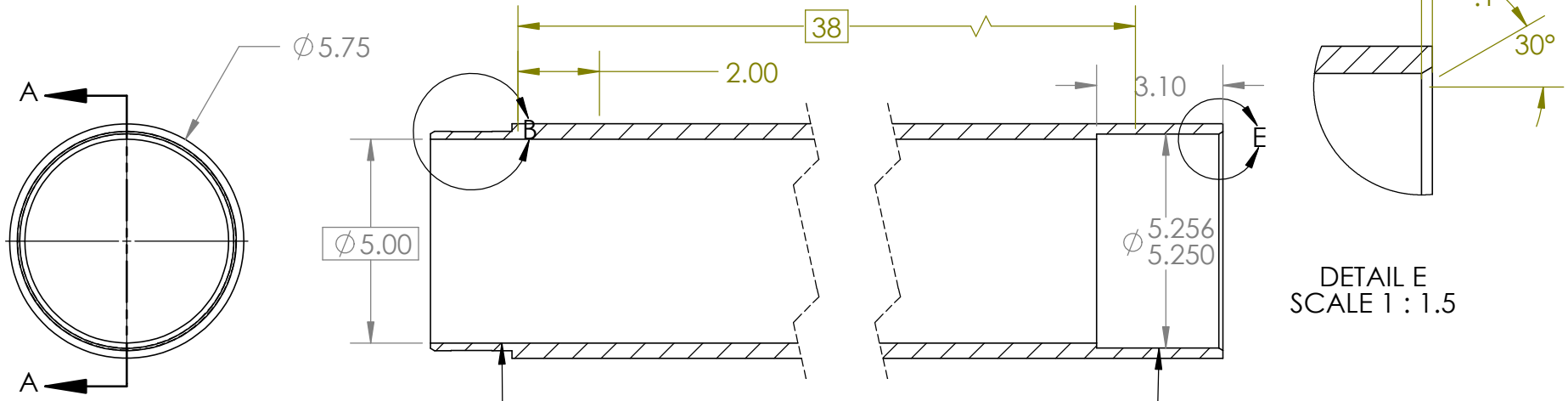

DETAIL E
SCALE 1 : 1.5

FIT WITH FORWARD PART 2
-.003"

SECTION A-A
SCALE 1 : 4

FIT WITH NOSECONE PART 2
+0.003"

Concordia University	MATERIAL **6061 T6 - ∅6"MAX x 86"**	UNLESS OTHERWISE SPECIFIED	SURFACE ROUGHNESS √63	TITLE **1004_FORWARD _SECTION_PART_1**	
	FINISH **CLEAN**		TOLERANCES X ± .1 .X ± .05 .XX ± .005 .XXX ± .002 ANGLE ± .5°		
PROPRIETARY INFORMATION NOT TO BE RELEASED WITHOUT WRITTEN AUTHORIZATION FROM CONCORDIA UNIVERSITY	DESIGNER **O.Khalimonov**	ALL DIMENSIONS IN **INCHES** UNLESS OTHERWISE SPECIFIED	⌖	A SIZE	DATE **10-Oct-2017** USED ON **SC-Rocketry**
	DRAFTER **O.Khalimonov**	APPROVED **O.Khalimonov**	SCALE **1:10**	SHEET **1 / 1** DWG NO. **0001**	REV NO. **00**

NOTES:

1- UOS. ALL DIA. ⌖ ∅ .010Ⓜ A

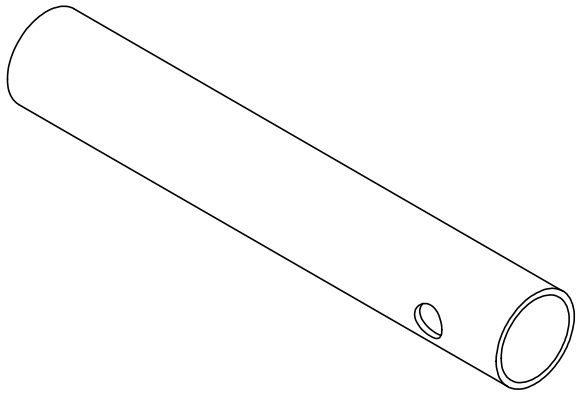

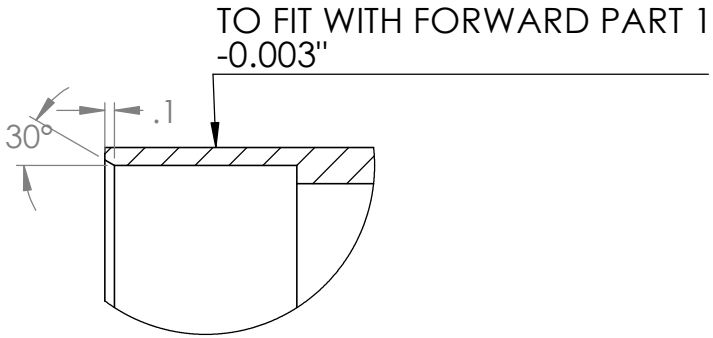

DETAIL O
SCALE 1 : 2

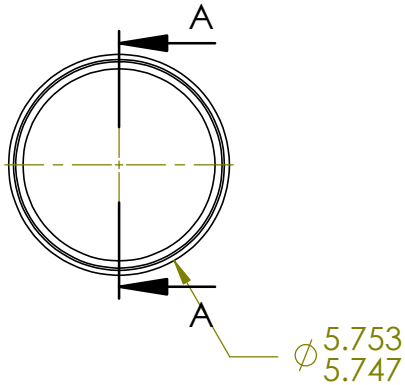

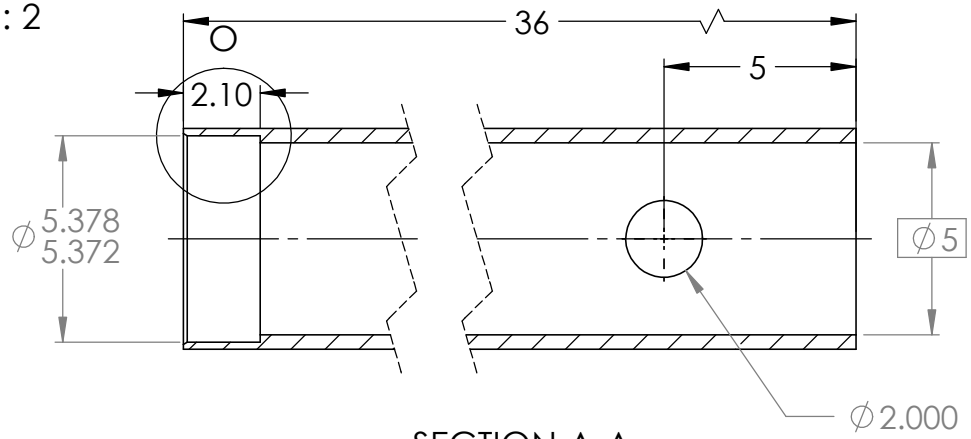

SECTION A-A
SCALE 1 : 5

Concordia University	MATERIAL **6061 T6 - ∅6" x 72-1/4"**	UNLESS OTHERWISE SPECIFIED	SURFACE ROUGHNESS √63	TITLE **1005_FORWARD_SECTION_PART_2**	
	FINISH **-**		TOLERANCES X ± .1 .X ± .05 .XX ± .005 .XXX ± .002 ANGLE ± .5°		
PROPRIETARY INFORMATION NOT TO BE RELEASED WITHOUT WRITTEN AUTHORIZATION FROM CONCORDIA UNIVERSITY	DESIGNER **O.Khalimonov**	ALL DIMENSIONS IN **INCHES** UNLESS OTHERWISE SPECIFIED	A SIZE	DATE **10-Oct-2017**	USED ON **ROCKET17**
	DRAFTER **O.Khalimonov**	APPROVED **O.Khalimonov**	SCALE **1:5**	SHEET **1 / 1**	DWG NO. **1005**	REV NO. **00**

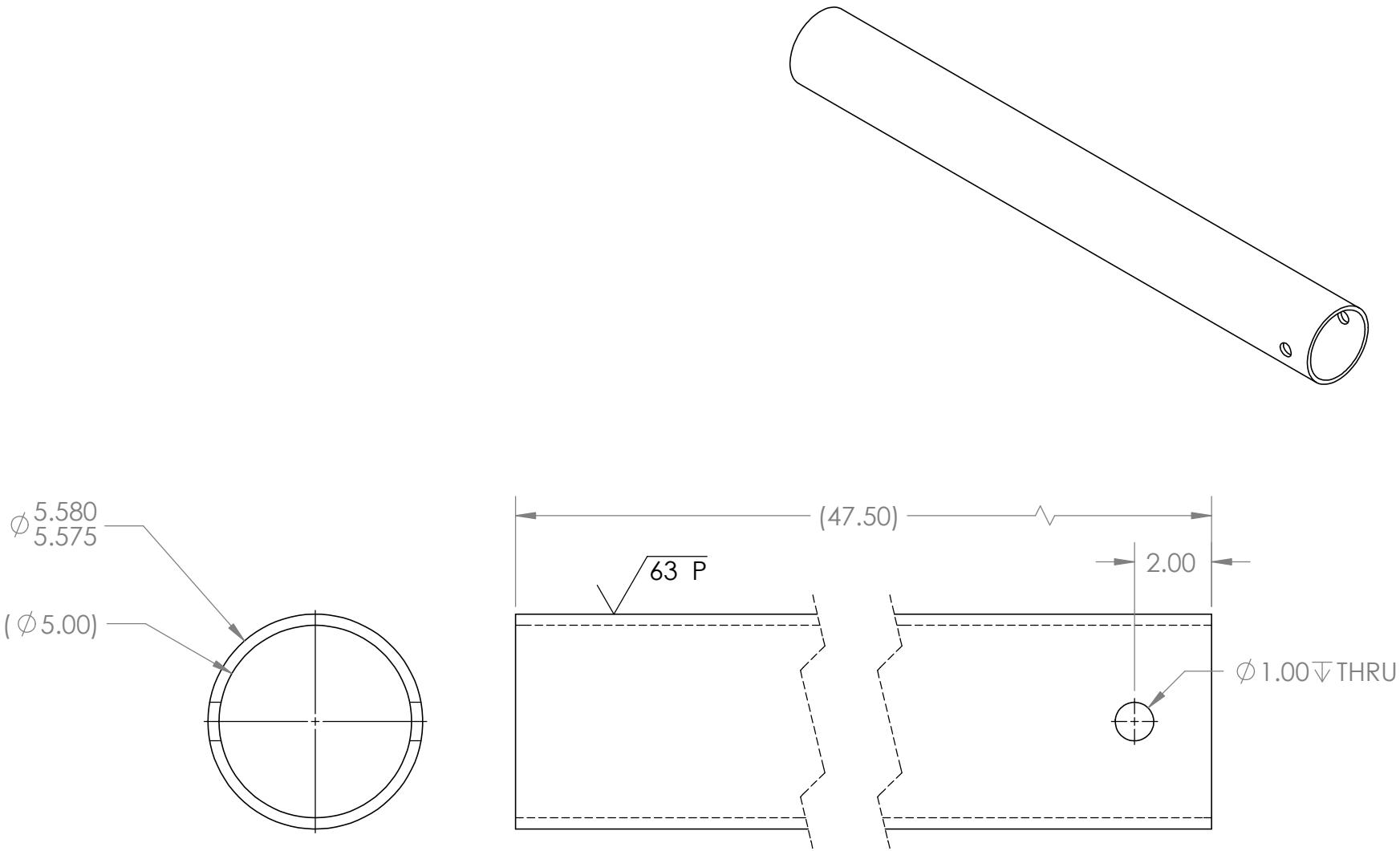

Université Concordia University	MATERIAL **Aluminum 60601 T6 6"ODx5"IDx48"**	UNLESS OTHERWISE SPECIFIED	SURFACE ROUGHNESS √63	TITLE **Coupler Mandrel**	
	FINISH **Clean**		TOLERANCES X ± .1 .X ± .05 .XX ± .005 .XXX ± .002 ANGLE ± .5°		
PROPRIETARY INFORMATION NOT TO BE RELEASED WITHOUT WRITTEN AUTHORIZATION FROM CONCORDIA UNIVERSITY	DESIGNER **O.Khalimonov**	ALL DIMENSIONS IN **INCHES** UNLESS OTHERWISE SPECIFIED		A SIZE	DATE **21-Mar-2018**	USED ON **SC- Rocketry**
	DRAFTER **O.Khalimonov**	APPROVED **O.Khalimonov**	SCALE **1:10**	SHEET **1 / 1**	DWG NO. **00018**	REV NO. **00**

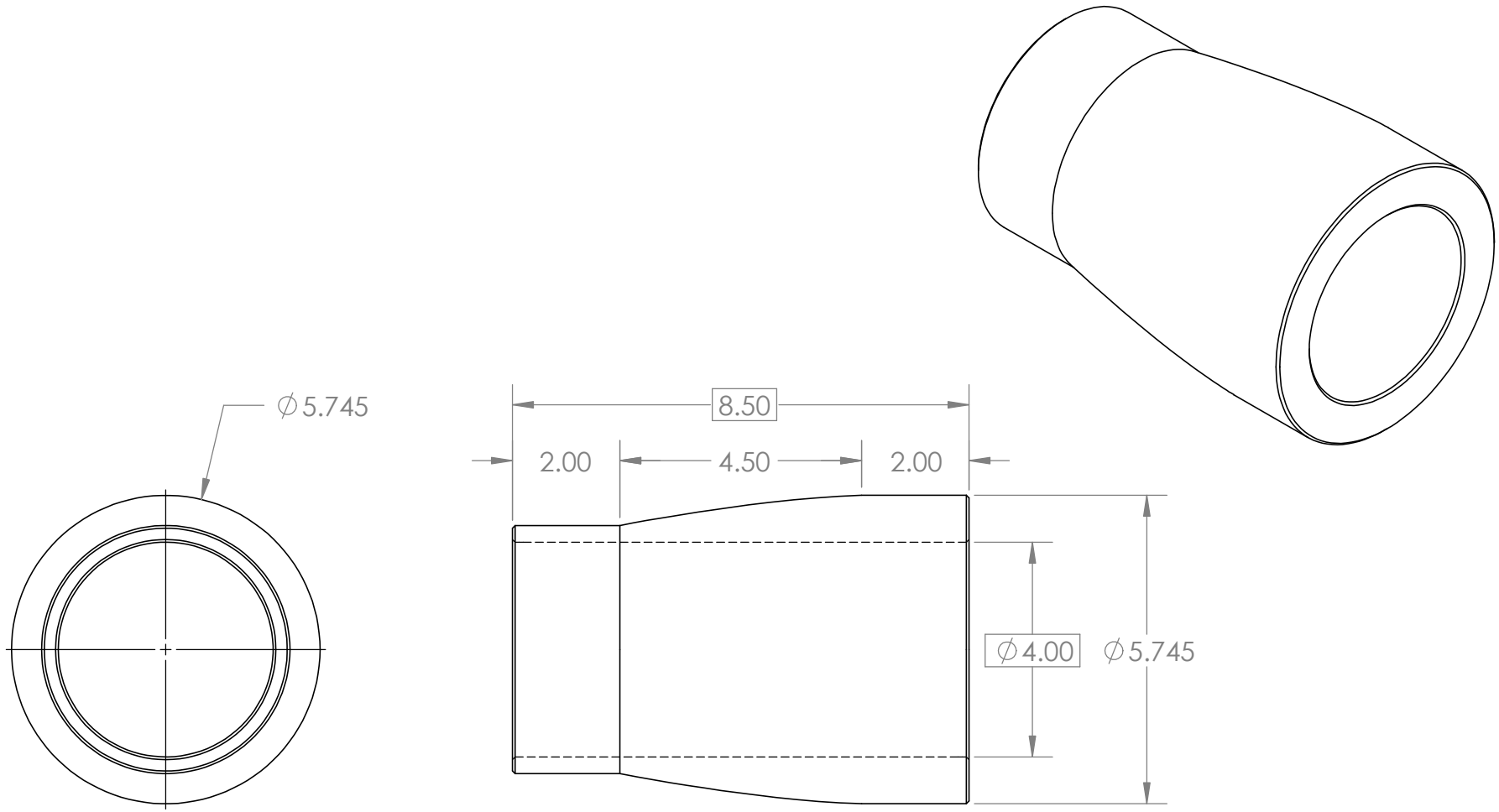

Université Concordia University	MATERIAL **6061 T6 - ∅5.75" OD x 4" ID**	UNLESS OTHERWISE SPECIFIED	SURFACE ROUGHNESS √63	TITLE **Boattail Mandrel**	
	FINISH **Clean**		TOLERANCES X ± .1, .X ± .05, .XX ± .005, .XXX ± .002, ANGLE ± .5°		
PROPRIETARY INFORMATION NOT TO BE RELEASED WITHOUT WRITTEN AUTHORIZATION FROM CONCORDIA UNIVERSITY	DESIGNER **O.Khalimonov**	ALL DIMENSIONS IN **INCHES** UNLESS OTHERWISE SPECIFIED		A SIZE	DATE **14/11/2017**	USED ON **SC-Rocketry**
	DRAFTER **O.Khalimonov**	APPROVED **O.Khalimonov**	SCALE **1:3**	SHEET **1 / 1**	DWG NO. **0001**	REV NO. **00**

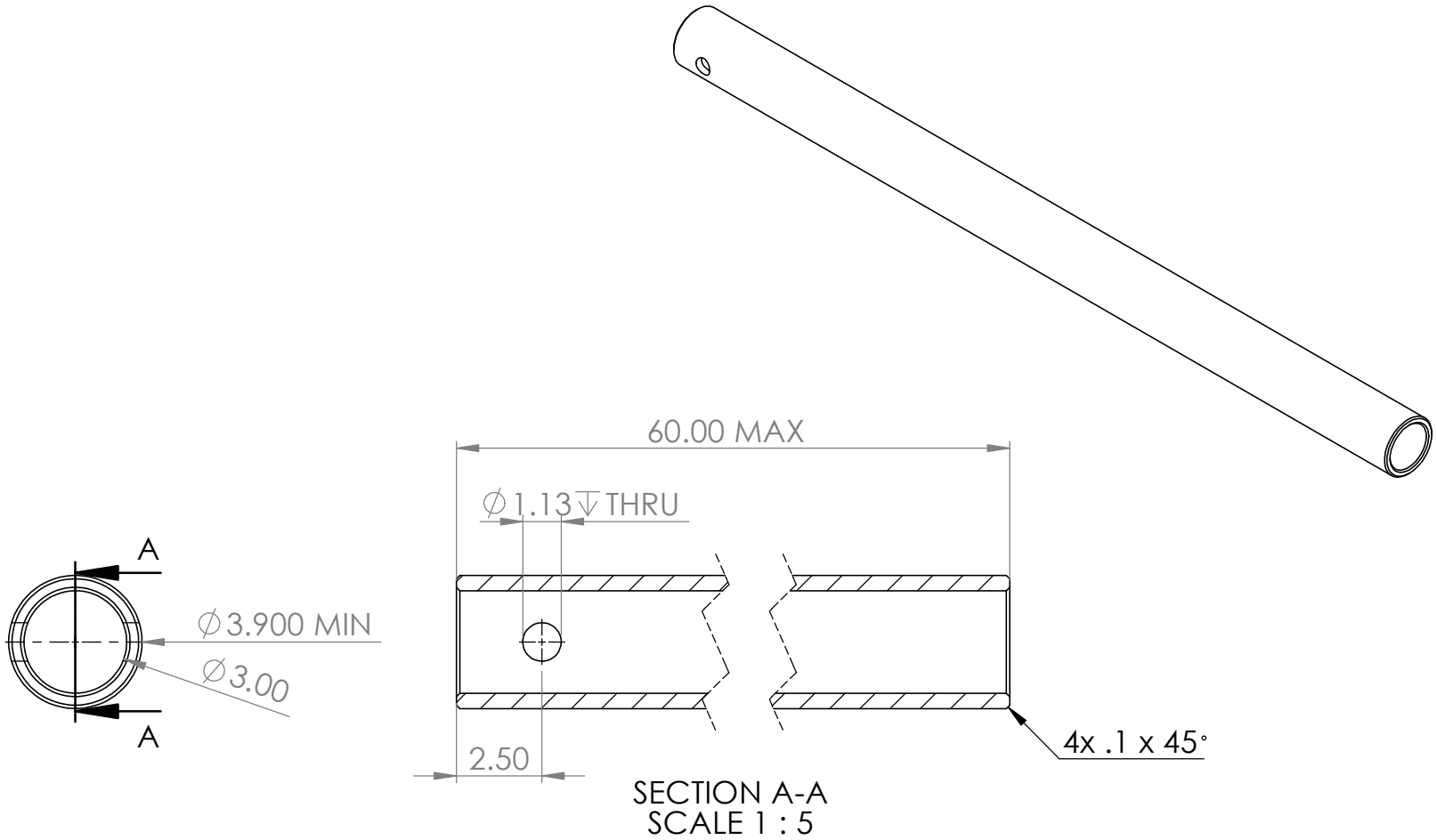

Université Concordia University	MATERIAL **6061 T6 - ∅4" x .5" x 60"**		SURFACE ROUGHNESS √63	TITLE **Motor Tube Mandrel**	
	FINISH **Clean**		TOLERANCES X ± .1, .X ± .05, .XX ± .005, .XXX ± .002, ANGLE ± .5°		
PROPRIETARY INFORMATION NOT TO BE RELEASED WITHOUT WRITTEN AUTHORIZATION FROM CONCORDIA UNIVERSITY	DESIGNER **O.Khalimonov**	ALL DIMENSIONS IN **INCHES** UNLESS OTHERWISE SPECIFIED		A SIZE	DATE **26-Nov-2017**	USED ON **SC-Rocketry**
	DRAFTER **O.Khalimonov**	APPROVED **O.Khalimonov**	SCALE **1:5**	SHEET **1 / 1**	DWG NO. **0008**	REV NO. **00**

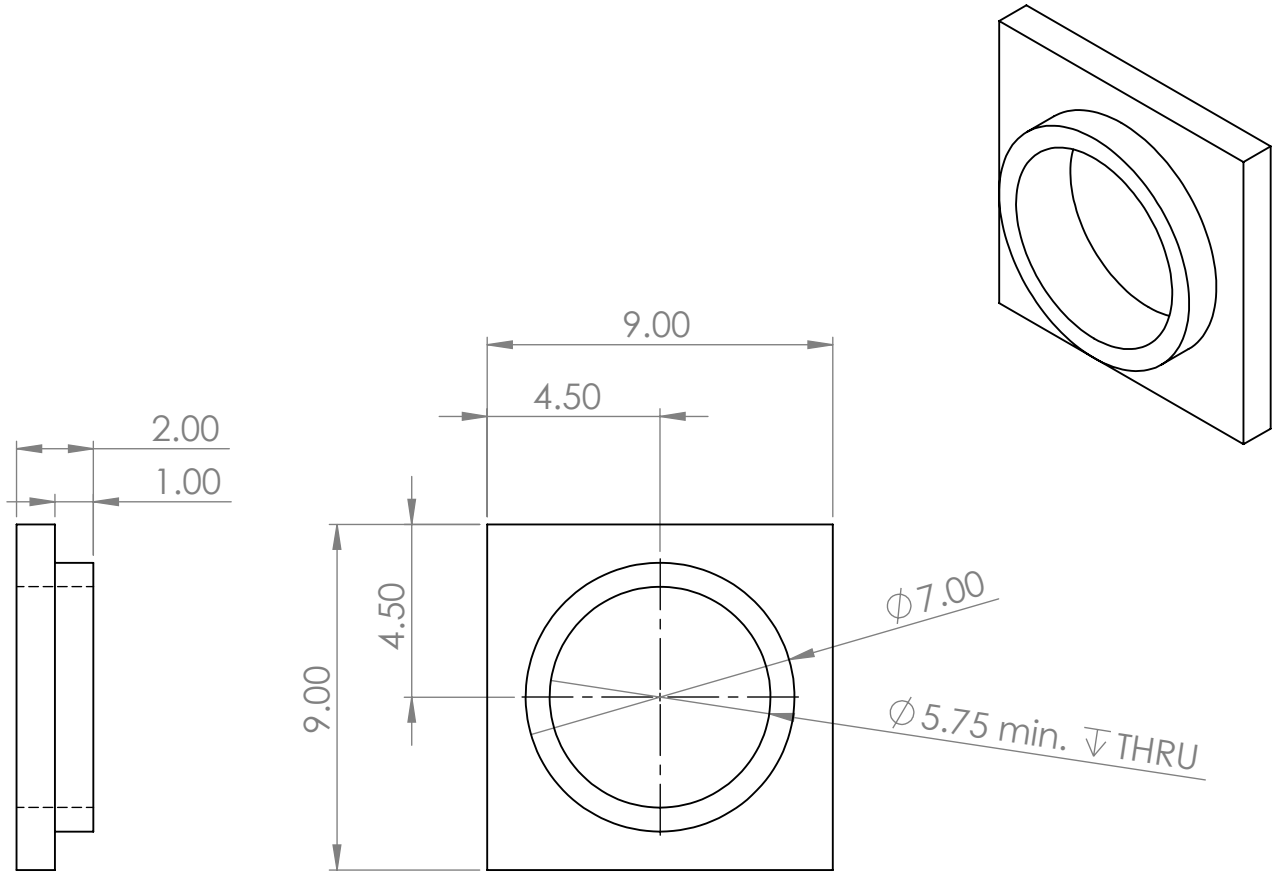

Concordia	MATERIAL **6061 T6 - 9" x 9"**		SURFACE ROUGHNESS √63	TITLE **Extractor Adapter Plate**	
	FINISH **Clean**		TOLERANCES X ± .1 .X ± .05 .XX ± .005 .XXX ± .002 ANGLE ± .5°		
PROPRIETARY INFORMATION NOT TO BE RELEASED WITHOUT WRITTEN AUTHORIZATION FROM CONCORDIA UNIVERSITY	DESIGNER **O.Khalimonov**	ALL DIMENSIONS IN **INCHES** UNLESS OTHERWISE SPECIFIED		A SIZE	DATE **25-May-2018** USED ON **SC-Rocketry**
	DRAFTER **O.Khalimonov**	APPROVED **O.Khalimonov**	SCALE **1:5**	SHEET **1 / 1**	DWG NO. **0001** REV NO. **00**

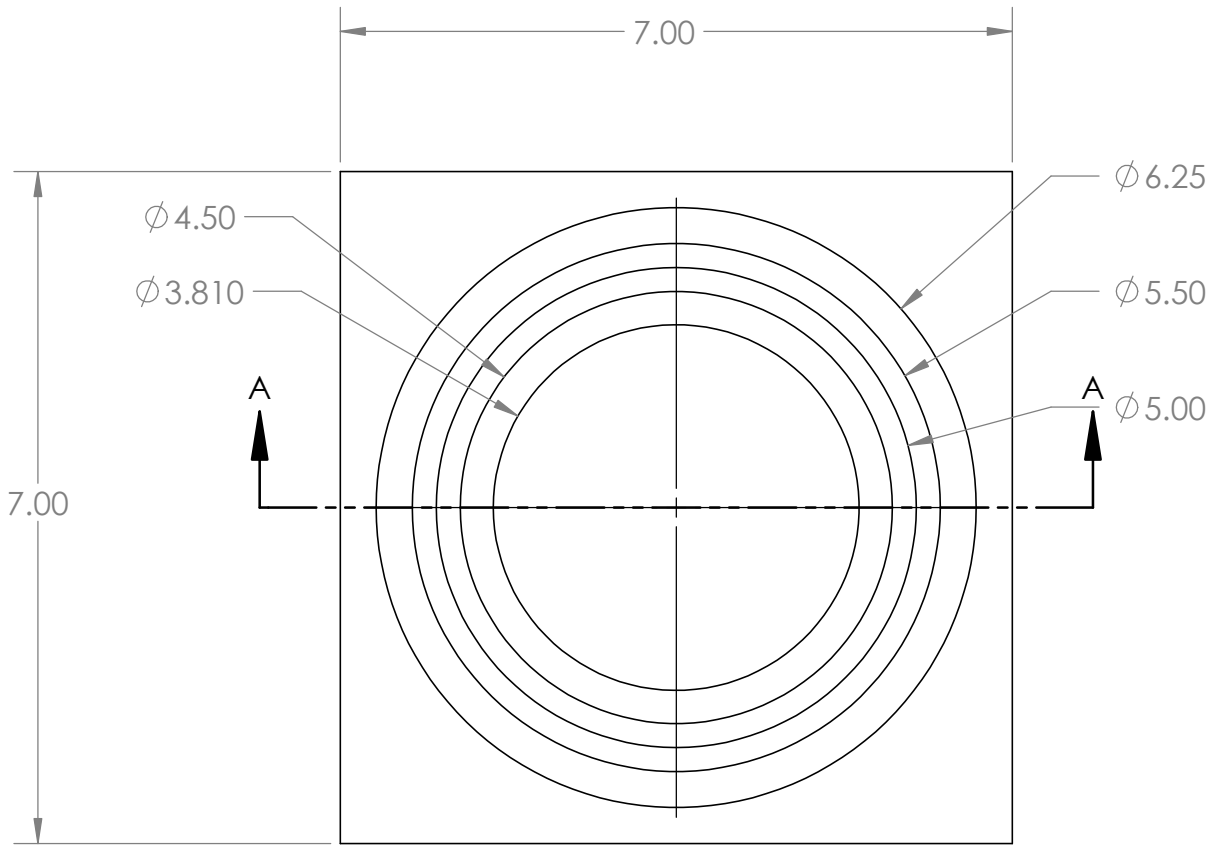

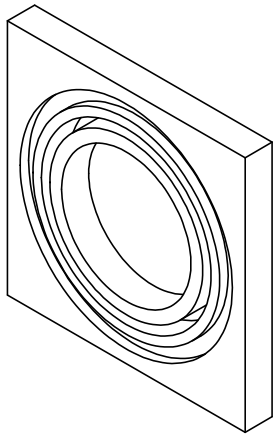

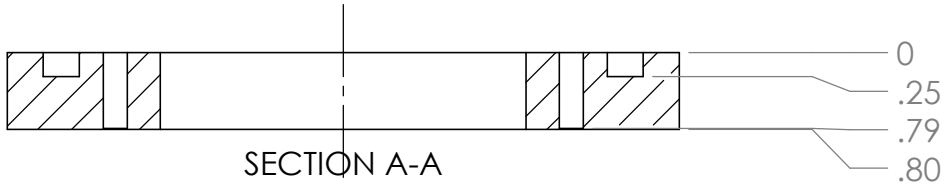

SECTION A-A

Concordia University	MATERIAL **Aluminum 60601 T6 8"x7"x1"**	UNLESS OTHERWISE SPECIFIED	SURFACE ROUGHNESS √63	TITLE **Compression ring and Extractor Plate**	
	FINISH **Clean**		TOLERANCES X ± .1, .X ± .05, .XX ± .005, .XXX ± .002, ANGLE ± .5°		
PROPRIETARY INFORMATION NOT TO BE RELEASED WITHOUT WRITTEN AUTHORIZATION FROM CONCORDIA UNIVERSITY	DESIGNER **O.Khalimonov**	ALL DIMENSIONS IN **INCHES** UNLESS OTHERWISE SPECIFIED		A SIZE	DATE **14-Mar-2018**	USED ON **SC- Rocketry**
	DRAFTER **O.Khalimonov**	APPROVED **O.Khalimonov**	SCALE **1:2**	SHEET **1 / 1**	DWG NO. **00018**	REV NO. **00**

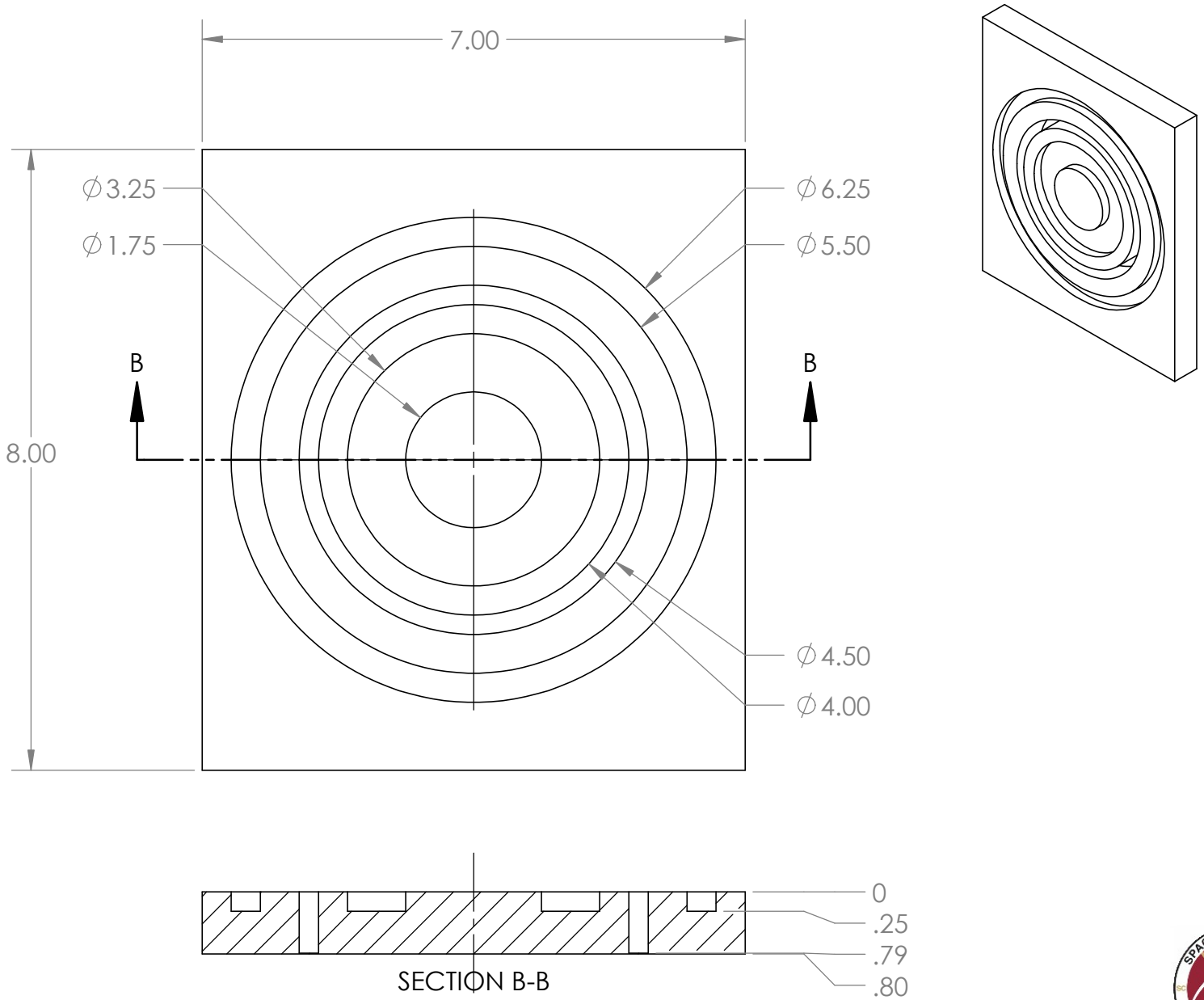

Concordia University	MATERIAL **Aluminum 60601 T6 8"x7"x1"**		SURFACE ROUGHNESS √63	TITLE **Compression rings**	
	FINISH **Clean**		TOLERANCES X ± .1 .X ± .05 .XX ± .005 .XXX ± .002 ANGLE ± .5°		
PROPRIETARY INFORMATION NOT TO BE RELEASED WITHOUT WRITTEN AUTHORIZATION FROM CONCORDIA UNIVERSITY	DESIGNER **O.Khalimonov**	ALL DIMENSIONS IN **INCHES** UNLESS OTHERWISE SPECIFIED		A SIZE	DATE **14-Mar-2018**	USED ON **SC- Rocketry**
	DRAFTER **O.Khalimonov**	APPROVED **O.Khalimonov**	SCALE **1:2**	SHEET **1 / 1**	DWG NO. **00019**	REV NO. **00**

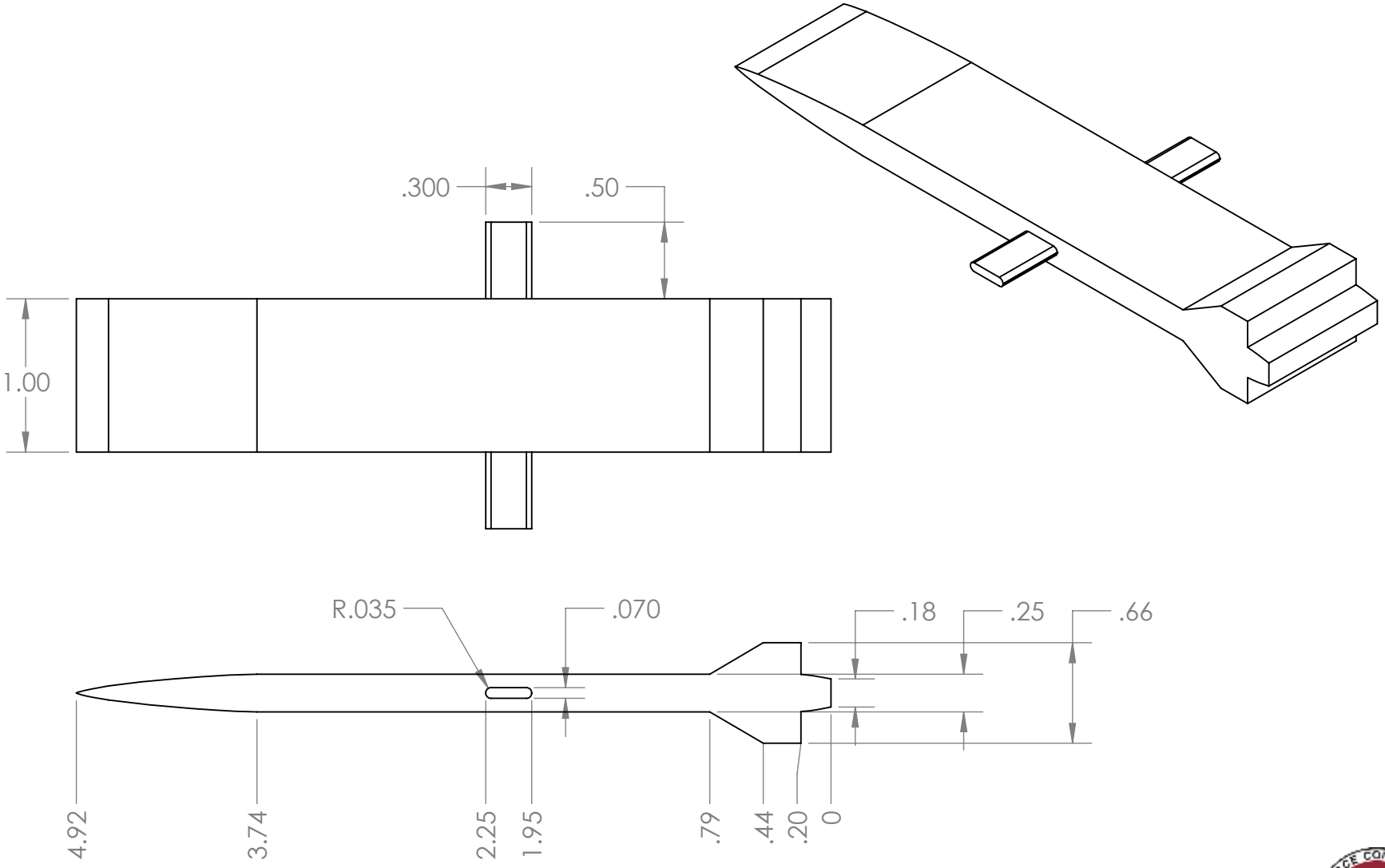

	MATERIAL **Mild Steel**		SURFACE ROUGHNESS √6.3	TITLE **Supersonice Profile**	
	FINISH **Clean**		TOLERANCES X ± .1, .X ± .05, .XX ± .005, .XXX ± .002, ANGLE ± .5°		
PROPRIETARY INFORMATION NOT TO BE RELEASED WITHOUT WRITTEN AUTHORIZATION FROM CONCORDIA UNIVERSITY	DESIGNER **O.Khalimonov**	ALL DIMENSIONS IN **INCHES** UNLESS OTHERWISE SPECIFIED		A SIZE	DATE **25-May-2018**	USED ON **SC- Rocketry**
	DRAFTER **O.Khalimonov**	APPROVED **O.Khalimonov**	SCALE **1:2**	SHEET **1 / 1**	DWG NO. **00018**	REV NO. **00**

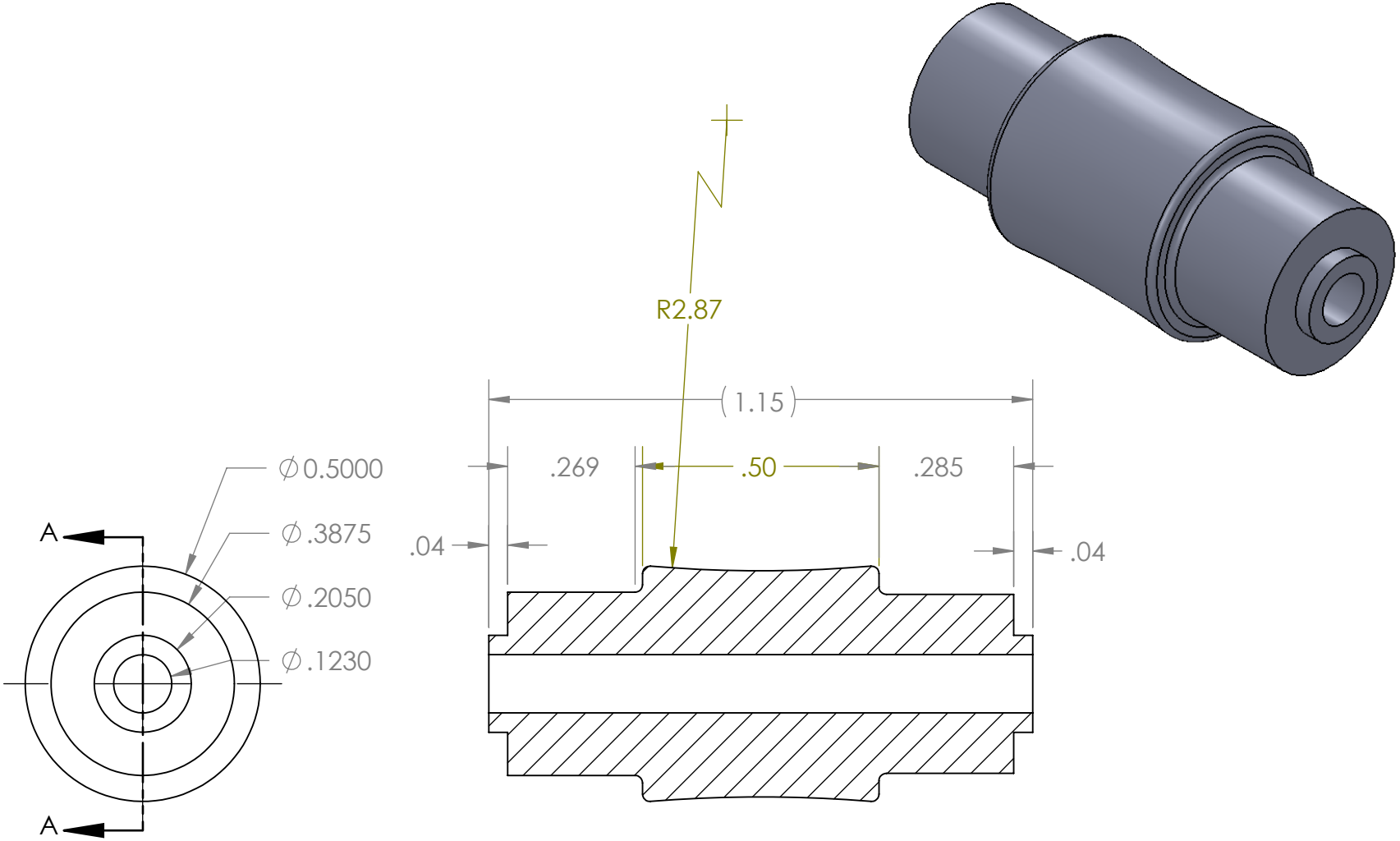

SECTION A-A
SCALE 3 : 1

Concordia	MATERIAL **Steel - ∅.5" x 1.25"**	UNLESS OTHERWISE SPECIFIED	SURFACE ROUGHNESS √63	TITLE **0 degree Roller**	
	FINISH **Clean**		TOLERANCES X ± .1 .X ± .05 .XX ± .005 .XXX ± .002 ANGLE ± .5°		
PROPRIETARY INFORMATION NOT TO BE RELEASED WITHOUT WRITTEN AUTHORIZATION FROM CONCORDIA UNIVERSITY	DESIGNER **O.Khalimonov**	ALL DIMENSIONS IN **INCHES** UNLESS OTHERWISE SPECIFIED		A SIZE	DATE **14/11/2017**	USED ON **SC-Rocketry**
	DRAFTER **O.Khalimonov**	APPROVED **O.Khalimonov**	SCALE **3:1**	SHEET **1 / 1**	DWG NO. **0001**	REV NO. **00**

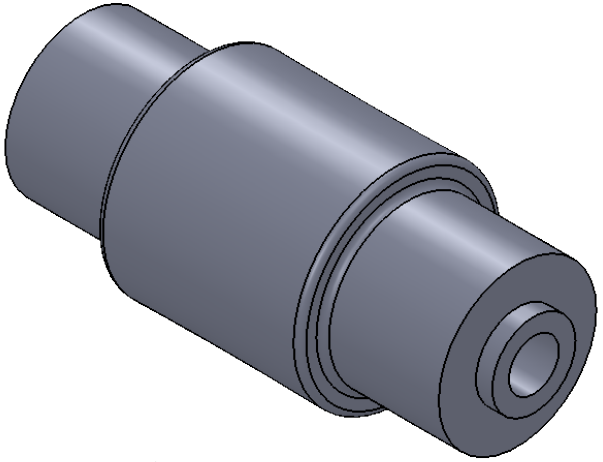

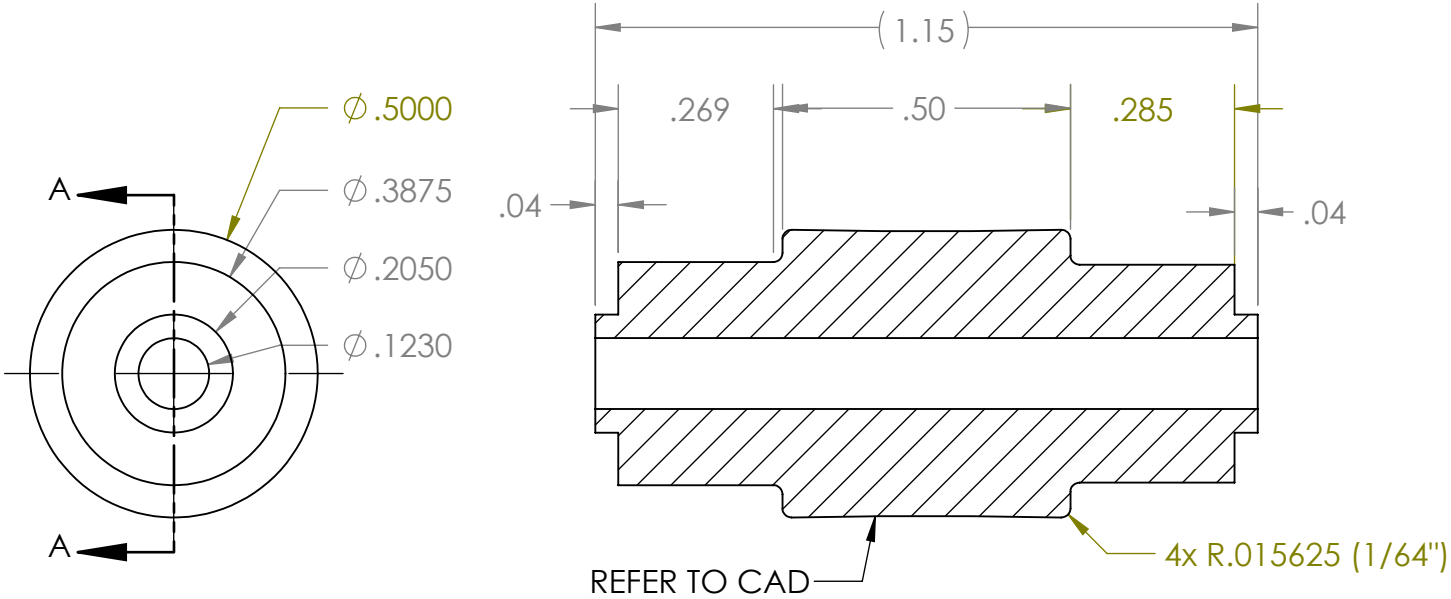

SECTION A-A
SCALE 3 : 1

Concordia	MATERIAL **Steel - ∅.5" x 1.25"**	UNLESS OTHERWISE SPECIFIED	SURFACE ROUGHNESS √63	TITLE **45 degree Roller**	
	FINISH **Clean**		TOLERANCES X ± .1 .X ± .05 .XX ± .005 .XXX ± .002 ANGLE ± .5°		
PROPRIETARY INFORMATION NOT TO BE RELEASED WITHOUT WRITTEN AUTHORIZATION FROM CONCORDIA UNIVERSITY	DESIGNER **O.Khalimonov**	ALL DIMENSIONS IN **INCHES** UNLESS OTHERWISE SPECIFIED		A SIZE	DATE **14/11/2017**	USED ON **SC-Rocketry**
	DRAFTER **O.Khalimonov**	APPROVED **O.Khalimonov**	SCALE **3:1**	SHEET **1 / 1**	DWG NO. **0001**	REV NO. **00**